KLAIPĖDA UNIVERSITY
Faculty of Marine Technology and Natural Sciences
Department of Informatics and Statistics

Rasa Idzelytė

A VISUALISATION SYSTEM FOR BIOGEOCHEMICAL AND HYDRODYNAMIC MODELLING AND ITS APPLICATION TO THE CURONIAN LAGOON

Geoinformatics master's thesis

Geoinformatics study program 621F74001

Klaipėda, 2016

MAGISTRO BAIGIAMŲJŲ DARBŲ LYDRAŠTIS

Pildo magistro baigiamojo darbo autorius

.... Rasa Idzelytė ....
(magistro baigiamojo darbo autoriaus vardas, pavardė)

.... Biogeocheminio ir hidrodinaminio modeliavimo vizualizacijos..............................
.... sistema ir jos pritaikymas kuršių marioms...
(magistro baigiamojo darbo pavadinimas lietuvių kalba)

Patvirtinu, kad magistro baigiamasis darbas parašytas savarankiškai, nepažeidžiant kitiems asmenims priklausančių autorių teisių, visas baigiamasis magistro darbas ar jo dalis nebuvo panaudotas Klaipėdos universitete ir kitose aukštosiose mokyklose.

.... Rasa Idzelytė ....
(magistro baigiamojo darbo autoriaus vardas, pavardė ir parašas)

Sutinku, kad magistro baigiamasis darbas būtų naudojamas neatlygintinai 5 m. Klaipėdos universiteto studijų procese.

.... Rasa Idzelytė ....
(magistro baigiamojo darbo autoriaus vardas, pavardė ir parašas)

Pildo magistro baigiamojo darbo vadovas

Magistro baigiamąjį darbą ginti ....
(įrašyti – leidžiu arba neleidžiu)

....doc.dr. Petras Zemlys....................................
(data) (magistro baigiamojo darbo vadovo vardas, pavardė ir parašas)

Pildo katedros, kuruojančios studijų programą, administratorius (sekretorius)

Baigiamasis darbas įregistruotas katedroje ....
(data)
Laima Brazdeikienė..............................
(katedros sekretorės vardas, pavardė ir parašas)

Pildo katedros, kuruojančios studijų programą, vedėjas

Magistro baigiamąjį darbą ginti ....
(įrašyti – leidžiu arba neleidžiu)
.... prof. dr. Vitalijus Denisovas ....
(data) (katedros vedėjo vardas, pavardė ir parašas)

Recenzentu(-ais) skiriu ....
....
(įrašyti recenzento(ų) vardą, pavardę)

.... prof. dr. Vitalijus Denisovas.....................
(data) (katedros vedėjo vardas, pavardė ir parašas)

SANTRAUKA

Rasa Idzelytė

BIOGEOCHEMINIO IR HIDRODINAMINIO MODELIAVIMO VIZUALIZACIJOS SISTEMA IR JOS PRITAIKYMAS KURŠIŲ MARIOMS

Geoinformatikos magistro studijų programos baigiamasis darbas

Darbo vadovas: prof. dr. Petras Zemlys

Konsultantas: prof. dr. Georg Umgiesser

Klaipėdos Universitetas

Jūros technologijų ir gamtos mokslų fakultetas

Informatikos ir statistikos katedra

Klaipėda, 2016

Darbo apimtis: 64 psl., 5 lent., 33 pav.

Raktažodžiai: Kuršių marios, hidrodinaminis-ekologinis modelis, Shyfem, AQUABC, vizualizacija, ledo danga.

Darbo tikslas – sukurti skaitinio modelio Shyfem/AQUABC modeliavimo rezultatų vizualizacijos sistemą ir pritaikyti ją ledo įtakos natūraliai aeracijai Kuršių Marių ekosistemose tyrimui.

Darbo uždaviniai - suformuluoti reikalavimus modeliavimo rezultatų vizualizacijos sistemai; suprojektuoti ir programiškai įgyvendinti vizualizacijos sistemą; suformuluoti scenarijus ledo įtakos tyrimui; atlikti modelinius eksperimentus su integruotu modeliu; pritaikyti vizualizacijos sistemą modeliavimo rezultatų analizei; pateikti rekomendacijas sistemos tolimesniam vystymui.

Teorinėje darbo dalyje (literatūros apžvalgoje) analizuojami darbo su skaitiniais modeliais žingsniai – būtini veiklos etapai prieš atliekant skaičiavimus ir gautų rezultatų apdorojimas, t.y. vizualizavimas ir statistinė analizė. Taip pat apžvelgiamos ekologinių modelių rūšys ir jų rezultatų priklausomybė nuo hidrodinaminio režimo. Pristatytas hidrodinaminis-ekologinis modelis Shyfem/AQUABC bei jo vidinės gautų duomenų vizualizavimo galimybės. Šioje darbo dalyje taip pat apžvelgta Kuršių marių ekosistema ir jos hidrodinaminiai ypatumai, bei ledo dangos įtaka fiziniams ir biogeocheminiams procesams.

Metodinėje dalyje aprašomas modelio vizualizacijos sistemos kūrimas – suformuluoti sistemos reikalavimai, naudojami kūrimo įrankiai ir metodai. Pagrindiniai sistemai iškelti reikalavimai yra nesudėtinga modeliu apskaičiuotų duomenų vizualizacija grafikų pavidalu (laiko eilutės, priklausomybės nuo gylio), interaktyvumas, galimybė grafiškai palyginti kelių modelio skaičiavimų rezultatus, gauti duomenų failus su statistiniais matavimo duomenų ir modelio rezultatų

įverčiais, bei galimybė nulemti grafiko matmenis ir failo formatą. Vizualizacijos sistema sukurta naudojantis GNU Octave programine įranga Linux Red Hat Enterprise operacinėje sistemoje, kuri veikia 64-branduolių serveryje, priklausančiame Klaipėdos universiteto jūros tyrimų atviros prieigos centrui. Akcentuojamas sistemos greitaeigiškumas – naudojami lygiagretūs skaičiavimai leidžiantys išnaudoti turimą techninę įrangą.

Sukurta vizualizacijos sistema susideda iš 8 skirtingų modulių, atsakingų už įvesties failų nuskaitymą, skaičiavimų lygiagretinimą, biogeocheminių ir hidrodinaminių kintamųjų duomenų apdorojimą. Sistema reikalauja įvesties failų, kuriuose yra nurodyti vizualizacijos parametrai, stočių ir kintamųjų vizualizacijos informacija. Nustatyta, kad laikas per kurį nubraižomi 54 kintamųjų grafikai didėja eksponentiškai mažinant naudojamų branduolių skaičių ir maksimalus našumas pasiekiamas tada, kai visi kintamieji yra apdorojami atskiruose branduoliuose. Darbe taip pat pateikiamos rekomendacijos tolimesniam sistemos tobulinimui.

Vizualizacijos sistema pritaikyta studijuojant ledo dangos poveikį natūraliai aeracijai Kuršių mariose. Buvo modeliuojami penki scenarijai, kurių rezultatų analizė parodė, kad didžiausią poveikį ištirpusio deguonies koncentracijai turi ledo slopinama reaeracija. Be to, yra pastebimi koncentracijos pokyčiai vasaros metu (ledo dangos poveikis nusitęsia į vasarą), kurie priklauso nuo fitoplanktono (stebimas jo koncentracijos poslinkis) išskiriančio deguonį fotosintezės metu.

Deguonies prisotinimo analizė parodė akivaizdų jo sumažėjimą esant ledo dangai, tačiau hipoksijos riba – nepasiekta. Taip pat pastebimas prisotinimo reikšmių kritimas baigiantis ledo periodui, tam gali turėti įtakos pradinės sąlygos, su kuriomis modelis nespėja „įsisukti“, t.y. pereiti stabilų režimą.

Naudojamas modelis atsižvelgia tik į ledo dangos procentiškumą (ne ledo ar sniego dangos storį), taip pat nėra sumažinamas sugeriamos saulės spinduliuotės kiekis esant ledui ir ledo danga buvo gaunama interpoliuojant tik keturių monitoringo stočių duomenis. Patobulinus ledo dangos modeliavimą ir naudojant palydovinius duomenis, ledo dangos poveikio natūraliai aeracijai tyrimas būtų tikslesnis ir geriau atspindėtų natūralią situaciją.

SUMMARY

Rasa Idzelytė

A VISUALISATION SYSTEM FOR BIOGEOCHEMICAL AND HYDRODYNAMIC MODELLING AND ITS APPLICATION TO THE CURONIAN LAGOON

Master thesis of Geoinformatics study program

Supervisor: prof. dr. Petras Zemlys

Advisor: prof. dr. Georg Umgiesser

Klaipėda University

Faculty of Marine Technology and Natural Sciences

Department of Informatics and Statistics

Klaipėda, 2016

Work size: 64 pages, 5 tables, 33 figures.

Keywords: Curonian Lagoon, hydrological model, Shyfem/AQUABC, visualisation, ice cover.

The main goal of the thesis is to create a visualisation system for the simulation results of numerical coupled model Shyfem/AQUABC and apply it for the investigation of ice cover effect to the natural aeration in the Curonian Lagoon ecosystem. The tasks of the work are to formulate the requirements for the visualisation system of modelling results; design and programmatically implement the visualisation system; formulate different scenarios for the investigation of ice cover effect; perform simulations of the model; apply the visualisation system for the analysis of model simulation results; and provide recommendations for further development of the system.

The developed visualisation system consists of 8 different modules responsible for reading input files and parallelisation of the computations, processing biogeochemical and hydrodynamic variable data, and data conversion if needed. The system requires input files, in which the visualisation parameters, and station and variable visualisation information are specified.

The parallelisation of the computations increases the speed of the processes. Analysis showed that the speed increases with the increased number of processors and reaches the maximum speed, when each variable is computed (plotted) on a separate core. Due to this the system allows user to quickly and easily obtain time series and depth profile (3D case) graphs of biogeochemical and hydrodynamic variables, time series graphs of biogeochemical state and derived variables data comparison of several model simulations, and files with statistical estimates. Several recommendations were presented for the further development of the system.

Visualisation system was applied to studying ice cover effect on natural aeration in the Curonian lagoon. Five simulations have been carried out for studying the variations of dissolved

oxygen. The analysis showed that during the ice cover period the greatest impact on dissolved oxygen concentration has the suppressed reaeration. Additionally there are noticeable concentration shifts in the summer time (ice cover effect on dissolved oxygen drags into the summer), this is due to the shift of phytoplankton growth, which also adds oxygen to the water in a process of photosynthesis.

The analysis of oxygen saturation showed a noticeable decrease during the ice cover period, however the level of hypoxia (<30%) was not reached, and the decrease of values in the end of ice period, this might occur due to the long model spin up time, which might be resolved by adjusting initial conditions.

The model takes into account just the percentage of ice cover (not the thickness of it or the snow cover on top of it), the solar radiation is not reduced when ice is present and ice cover data was interpolated over the entire lagoon from the data of just four monitoring stations. Overall, an improved model (and the use of satellite data) would improve the knowledge of ice cover effect on natural aeration in the water body.

LIST OF TABLES

LIST OF FIGURES

TABLE OF CONTENTS

INTRODUCTION

Modelling is of great use for assessing the changes of the hydrological and biogeochemical processes in the water body. It is a basic tool for investigation of the interactions between different elements of the ecosystem. Though model is a simplified version of the real system and cannot contain all of its elements and processes, it can give a great insight on studied problems.

Numerical finite element model Shyfem was notably used to investigate hydrodynamic processes of the Curonian lagoon. This model has the ability to be coupled with ecological models. This was done with biogeochemical model AQUABC, which is a relatively new model and currently under development, thus the visualisation system of the modelling results (both the ecologic and hydrodynamic) should be developed in order to get fast depiction of the output, which facilitates the calibration and validation of the model as well as studying the ecological processes.

There are thorough studies of the Curonian lagoon ecosystems done by investigating the observational data. However the research done through modelling is not as profound and more attention is needed, especially studying the fields, where observations are costly or hard to obtain.

Ice cover is of great importance to the hydrodynamical and biogeochemical processes of the shallow lagoons. Its presence alters water level oscillations, mixing, heat balance, and gas exchange with the atmosphere. During cold winter periods when the thick ice cover forms, it suppresses the natural aeration, light penetration and wind stress, these processes (through various chemical processes) have impacts on lagoon's ecosystem structure and productivity. Therefore it is important to investigate the influence of ice cover for physical and biogeochemical processes. Modelling is useful for examination of the processes occurring during and after the ice cover period.

The object of the thesis: visualisation system, coupled hydrodynamic-biogeochemical numerical model, and the ecosystem of the Curonian lagoon.

The aim of the thesis: to create a visualisation system for the simulation results of numerical coupled model Shyfem/AQUABC and apply it for the investigation of ice cover effect to the aeration in the Curonian Lagoon ecosystem.

Tasks of the thesis:

1. Formulate the requirements for the visualisation system of modelling results;
2. Design and programmatically implement the visualisation system;
3. Formulate different scenarios for the investigation of ice cover effect;
4. Perform simulations of the model;
5. Apply the visualisation system for the analysis of model simulation results;
6. Provide recommendations for further development of the system.

The presented products: developed visualisation system for coupled hydrodynamic-biogeochemical model (Shyfem/AQUABC) simulation results.

1. LITERATURE OVERVIEW

Everything in this world is made of parts – car, human body, water body and etc. To say this in a more formal, scientific way – a set of interconnected elements forms a system. A system acquires characteristics that its individual elements do not have. Usually those elements are also systems themselves and they are made up of other elements which can be systems too, and so on. An example of such complex system is an ecosystem, which has various biotic and abiotic elements interacting with each other.

To understand ecological systems such as Curonian lagoon, it is not sufficient to identify and characterize only individual elements in the system. It is also necessary to obtain a thorough knowledge of the interactions between them, like nutrient cycles and energy flows. The technological advances enable researchers to monitor complex processes, so the main focus is on interpreting the observed data. Numerical models allow scientists to investigate how these complex processes are connected. Furthermore, these models help investigators to systematically analyze systems disruptions and develop predictions to increase the benefits of this complex system.

Models give a simplified picture of reality and will never contain all the features of the real system because then it would be the real system itself. It is, however, important that the model contains the characteristics of the system that are essential in the context of the management or scientific problem to be solved or comprehended.

1.1. Numerical models

Most of the mathematical models used in the natural sciences are based on differential or integral equations, which consist of continuous functions. However, computers can only perform discrete calculations, so instead of solving complicated continuous equations (which usually cannot be solved analytically), there has to be developed an appropriate numerical model – approximation to the mathematical model.

Work with developed numerical model usually can be divided into three stages: pre-processing, processing and post-processing. The pre-processing stage requires most of the model developers' time, because there has to be defined discretized computational grid, initial and boundary conditions, constants and coefficients, and other properties or methods concerning the problem. In the processing step the computer solves the problem (defined equations); the user interference is minimum or none. In the post-processing stage the derived solution is visualised and analysed.

1.1.1. Pre-processing

A very important part of pre-processing is generation of the grid. The continuous domain is discretized into elements or cells and the position of grid points (vertices of these elements, called nodes) are determined. Afterwards, nodes and elements are numbered and nodal positions and connectivity between elements are specified such that the processor can identify the problem domain, discretisation and nodal position (Desai et al., 2011). There are two main types of grids used for numerical solution of continuous equations – structured and unstructured grids (Figure 1).

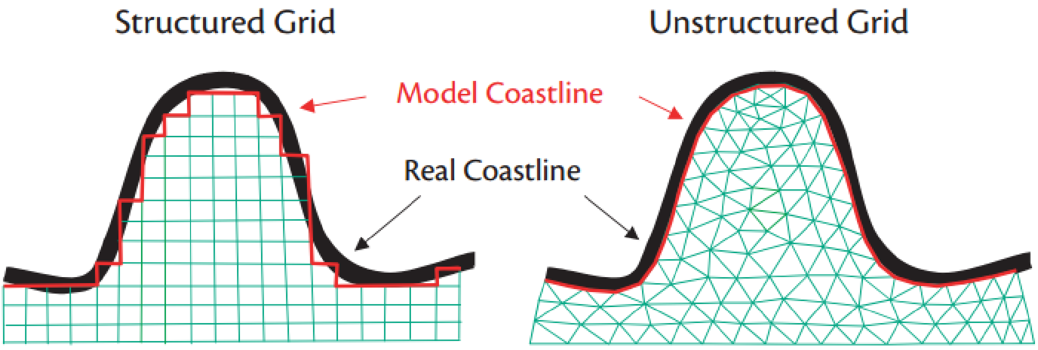

Figure 1: Structured and unstructured grids in 2d (Chen et al., 2006).

Structured grid models tend to use quadrilateral grid cells in 2D and cubes in 3D this offers straightforward and efficient algorithms, because the grid points can be stored as an array $x(i_1, i_2)$ and the neighbours of a given grid point are simply found as the neighbours in index space $x(i_1 \pm 1, i_2 \pm 1)$ (Henshaw, 1996). But this approach limits the grid's flexibility in resolving the complex coastlines, islands, barriers or inlets. For good representation of these geometries the resolution of the grid has to be increased, which results in unnecessarily high resolution of the not so geometrically complex areas of the analysed domain (requires more elements than an unstructured grid for the same problem). Nonetheless this type of model is relatively fast and can be used for modelling shallow water hydrodynamics (Kelin et al., 2008; Ateljevich et al., 2009; Liungman et al., 2010; Zhang et al., 2012).

Unstructured grid models have much more flexibility in their grid resolution than structured grid models. Grid size can vary from place to place in the computational domain. Unstructured grids tend to use triangles in 2D and tetrahedra in 3D. This model requires higher storage space, because there have to be stored all the elements (as a list) and their neighbourhood relationships (relationships cannot be defined implicitly as in structured grid model). This grid creation approach also tends to be more time consuming to run and more sensitive to numerical errors (Holleman et al., 2013), nevertheless this method's applicability for complex computational domains is widely used for estuarine hydrodynamical modelling (Holleman et al., 2013; Ferrarin et al., 2008; Zemlys et al., 2013; MacWilliams et al., 2007 and 2015, Umgiesser et al., 2016).

These two grid models can be combined together and used as so called hybrid grid model. When the computational domain has regular and complex geometry, the structured and unstructured grids can be used respectively or grids of the same type can be nested. Some models are run with finer-resolution grids nested inside coarser-resolution grids (Figure 2) within the same model. This configuration can reduce the CPU time compared to the standard approach of using only one fixed grid size (Rasmussen et al., 2004).

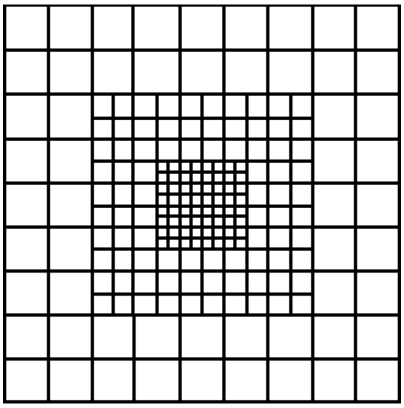

Figure 2: Nested structured grid.

Nesting can be one-way or two-way, considering the sharing of information between grids. Advantages of the two-way nested grid include, fine-scale processes resolved on the finer grid are allowed to affect the larger-scale flow on the coarse grid, because the small-scale processes in greatly influence the large-scale processes. Two-way nested grid models are also used for studying hydrodynamics of water bodies – Zhai et al. (2003) combined ocean circulation model (outer coarse grid) with Scotian shelf and slope (inner fine grid) model by adding a two-way interaction term to the horizontal momentum equations of each sub-model. The results showed that the inner model produces not only large-scale circulation features which are consistent with observations and those produced by the outer model, but also more meso-scale features than those in the outer model. Nested grid technique is also used for studying the circulation and thermal structure of lakes (Sheng et al., 2006) and coastal waters (Sheng et al., 2009).

The generation of the grid also depends on the dimension of the model (1D, 2D or 3D). One-dimensional models include one space dimension only and are used when physical properties vary mainly in one direction (e.g. depth) and remain constant in the other two dimensions. 2D models include two space dimensions; they vertically average the processes. 3D models are the most complicated and treats the full domain in depth and both the horizontal and vertical directions.

After generating the grid, the process handling equations have to be discretized. Numerical methods for solving the continuous equations are primarily of two types. The first type of numerical method approximates the equation of interest, usually by approximating the derivatives or integrals in the equation. The approximating equation has a solution at a discrete set of points, and this solution approximates that of the original equation (Atkinson, 2016). Such numerical procedure is called finite difference method (FDM). This method usually uses structured grid, which makes it a relatively simple, fast and easily programmed method, however it can also be used for unstructured grids (Fernandez et al., 2004).

The second type numerical method approximates the unknown function in the equation by a simpler function, often a polynomial or piecewise polynomial function, chosen to closely follow the original equation (Atkinson, 2016). Such numerical procedure is called finite element method (FEM). This method directly approximates the solution of the continuous equation, rather than the equation itself (Likens, 2009). FEM uses unstructured triangular grid, which is preferable for flows (Ghorbani, 2011) and complex geometries (Church, 2008). As FDM method can be applied both to structured and unstructured grids, the FEM can be applied to structured grid also (Kumar et al., 2008).

Finite difference and finite element methods are used not only separately, but they can also be coupled together. Kangping et al. (2012) proposed a numerical method for interaction between free surface and an elastic structure. FEM was used for solving dynamic structural deformation and FDM was applied for calculating the free surface flow. The investigation showed that this method has a great potential for studying such fluid-structure interaction problems. De Martin et al. (2007) also presented an approach of coupling these two methods for simulating regional seismic wave propagation to local site response – the advantages were taken of both methods: the portability of the FDM and the flexibility of the FEM.

When the equations are discretized, there are requirements for them and their solution to the continuous equations: (i) consistency – when time step and grid size goes to 0, discretized equation converges to the differential equation, (ii) accuracy – truncation error and the closeness of the numerical solution to the analytical solution (numerical scheme must be at least first-order accurate in order to be consistent (Blazek, 2005)), (iii) stability – not growing of round-off errors and/or initially small fluctuations in initial data which might cause a large deviation of numerical solution from the analytical solution (Ogunniye, 2015).

These equations have to be solved on the discrete points inside the grid of intersecting lines obtained by the discretisation process. The fluid motion and transport processes are not determined by just the governing equations, but it also depends on initial conditions and conditions applied on the domain boundaries.

Initial conditions are required only when the simulation is time dependent. It specifies the state of the water body at the beginning of the simulation and its influence on the solution lasts a limited period that can easily be determined. This period is the time taken for numerical model to reach the statistical equilibrium under the applied forcings and it depends on the retention time of the system, which depends on the boundary conditions (Gonenc et al., 2004).

The value of the boundary conditions cannot be obtained from the equations used to describe the physical phenomena, but must be inserted on the basis of the information. Boundary conditions and external forcing to the study area are driving forces for model simulations (circulation and water quality changes). A model does not calculate boundary conditions for itself, but are affected by them (Zhen-Gang, 2008). In fluid dynamics there are two main boundaries – vertical and horizontal. Vertical boundary conditions include surface and bottom boundary conditions (wind stress, heat fluxes, bottom stress). Horizontal boundary conditions are of two types: (i) closed – e.g. coast line, this type of boundary can be classified as no slip (no flow along or through the boundary) and free slip (flow can be along the boundary, but not perpendicular to it), (ii) open – conditions for the sides of the domain not bounded by land, it can be classified as inflows and outflows. Open boundary conditions are very important for determining flows in ocean (Jensen, 1998) and coastal (Ma et al., 2011) models.

Another step in pre-processing is specification of initial values of the model parameters. Such parameters can be bathymetry, domain geometry, and the flow resistance properties (friction forces) within the water body (at the surface and bottom).

Numerical models have to be valid for their application and must provide credible and reliable results. The process of ensuring it typically consists of three elements - verification, validation and calibration. The first two – is the model internally correct (are the parameters, equations, and code true) and does the model perform well (model output compared to field data), are the components of testing the model. The third element – calibration, improves the parameterization of a model, so that the model output would be the closest approximation of the measurement data. Calibration can occur as part of either verification or validation (Rykiel, 1996; Mazzotti et al., 2007). At least two data sets are required to adequately calibrate and validate a numerical model.

Parameters are used for the calibration of the model, but considering the large amount of them, it is best to reduce this number by performing the sensitivity analysis and keep just those parameters that can significantly affect the solution (Gonenc et al., 2004).

Once the domain and governing equations are discretized, and the parameters and conditions are set, then it is time for processing step – simulation of the numerical model (deriving the solution). For example, processing in the context of FEM includes generation of element matrices, assembly of element equations imposition of boundary conditions and solution of system of equations (Desai et al., 2011). Computer generates results which are stored in files and can be reviewed in the post-processing step.

1.1.2. Post-processing

The primary goal of the data visualisation is to represent information clearly and efficiently for users to analyse and understand patterns or relationships in the data for one or more variables, obtain insights that directly support assessment, planning, and decision making. There are several numerical computational packages that can serve as visualisation tools: Excel, Matlab, Octave, R, Maple, Model Maker, gnuplot and etc. For representing the spatial or geographical data the GIS tools, such as ArcGIS, Idrisi, QGIS, GRASS GIS, and etc., can be used.

When working with numerical models, in the post-processing stage, the results of the numerical simulation (or processing) are visualised or/and other computations (statistical evaluation) are made. Scalars and vectors are visualised in one, two or three dimensions and time in form of time series (temporal graphs), isolines, isoareas, vector fields, path lines, animations, maps, tables and diagrams.

In 1D the computed results are plotted along the coordinate axis, for time-dependant problems at a certain time, at different time steps or in an animation. The temporal development of a variable at a certain location is shown in time series. In 2D the results of scalars, such as water level, concentrations or saturations, are presented with isoline or isoarea plots, the results of vectors (such as flow) in vector plots. For time-dependant problems time series and animations are suitable for the analysis of the results. For particle models – the path lines are used. Sometimes to analyse the simulated processes it is good to combine several visualisation techniques or to plot differences between results of different simulations, e.g. the reference (original) situation and the one after an interaction with the system. The visualisation of time-dependant 3D simulation can be very complex. A first impression can be obtained by looking at the results in certain cuts or cross sections and all the 2D visualisation techniques can be applied to it. For detailed view of 3D results, the user’s interaction is needed (for defying point of view, shading, light intensity and etc.). This requires advanced visualisation tools (Hinkelmann, 2005).

Estuarine hydrodynamic models always require management of large amounts of geographically referenced information, so it is good to represent the results on maps using geospatial tools like GIS (Basos, 2013), which can also be used for pre-processing of input data including editing, transformation, interpolation, and the derivation of parameters. GIS also can be used for statistical analysis of the model output.

Hadaś E. (2014) presented information technology system (ISOK) dedicated for protection against extreme hazard (especially floods) that is a valuable source of high-quality spatial data and maps. The author presented how numerical model results can be visualised using GIS system for 3D visualization of hydrodynamic modelling of flood, the impact of increased water level on buildings and land can be easily assessed. This technique is an enormous advantage for less experienced people, because the final result is very detailed.

Both the visualisation and statistical analysis of the simulation results contributes also to the calibration and validation of the numerical model. In this (post-processing) step the validity of the solution is investigated, or (when validity is good enough) simulation results are analysed in order to achieve the modelling goal.

Most numerical modelling software systems have their own data formats and structures, thus it is needed to process the data individually depending on the output. However there are tools for visualisation of the result of several models, e.g. Pan et al. (2014) presented the development of an open visualization tool for grid based water models, which has functions for loading and visualizing results from a suite of modelling systems, regardless of their data structures.

The application of numerical methods and models is wide – from hydrodynamics, meteorology to mechanics and etc. But it cannot be forgotten that, a reliable numerical model cannot be expected to represent every aspect of the physical/real object (e.g., temporal resolution of the model is coarser than real time) neither is the representation exactly accurate as there is always some quantitative error. Development of an effective model often involves a series of iterative testing and revision cycles.

1.2. Ecological models

Ecological models are an instrument to understand the properties of the complex ecosystems and also used as a sustainable management tool. For instance, an increased nitrogen use in agriculture and untreated industrial and urban discharges leads to water contamination and eutrophication of freshwater and estuarine ecosystems (Zhang et al. 2015). It is not practical or affordable to sample at sufficient spatial and temporal resolution for hundreds of individual chemicals within fresh and marine waters, including aquatic biota and sediments, for this reason modelling is required (Collins, 2011).

As the development of computer technologies increased so did the spectrum of applications of the models. There are 11 types of ecological models (Jørgensen, 2009; Chatzinikolaou, 2012):

1. Biogeochemical and bioenergetic dynamic models – applied for describing the state of an ecosystem in terms of matter or energy distribution when a good dataset is available;
2. Static models – can be considered as a special category of the biogeochemical or bio-energetic dynamic models where all differential equations are set to zero in order to describe a static situation.

3. Population dynamics models – for observing the development or recovery of a population; require a homogenous and good database;
4. Structural dynamic models – describe ecosystem adaptations and shifts in species composition. They can include more than one species (even with slightly different properties), and they can be used to model biodiversity and ecological niches;
5. Fuzzy models – applied when no data are available or when the data are uncertain;
6. Artificial neural networks – give relationships between state variables and forcing functions based on a heterogeneous database, which has to be sufficiently big;
7. Individual based models (IBM) and cellular automata – IBM models are able to derive the properties of a system from the properties of the components of this system. These models often use cellular automata models, which are spatio-dynamical models where space, time and states are discrete;
8. Spatial models – investigate the spatial distribution of the forcing functions and of the non-biological and biological state variables. Effective for investigating spatial patterns;
9. Ecotoxicological models – includes simple to use bio-geochemical models or population dynamic models which additionally include an effect component;
10. Stochastic models – can be a biogeochemical, a population dynamic, a spatial, an IBM, or a structural dynamic model, which will be able to consider randomness of forcing functions or processes;
11. Hybrid models – combination of any two of the previously mentioned model types, resulting in the composition of advantages and the elimination of disadvantages of the existing models.

There are numerous ecological processes acting in the ecosystem (Jørgensen et al., 2001) and the selection of the proper ecological model depends on the type of the available dataset and on the problem that is needed to be solved or understood.

All of the biological processes react on physical conditions both directly and indirectly via chemistry (Jørgensen, 2011). The hydrodynamic conditions are described in terms of the circulation, temperature, salinity and water level. The vertical distribution of temperature and salinity gives an indication of how stratified or well-mixed the water column is, which is of great importance for the ecological processes (Liungman et al., 2010). These interactions between biotic and abiotic processes make it necessary to couple hydrodynamic and ecological models. There are three ways of coupling these models: (1) offline with no feedback; (2) online with no feedback; (3) online with feedback (Figure 3).

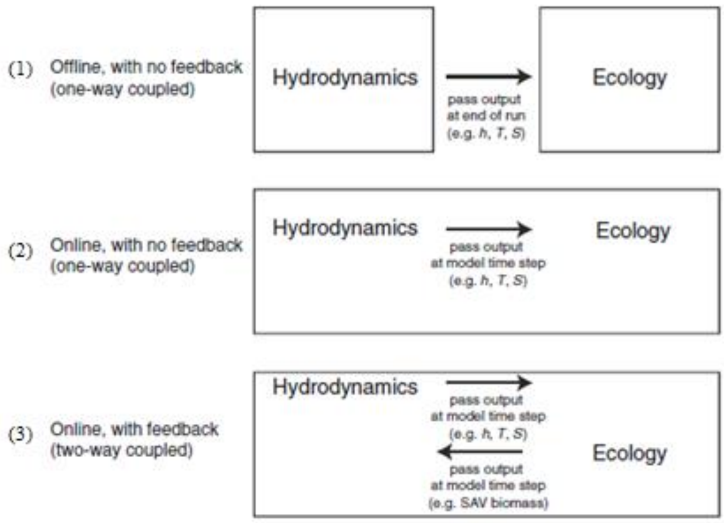

Figure 3: Examples of three model coupling configurations; h – water depth, T – temperature, and S – salinity (Ganju et al., 2015).

When offline coupling technique is applied then there is no feedback between these models. The hydrodynamics is run first and then the ecological model is run using physical outputs with or without spatial and temporal modifications. The benefit of this technique is that the ecological model can be run several times using the same hydrodynamic model output, however some post-processing of hydrodynamic model output may be necessary, and this may change the fidelity of the hydrodynamic results (Ganju et al., 2015). Filgueira et al. (2012) presented an offline physical–biogeochemical coupling scheme for marine systems, which was developed using graphical modelling software and it showed that it is a generic and flexible tool for modelling long-term processes in coastal waters. Nobre et al. (2010) used this technique in multilayered ecosystem modelling approach for marine resource management, where the output from the catchment, hydrodynamic and aquatic resource sub-models was collected for offline coupling with biogeochemical model.

Applying the second technique, online with no feedback (also called forcing), the hydrodynamic model output is passed internally to the ecological model with no need for modification; these models are integrated into the same compiled executable. There is no loss of fidelity in this case, because the models are running on the same grid and time step; however the hydrodynamics has to be re-run each time an ecological parameter is changed, even though the ecological parameter change has no effect on hydrodynamics (Ganju et al., 2015). An example of this type of coupling is shallow water hydrodynamic finite element model Shyfem coupled with biogeochemical model AQUABC, both of them will be presented in the next section of this chapter.

The last configuration is online with feedback; here the models are also integrated in the same compiled executable. In this case the hydrodynamic model output is passed internally to the ecological model and then it gets feedback from it. Sonntag et al. (2011) used this coupling technique for studying the effect of a changing phytoplankton community composition to one dominated by buoyant cyanobacteria on the physical oceanic properties. The coupled model results suggest that the development of cyanobacterial surface blooms and their feedbacks on light absorption and wind drag need to be taken into account in order to capture changes in the dynamics of the upper ocean.

Ecological model results are quite sensitive to the hydrodynamic framework so robust evaluation of the hydrodynamic component is imperative for coupled models. For numerical models, the equations governing hydrodynamics are well constrained and tractable when compared with ecological processes (Ganju et al., 2015).

Since the model is a simplified version of the real system, the biological processes of the ecosystem are aggregated into functional groups. For example, all phytoplankton and zooplankton are considered as groups and population dynamics are described in terms of fluxes of carbon and nutrients between functional groups and between organic and inorganic material (James, 2001). The simultaneous simulation of physical, chemical and biological processes at the relevant spatial and temporal scales are very useful for investigating the estuarine ecosystems (Park et al., 2015), thus it is necessary to couple hydrodynamic and biogeochemical models.

1.3. Coupled numerical model Shyfem/AQUABC

Shyfem is an open source hydrodynamic finite element model for shallow water bodies developed by G. Umgiesser (and constantly improved by him and his team) at the Institute of Marine Sciences of the Italian National Research Council (CNR-ISMAR) in Venice. It is based on unstructured grid, thus makes it suitable for application to lagoons, coastal seas, estuaries and lakes with complicated geometry and bathymetry.

The hydrodynamic model solves the shallow water equations with the hydrostatic and Boussinesq approximation. It uses a semi-implicit time resolution and a staggered finite element approach for the horizontal spatial integration. The model takes into account the main physical forcings characterizing the water circulation such as barotropic and baroclinic forcing, horizontal and vertical viscosity effects, and non-linear inertial processes (Cucco et al., 2013; Umgiesser et al., 2004). This model is able to provide 2D as well as 3D simulations. More about the model can be found in section *2.2.1. The modelling framework*.

The finite element program Shyfem was originally created for studying Venice lagoon, which has a very complicated bathymetry and needed a better investigation, and now it has been applied to open seas (Roland et al., 2009), river delta in Romania (Bajo et al., 2014), numerous lagoons in Italy (Umgiesser et al., 2004; Bellafiore et al., 2009; Ferrarin et al., 2005 and 2010), Spain (De Pascalis et al., 2011), Japan (Chikita et al., 2015), Vietnam (Umgiesser et al., 2007) and the

Curonian lagoon in Lithuania (Ertürk et al., 2008; Zemlys et al., 2008 and 2013; Umgiesser et al., 2015).

AQUABC (AQUAtic Biogeochemical Cycling) is a biogeochemical model based on the kinetic part (ALUKAS) of the box model ESTAS (Ertürk et al., 2008). This model was coupled with Shyfem using online with no feedback coupling technique. AQUABC was developed initially as a model focusing on pelagic ecological processes, later incorporated with the bottom sediment model, which is currently under development. The linkage between the water column and sediment model is ensured by coupling the state variables in pelagic ecology and bottom sediments sub-models where the transport processes in the bottom sediments model make the two way transfer of nutrients and organic matter possible (Eilola et al., 2015).

The main goal of biogeochemical models is to describe the cycles of chemicals (dynamics and spatial distribution of concentrations). AQUABC has 33 water column state variables (Table 1). Meteorological forcings, salinity and temperature data is obtained from hydrodynamic model and the kinetic part is called every hydrodynamic time step.

Table 1: The list of water quality state variables.

No	Name
1	Ammonium nitrogen
2	Nitrate nitrogen
3	Orthophosphate phosphorus total in water and in particles
4	Dissolved oxygen
5	Chemoautotrophic(nitrification) bacteria Carbon
6	Aerobic-anaerobic heterotrophic bacteria Carbon
7	Facultative anaerobic heterotrophic bacteria Carbon
8	Diatoms carbon
9	Zooplankton Carbon
10	Zooplankton nitrogen
11	Zooplankton phosphorus
12	Detritus particulate organic Carbon
13	Detritus particulate organic Nitrogen
14	Detritus particulate organic Phosphorus
15	Dissolved organic Carbon
16	Dissolved organic nitrogen
17	Dissolved organic phosphorus
18	Cyanobacteria Carbon
19	Other phytoplankton Carbon
20	Dissolved silica
21	Biogenic silica
22	Nitrogen fixing cyanobacteria Carbon
23	Dissolved inorganic Carbon

24	Total alkalinity
25	Ferrous total (water and particles)
26	Ferric total
27	Manganous total
28	Manganese 4+ total
29	Calcium total
30	Magnesium total
31	Sulphate sulphur total
32	Sulphide sulphur total
33	Methane carbon total

The coupled Shyfem/AQUABC model was presented by Zemlys et al. (2011) as a water quality forecast model. In this technical report the AQUABC model calibration and validation was described and the results showed that in general model demonstrates satisfactory performance and can be used for the research. However the creation of the water quality model is an endless process and the improvements are expected.

1.3.1. Model visualisation tools

Shyfem has a program *plots* for representing simulation results on a map. There are several options to choose for plotting: basin (grid, bathymetry, etc.), velocities, transports, water levels, generic concentration (tracer), temperature, salinity, wave height, period and direction, etc.

In the model framework program *gnuplot* is applied to visualise the time series (command *gp*). When using this program it is possible to specify the scaling of axes, the line type, legends for the axis and colour plots. There are also utility routines (*splitets*, *nosextr_node*, and etc.) that can extract data from the output binary files. These data are written in a way that it can be imported into a spreadsheet or any other program for proper visualisation or calculation of the statistics.

A set of scripts are available for visualisation of AQUABC model results. It allows plotting time series of all the water columns and sediment state variables of a single model run, as well as comparison of two simulation results. However, the use of these scripts is cumbersome and requires an adaptation after each change of the number of state, derived and diagnostic variables, and number of vertical layers. Thus it is necessary to develop a visualisation system, which would be independent of these numbers, could provide fast generation of graphs of biogeochemical and hydrodynamical variables time series, and depth profiles (for 3D simulations), be an interactive system if needed, and compare several simulations at once, with additional options concerning the visualisation of the model results.

1.4. Curonian lagoon

Lagoons are ecologically defined as "shallow water bodies separated from the ocean by a barrier, connected at least intermittently to the ocean by one or more restricted inlets, and usually oriented shore parallel" (Cataudella et al., 2015). Lagoons are the most valuable components of the coastal areas (Gonenc et al., 2004). Lagoon ecosystems play a significant role in regulation of freshwater inputs to the marine environment, are sinks and biogeochemical reactors for nutrients and toxic substances originated from terrestrial sources as well as nurseries for many marine species (Razinkovas et al., 2008). Coastal lagoons are most vulnerable to direct impacts of natural environmental and anthropogenic factors (Aleksandrov, 2010). The influence on ecosystem (e.g. pollution) and the benefits provided by it (e.g. fisheries, tourism) have to be sustainable, so that the ecosystem of the lagoon would be healthy and productive.

The Baltic Sea is one of the largest brackish water systems in the world (Arheimer et al., 2015) and the Curonian lagoon (Figure 4) is the largest lagoon of the Baltic Sea and in Europe. The lagoon is located in the south-east of the sea and separated from it by narrow sand spit (Curonian Spit) with the connection to the sea in the Klaipėda Strait (width of 400 m). The lagoon has a shape of a right-angled triangle with the widest part being in the south and gradually narrowing to the north. Politically Curonian lagoon can be divided in two parts: the northern part belongs to Lithuania's territory and southern part belongs to Russia's Kaliningrad Oblast.

Figure 4: Curonian lagoon (interactive, available at: http://www.sfgate.com/travel/article/Exploring-a-sliver-of-the-real-Lithuania-on-the-6190642.php).

Curonian lagoon is a large estuarine coastal freshwater body with volume of 6.3 km^3. The lagoon is relatively shallow with the mean depth of approximately 3.8 m, the greatest natural depth of 5.8 m and artificially deepened in Klaipėda Strait (the only lagoon outlet) to the depth of approximately 14.5 m (Balevičienė et al., 2007; Schiewer, 2008). The total surface area is 1584 km^2 and only around 380 km^2 belongs to Lithuania's territory, studies show that this extent is decreasing (as in the whole lagoon) because of accumulation processes in the Nemunas delta and sand gliding into the lagoon from the active dune areas of the Curonian spit (Žilinskas et al., 2012).

It is an open system, influenced by a discharge of the fresh water from Nemunas River (main water inflow) and other smaller rivers, and saline water from the Baltic Sea. Every year the rivers carry the amount of fresh water about 4 times the lagoon volume, thus it is the main water renewal source. Therefore, the southern and central parts of the lagoon are freshwater (average annual water salinity is 0.08 ‰), while the northern part has an average annual water salinity of 2.45 ‰, with irregular salinity fluctuations of up to 7 ‰ due to the Baltic sea water intrusion (Zemlys et al., 2013).

1.4.1. Hydrology

The perennial change of water balance in the Curonian lagoon is related to both natural and anthropogenic effects. The natural changes are in sea level rise and Nemunas run-off, precipitation and evaporation; these changes modify the water balance of the lagoon during the year. The main changes are observed in the winter-spring period, when in the month of January and February the Nemunas discharge increases due to warmer winters, meanwhile floods in the spring time decreased, therefore, run-off during the year becomes more even (Žilinskas et al., 2012).

The studies of long term observational data (Dailidienė, 2007) showed that water level, precipitation, air and water temperatures have increased and pressure at sea level and the average annual wind speed have decreased. Comparing two periods of 1960–1975 and 1991–2005, the mean water level in Klaipėda strait has increased by 11 cm and in the lagoon (stations in Nida and Juodkrantė) – by 8 cm. Water level regional analysis is very important to assessing climate change. Lagoon environmental features such as depth, connections with the sea, sediment dynamics, size, as well as water temperatures and productivity, can be affected by global climate change and the rise of water level (Cataudella et al., 2015).

Čerkasova et al. (2016) presented a sophisticated hydrological model SWAT for the assessment of the impact of climate change scenarios (pessimistic and optimistic) on the run-off of the Nemunas River and the Minija River. The pattern of the simulations of these scenarios is similar: a strong increase in the winter months (especially in February), a decrease during the spring and summer, and a slight increase during the autumn (up to 22%, 10%, 18% and 10% respectively).

Due to the inflowing rivers the average water level in the lagoon is normally higher compared to the sea level of the Baltic Sea and it makes up to 5% of the fresh water inflow to it (Davulienė et al., 2003). The predominant flow of water is from the south to the north discharging approximately 22 km^3/year (Gasiūnaitė et al., 1998).

Atmospheric processes also have an impact for water level increase – due to increased cyclonic activity and more frequent storms, the stronger western winds formed higher water level in the southeastern coast of the Baltic Sea, thus in the Klaipėda strait also (Žilinskas et al., 2012). The variation of water level is also associated with the annual changes of ice cover duration in the coast of the Baltic Sea, which had not formed very often due to warm winters, and the prevailing western winds could form higher water levels and affluents (Dailidienė, 2007).

The interactions between the lagoon and sea were studied by Zemlys et al. (2013). The results of one year simulation, got from running finite element model Shyfem, showed that the saline water intrusions are determined by barotropic inflows driven by the sea-lagoon water level difference. Saline water inflow is gradually decreasing with distance from the sea. The saline water reaches southern part of the lagoon through the western coast, due to the weaker influence of the fresh water discharge from Nemunas River. The strongest salinity gradient is in the Klaipėda Strait (difference between annual average salinity of the bottom and surface layers is 2.5–3 ‰), which creates conditions for three types of flow regime: one-directional inflow, one-directional outflow, and two-directional flow, which differ in duration of each flow regime and intensity of opposite-direction flows. However the Baltic Sea influence on water level has direct impact just in Klaipėda Strait and changes of water level of the lagoon is more affected by river run-off and precipitation.

The fluctuations of water levels in the Baltic Sea and the lagoon, surface run-off, wind, affluents and low-tides cause currents in the lagoon. Furthermore, they are affected by the bottom relief and the shoreline. Horizontal water circulation pattern studies (Davulienė et al., 2003; Ferrarin et al., 2008) showed that the wind (depending on its direction) creates different circulation subsystems in the southern part of the lagoon. In most cases the system evolves into a dominant gyre, with anticlockwise (wind from west) and clockwise (wind from south-east) directions and some smaller gyres. In case of south-west wind, the circulation pattern is characterized by a two-gyre system. In the northern part of the lagoon there is a south-north current due to the Nemunas River run-off. The brackish sea water is pushed into the lagoon only in case of strong north or north-west winds.

Ferrarin et al. (2008) proposed a hydraulic regime based zonation scheme of the Curonian lagoon identifying transitional, intermediate, and stagnant zones. Transitional zone can be referred to northern part of the lagoon, where the influence of Baltic Sea and Nemunas River discharge is the greatest, and the whole southern part of the lagoon – stagnant. However, the zonation scheme can vary seasonally – in summer transitional zones can shrink significantly turning most of the lagoon into the stagnant water body.

The hydrodynamics of the Curonian lagoon was further studied by Umgiesser et al. (2016). The investigation of circulation patterns in the Curonian lagoon for 10 years showed that the variability depends mainly on seasonal changes in hydrographic forcing and on the dominant wind regimes. Winds enhance the water exchange with the Baltic Sea and they contribute to the internal mixing and redistribution of the water masses inside the lagoon. Exchanges between the southern and the northern part of the lagoon are much less impacted by river discharge. However, Nemunas River discharge is the most important factor for water renewal time (WRT), especially in the northern basin. Lowest WRTs are always during winter and spring, and highest during summer. The variability is much lower in the northern basin compared to southern. In the northern part of the lagoon the inflow of the Nemunas is stabilizing the water exchange and in the southern part – the only physical forcing is the meteorological forcing which may vary considerably between different years.

The same study (Umgiesser et al., 2016) investigated also an ice cover impact on WRT. The results showed that the influence is very small, because most of the time when ice is present, it is land locked, therefore completely inhibiting the momentum transfer between the atmosphere and the water. Only during strong winters, when ice cover is lasting for a considerable amount of time, the ice cover will be able to change the WRT, but just inside the lagoon, not the exchanges with the Baltic Sea, however, this does not change the absolute value of the water renewal times.

1.4.2. Ecology

The close relationship of lagoons with terrestrial ecosystem boundaries make these environments very vulnerable to hydrological modifications (freshwater diversions or drainage discharges), water pollution and various other anthropogenic activities (such as dredging and widening of the seaport navigation channel (Gulbinskas et al., 2012)) deeply change the structure of the lagoons' ecological dynamics (Cataudella et al., 2015).

The ecological state of the Curonian lagoon highly depends on the Nemunas River discharge and its water quality. Huge amounts of various nutrients, chemical elements, and biogens are discharged by rivers (Raškauskienė, 2008). Calculations (Žilinskas et al., 2012) show that approximately 80% of total nitrogen and 40% of total phosphorus prevails in the Nemunas River basin.

The strong interactions between not only the physical processes, but also the ecological processes are in the transitional area between the marine and the freshwater environments. The interaction between sea and lagoon (river discharge) flows influences the transport of dissolved and particulate matter (e.g. nutrients) and of organisms within the estuaries, affecting, consequently, the biological activity (e.g. primary production) (Park et al., 2015).

A combination of enclosure nutrient enrichment experiments and historical data analysis (Pilkaitytė et al., 2006) showed that the highest concentrations of nutrients in the Curonian lagoon are in early spring. A rapid decrease in phosphate concentration occurs later in spring. Nitrogen concentration could decrease to analytical zero in May. Due to fast regeneration of phosphorus compounds, phosphate concentrations already begin to increase in early summer. However, mean phosphate levels remained lower than early spring values. Nitrate concentration also tended to increase from midsummer. The lowest concentrations of silica are during spring after the diatom bloom. Silica concentration remains low almost throughout all of the summer and in early autumn it starts to increase again.

Shallow water eutrophication is a natural process. It occurs in intensive algal bloom caused by planktonic algae. High temperatures in summer and other factors, such as slow water exchange and high nutrient concentrations, stimulate the blooming. Eutrophication of the Curonian Lagoon affects all trophic levels and primarily the intensity of phytoplankton development. Phytoplankton production exceeds mineralization of organic matter, which accumulates in water and sediments.

Phytoplankton seasonal succession in the Curonian lagoon occurs in three phases: (1) growth controlled only by ambient physical conditions, (2) growth controlled by phosphorus limited conditions, and (3) growth controlled by nitrogen and light limited conditions. Phytoplankton is the most important autochthonous organic matter producer both in Baltic Sea and in the Curonian lagoon. Its seasonal dynamics is highly related to the seasonal changes in the water quality. The spring bloom, mostly formed of diatoms is not so critical to the water quality because of lower temperatures. However, the summer cyanobacteria bloom is often of higher intensity (up to 20 mgChlA/l) and often cases of a number of water quality problems inside the lagoon – hypoxia, fish kills, cyanotoxins (Pilkaitytė et al., 2006; Razinkovas et al., 2008).

The modelling of ecological processes in the Curonian lagoon is not as profound as investigations of hydrodynamics. Up to 2008 the hydrodynamic models were not linked to biological models, but Zemlys et al. (2008) filled this gap, when the results of calibration of coupled model Shyfem/EUTRO were presented. The model was two dimensional and did not give good results and needed further development, however, it met the objectives set by the researchers – to synthesise the existing knowledge and identify the gaps to be covered for future work.

1.5. Ice cover

Ice begins to form when fresh water is cooled to 0^{o}C and continues to lose heat. The freezing temperature for saline water varies – the higher the concentration of salinity, the lower freezing temperature. Ice cover formation is controlled by variations in heat exchange and mixing, as well as the heat storage capacity of the water body. The initial ice formation can be rather complex with many ice formations and break up events depending on the strength of the heat loss and the wind stress at the surface.

Ice cover has a great impact on the heat balance, mixing characteristics, and water quality. Once the lagoon freezes over, sensible heat loss and evaporation nearly stop, but a strong net loss of heating continues, resulting in more or less steady ice growth during the early winter months. During winter less solar radiation reaches the surface and the atmosphere is colder, thus ice cover reflects more heat also the heat flux from the bottom becomes important in the heat balance, which is negligible during the ice-free period (Martin et al., 1999).

The ice cover not only alters the physical and thermal properties of water body, but it also has ecological consequences. Since there is no exchange with the atmosphere, the oxygen content of the water decreases. Man's impact on ice cover is mainly from release of oxygen consumption substances. All releases from industries and waste water treatment plants and also the increased winter flows in regulated rivers have local effects on the ice cover.

1.5.1. Physical processes

Ice cover affects the lagoon in several ways. First, the amount of solar radiation entering the water body per day is not only at its lowest in the yearly cycle, but it is also further reduced by the formation of ice and snow cover on it. The temperature, which affects all biological and chemical processes, is not much above the freezing point throughout the water column. The layer of ice rests on water at 0C with a transition from 0 to 4 or 5C descending in the water column. Thus, the uppermost layers of water, which are receiving the most light, are at the same time the coldest. When ice forms on the lagoon it seals it from the wind induced movement, thus preventing circulation and the exchange of gases with the atmosphere.

The momentum flux from the atmosphere into the water body depends on various factors such as wind speed, surface layer stability, surface roughness, and sea ice conditions. Roughness changes in response to changing surface waves and variations in the geometry of ice floes and ridges (Martin et al., 2014). Ice cover diminishes mixing leading to stabilization and stratification of the water column. It suspends airborne particles drastically reducing sediment transport, limiting reaeration and other gaseous exchanges (Singh et al., 2011).

Oxygen levels are replenished by the addition of the oxygenated water and transfer of oxygen from the atmosphere. Water motion is primarily responsible for reaeration. When the ice cover blocks the wind stress, there is no motion on the surface, thus oxygenated water can only be get from the water inflow areas.

The light penetration is decreased or blocked by ice and snow, affecting the heat balance, the survival of aquatic organisms (by altering water quality) as well as the timing and energy required for breakup of the ice. Light is a source for heating the water and provides radiation for primary production. Where there is a sufficient light penetration, the algal blooms often occur. In particularly productive water bodies the limited light penetration causes dissolved oxygen depletion. The most significant factor affecting light penetrations is snow. It was found that 3cm of wind paced snow on 28 cm of clear ice reduced radiation transmittance up to 90% (Martin et al., 1999).

Light penetration is dependent on two processes: reflection (or albedo) and absorption. Air-snow interfaces have an albedo ranging from a few percentages to 95%, which means that the most of incoming light is reflected. Albedo ranges for different ice and snow conditions are provided in Table 2 (Martin et al., 1999).

Table 2: Variations in albedo with ice and snow cover (Martin et al., 1999).

Surface condition	Albedo, %
Freshly formed, snow-free, ”black ice”	2
Snow free ice with cracks, bubbles or previously melted snow on top that has refrozen	40-50
Freshly fallen snow	80-95
Old snow or moist wet snow	70-80
Wet snow	60-70
Slushy, grey melted snow layer	20-60
Completely wet top surface (water ponding)	5

The light that is not reflected can penetrate to the water column or be absorbed. In doing so the solar radiation heats the interior of the ice and the water column bellow it.

1.5.2. Dissolved oxygen

Non-compound oxygen, or free oxygen (O_2), is oxygen that is not bonded to any other element. Dissolved oxygen (DO) is the presence of these free O_2 molecules within water. Oxygen is needed for many forms of aquatic organisms: fish, plants, bacteria, etc. Bottom-dwelling microbes are not affected by DO changes as much as fish or plants. If all the oxygen at their water level gets used up, bacteria will start using nitrate to decompose organic matter (denitrification). If all of the nitrogen is used, they will begin reducing sulphate. If organic matter accumulates faster than it decomposes, sediment at the bottom of a lake becomes enriched by the organic material (Kemker, 2013). However an excessive amount of organic matter becomes a pollutant.

The amount of oxygen that is dissolved in the water is called oxygen saturation. In a stable, unstratified water body, the oxygen saturation is 100%, which means that water holds as much DO as it can in equilibrium (the percentage of gas in the water equivalent to the percentage of that gas in the atmosphere). The absorption of gas is accelerated by wind induced mixing, surface roughness and other sources of aeration. In deeper water levels DO can remain below 100% due to the stratification, respiration of aquatic organisms and microbial decomposition (Kemker, 2013).

DO saturation of over 100% (supersaturation) can occur because of the rapid reaeration (hydro power dams and large waterfalls), temperature changes (decreased water temperature increases oxygen solubility) and production of pure oxygen by photosynthetically active organisms (during the day in photosynthetically active water bodies).

DO levels are influenced by temperature and salinity. The oxygen's ability to dissolve in water decreases as the water's temperature and salinity increase. At the same temperature saltwater holds about 20% less dissolved oxygen than freshwater (Kemker, 2013). The initial conditions of water temperature are very important after the instance of freezing – the colder the water is after the autumn mixing, the more oxygen in contains.

Freshwater systems are more prone to hypoxia (DO saturation is 1-30%) and anoxia (DO saturation is <1%). Hypoxia refers to low oxygen concentration in the water. This might be a result of stratification of the water column, which occurs when less dense freshwater from an estuary mixes with heavier seawater. Hypoxic conditions can be reached in the lower layer of the water body where the dissolved oxygen concentration is the lowest compared to other layers closer to the surface, where the wind induced mixing is strongest (higher DO concentration). Hypoxia usually occurs as a result of human induced factors, especially nutrient pollution. Coastal areas with seasonal stratification tend to be highly sensitive to anthropogenic activities related to organic and nutrient enrichment which leads to eutrophication of freshwater and marine systems. A significant decrease of DO usually occur during the summer time with high temperatures in rich in nutrients and highly productive eutrophic water bodies (Richard et al., 2009).

At the air-water interface oxygen diffuses to the water directly from the atmosphere. The mixing of surface waters by wind and breaking waves increases the rate at which oxygen from the atmosphere can be dissolved into the water. For this the wind stress induced turbulence and mixing is crucial. The flowing water is richer in DO concentration than stagnant water, because of the water renewal at the surface – oxygen-rich water is replaced by the water that has less DO. During the ice cover period the wind is blocked by ice, thus there is no wind stress on the surface of the water body and the DO concentration decreases.

Without the aeration from the atmosphere, oxygen is also produced as a waste product of photosynthesis by plants, like phytoplankton, and consumed during respiration and decomposition.

Photosynthesis occurs only during daylight time, because it requires light, but the loss of oxygen through respiration and decomposition occurs all day. Thus the variations of oxygen level can be observed even daily. During the ice cover period the light cannot fully penetrate down to the water column, thus there is no (or not enough) light to allow photosynthesis and this affects the phytoplankton – reduced illumination limits its growth rates.

Water body also gets oxygen from inflow of oxygen rich water. In the Curonian lagoon water flows from rivers, streams and the Baltic Sea. The river waters are moving fast and this helps oxygen to dissolve from the atmosphere, although this running water can be large nutrient inputs. During winter it is important to ensure that no additional anthropogenic oxygen-depleting sources are discharged into the water system.

Dissolved oxygen levels have a significant impact on organisms in the water body, thus it is a very good water quality indicator. DO concentration and impact of its fluctuations, relation with flows and temperature and etc. are interesting topics for studying river (Wehmeyer et al., 2011), lake (Antonopoulos et al., 2003), estuary and coastal water (Nezlin et al., 2009; O'Boyle et al., 2009), and sea (Kress et al., 2001) ecosystems.

In the Curonian lagoon oxygen concentration fluctuates spatially and temporally (both diurnally and seasonally). Low concentrations down to 1.8 mg/l were found during the ice cover period and local anoxia may take place during the cyanobacteria "blooms" at night. (Zemlys et al., 2008). DO concentration in the Curonian lagoon was studied by Zilius et al. (2013). However, the study was targeted on the chlorophyll a concentration influence on DO and the analysed measurements (*in situ* and satellite) were of the period without the ice cover.

1.5.4. Ice cover in the Curonian lagoon

Curonian lagoon is shallow and freshwater body, thus 10-70 cm thick ice cover forms every year. On average, it forms in the beginning of December and about 12 days after the formation of ice the lagoon freezes. Because of the influence of saline water and inflow from the Nemunas river mouth, more turbid northern part of the lagoon freezes later. In spring ice breakage starts on average in the end of March. The breakage starts in the northern part of the lagoon and in Nemunas watershed. The ice is completely melted 6-13 days after the breakage. The average period of the ice season is 110 days (the shortest 12 the longest 169 days). The thickness of the ice cover is not the same throughout the winter season. Usually the ice cover forms and decomposes 2 or more times (Žilinskas et al., 2012; Schiewer, 2008).

Due to the climate change the winters are expected to get warmer thus the ice cover period in the lagoon will get shorter following with the increased probability of thaws and even more unstable ice cover. This can already be observed in Nida, where the number of days with ice phenomena decreased by 50% (comparing periods of 1961–1975 and 1991–2005). This may lead to coastal erosion, because ice on the coast is a natural breakwater, protecting the shore from winter storms, and prevents the deflation of the sand (Bukantis et al., 2007).

However, on the other hand, when the drifting of the ice begins, ice heap has a great impact of abrasion on the shoreline, which depends on the mass of the ice and direction and speed of wind and water currents. The ice drifts affects water level fluctuations in the lagoon by damming the rivers, thus significantly increasing flooded land areas and making partially or sometimes even completely change the riverbed. In the north of the lagoon (usually at the Kiaulės nugara island) floe clutters causes an increase of the overall water level, reducing the outflow into the sea.

Ice cover has strong effects on the physical, chemical and biological characteristics of the Curonian lagoon. An analysis of the changes in physical processes in the Curonian Lagoon was done by Rukšėnienė et al. (2015). The main purpose of this study was to analyse changes in the ice phenomena formation, their dependency on the related changes in the air temperature, sea surface temperature and water salinity by employing spatiotemporal analysis of hydrophysical data using linear models (multivariate linear regression and regression kriging).

It is clear that ice cover plays a major role in modulating the physical forcing of the lagoon. However, there are no investigations of the ice cover impact on ecological processes, such as ice cover influence on dissolved oxygen, thus one of the aims of this work is dedicated to studying physical limitations forcing the change of concentration and saturation of this substance.

2. MATERIALS AND METHODS

2.1. Visualisation system

2.1.1. Requirements

The visualisation system must have the following characteristics:

- Quick and easy visualisation of state (hydrodynamic and biogeochemical) and derived variables' time series and depth profiles (3D case) in the form of graphs at given points (stations) of the modelling domain.
- The ability to visualise time series of diagnostic biogeochemical variables.
- The ability to visualise time series of state (derived) biogeochemical variables for interactively given nodes of the computational grid.
- The ability to compare results of several model simulations. In case of 3D, the system has to be capable to compare all the layers, their average, and top and bottom layers. Additionally system has to provide the ability to plot differences between two simulations.
- The ability to calculate statistical estimates (RMSE, mean, standard deviation, min, max) of measurement data and model simulation results.
- The ability to select a graphic file format from several popular formats (png, jpg, tiff, and etc.) and to select the dimensions of the graph.
- To increase the high-speed of the visualisation by using parallel computations.

2.1.2. Development tools

The visualisation system was developed using GNU Octave software on Linux Red Hat Enterprise operation system running on 64-core SGI UV2000 server owned by an Open Access Centre for Marine Research of Klaipėda University.

Octave is a high-level interpreted language, primarily intended for numerical computations and their visualisation. It provides capabilities for the numerical solution of linear and nonlinear problems, and for performing other numerical experiments. It also provides extensive graphics capabilities for data visualization and manipulation. Octave is usually used through its interactive command line interface, but it can also be used to write non-interactive programs. The Octave language is similar to Matlab, thus most of the programs are easily portable. One of Octave's most important features is that it is free and open source software. However it may be slow in some cases (e.g file reading), but regarding the visualisation program it is somewhat solved with parallelisation of the processes.

Octave's *parallel* package is used to increase the performance of the developed visualisation system. The package contains functions for explicit local parallel execution, and functions for parallel execution over a cluster of machines, possibly combined with local parallel execution at each machine of the cluster. Explicit local parallel execution, with the intent to exploit more than one local processor (core), is performed by calling a user-defined function in parallel with several different arguments (parallel package documentation).

Earlier versions of Octave provided plotting through the use of *gnuplot*, which is a portable command-line driven graphing utility. This capability is still available. But, a newer plotting capability is provided by access to OpenGL (a cross-language, cross-platform application programming interface for rendering 2D and 3D vector graphics). Currently there are available two additional graphic libraries: FLTK and Qt, which can be used for working with the visualisation system.

2.1.3. Development methods

The parallel computations are used to achieve a high speed of the visualisation system. Parallel computing is a type of computing architecture in which several processors execute computations simultaneously (www.techopedia.com). This method is of great use for performing large computations by dividing the workload between several processors, all of which performs the computations at the same time. There are many forms of parallelism - bit-level, instructional level, data, task and etc. (Oshana, 2016).

Data parallelism was used for the development of the visualisation system. Using this approach the same task runs on different data in parallel. Task in this case is plotting of the graphs and calculation of statistics. Parallelisation in the visualisation system is implemented by using the command *parcellfun* provided by the Octave's *parallel* package. It evaluates specified function for multiple argument sets using multiple processes. The argument sets have to be cell arrays of equal size. When the station is indicated to be visualised, then parallel computations are applied to processing biogeochemical and hydrodynamical variables' data.

Performance of the visualisation system (for plotting time series of 54 biogeochemical variables of 2D simulation) is shown in figure 5. The time taken to plot the graphs increases exponentially as the number of used cores decreases. In figure 6 the drop of time required to plot all the graphs is noticeable. The maximum performance is reached when all the variables are plotted on separate cores.

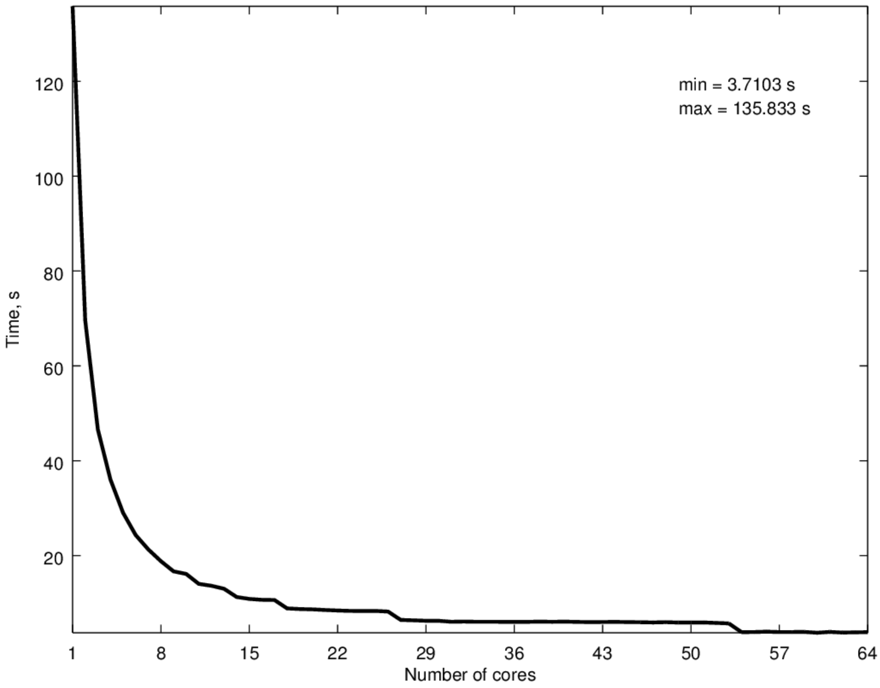

Figure 5: Performance of visualisation system.

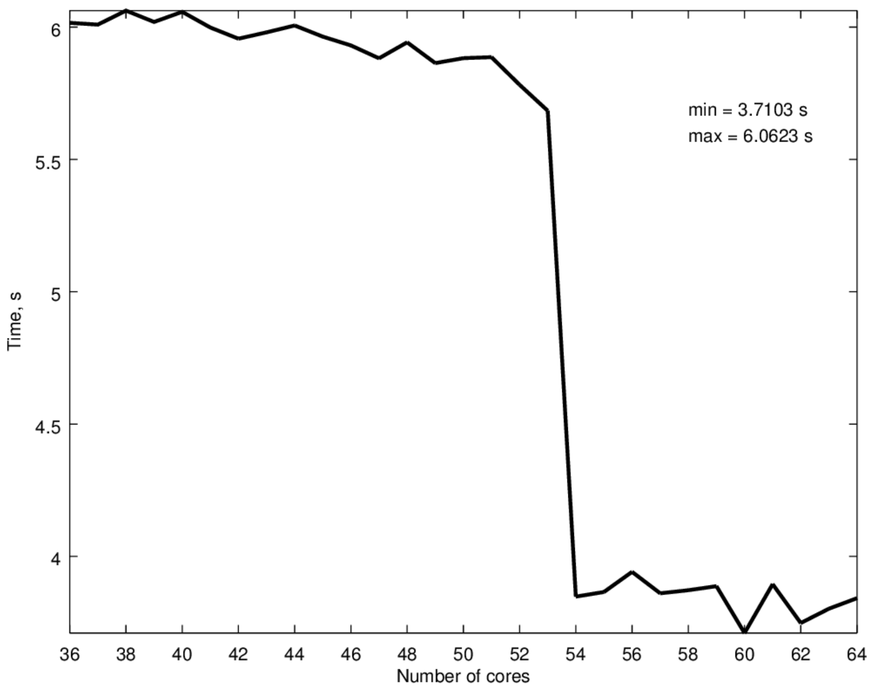

Figure 6: Maximum performance of visualisation system.

2.2. Numerical model

2.2.1. Data

All the used data are of the period of 2009. There are five open boundaries in the study domain – Baltic Sea, Nemunas, Minija, Matrosovka and Deima Rivers. Open sea boundary water temperature, salinity and water levels were obtained by spatial interpolation of 1 nautical mile spatial resolution forecasts by operational hydrodynamic model HIROMB (http:www.hiromb.org) provided by the Swedish Meteorological and Hydrological Institute. Daily river discharges were provided by Lithuanian hydro-meteorological service. The freshwater input into the Curonian Lagoon was considered as the sum of the discharge of its major rivers (Nemunas near Smalininkai, Minija, Šešupė, Jūra, Šešuvis, Deima) (Umgiesser et al., 2016).

Ecological open sea boundary condition is prepared using Baltic Sea stations data of the State monitoring carried out by Marine Research Department of the Environmental Protection Agency. Water quality input is provided by Open Access Centre for Marine Research (previously named CORPI - Coastal Research and Planning Institute).

Meteorological forcing fields were obtained by forecasts of the operational meteorological model HIRLAM (http:www.hirlam.org) provided by the Lithuania hydro-meteorological service.

Ice data were provided by the Marine Research Department of the Environment Protection Agency. Ice thickness and ice concentration have been measured daily at four points inside the lagoon (Nida, Ventė, Juodkrantė and Uostadvaris). In the study period (year 2009) the full freezing observed in these stations occurred approximately at the same day – the 5th of January. Till the end of the month the full freezing stayed in the Nida and Ventė, it lasted the whole month of February and started to break in the beginning of March – first in Ventė, then in Nida. In other stations the variation of ice cover was visible. The longest continuous full freezing periods were observed in January in Uostadvaris and in February in Juodkrantė. In March there were no full freezing in these stations, mostly drifting ice and ice along the shore. Ice cover observations are shown in Table 3.

Table 3: Observations of ice cover.

Months	Stations	Number of days				
		Without ice	With coastal and drifting ice	With drifting ice	With coastal ice	Full freezing
January	Nida	0	0	4	27	27
	Juodkrantė	1	7	3	20	13
	Ventė	0	0	4	27	27
	Uostadvaris	0	0	2	29	23
February	Nida	0	0	0	28	28
	Juodkrantė	0	1	0	28	26
	Ventė	0	0	0	28	28
	Uostadvaris	0	0	0	28	5
March	Nida	14	1	2	16	9
	Juodkrantė	20	11	0	11	0
	Ventė	10	3	13	9	5
	Uostadvaris	16	0	3	12	0

In the model the ice concentration is a value between 0 (ice free) and 1 (fully ice covered) and can be a fractional number. Due to the shallowness of the lagoon, freezing (and melting) happens in a short period (days) and once the lagoon is frozen the ice is land locked, not transmitting any wind stress to the underlying water. Although in reality Klaipėda Strait and Baltic Sea is always ice free, just the sea has been considered without the ice cover for all the simulations (Umgiesser et al., 2016).

2.2.1. The modelling framework

The equations used in the model are vertically integrated shallow water equations in their formulation with water levels and transports:

$$\frac{\partial U}{\partial t} - fV + gH\frac{\partial \zeta}{\partial x} + RU + X = 0$$
$$\frac{\partial V}{\partial t} + fU + gH\frac{\partial \zeta}{\partial y} + RV + Y = 0 \qquad (1)$$
$$\frac{\partial \zeta}{\partial t} + \frac{\partial U}{\partial x} + \frac{\partial V}{\partial y} = 0$$

where ζ – water level,

f – Coriolis parameter,

g – gravitational acceleration,

H – total water depth,

R – friction coefficient ($R = \frac{g\sqrt{u^2+v^2}}{C^2 H}$, where $C = k_s H^{1/6}$ is the Chezy coefficient with k_s being the Strickler coefficient),

U and V – vertically integrated velocities in x and y directions (total or barotropic transports), $U = \int_{-h}^{\zeta} udz$ and $V = \int_{-h}^{\zeta} vdz$ (u,v – current velocities),

X and Y – contain all other terms that may be added to the equations like the wind stress or the nonlinear terms and that need to not be treated implicitly in the time discretization.

At open boundaries the water levels are prescribed. At closed boundaries the normal velocity component is set to zero whereas the tangential velocity is a free parameter (this corresponds to a full slip boundary condition).

Time is integrated using semi-implicit discretisation scheme, which combines the benefits of the implicit and explicit schemes. It is unconditionally stable for any time step (Δt) chosen and allows the two momentum equations to be solved explicitly without solving a linear system. The only equation that has to be solved implicitly is the continuity equation.

The discretized equations (1) are:

$$\frac{U^{n+1}+U^n}{\Delta t}-f\frac{1}{2}(V^{n+1}+V^n)+gH\frac{1}{2}\frac{\partial(\zeta^{n+1}+\zeta^n)}{\partial x}+RU^{n+1}+X=0$$
$$\frac{V^{n+1}+V^n}{\Delta t}+f\frac{1}{2}(U^{n+1}+U^n)+gH\frac{1}{2}\frac{\partial(\zeta^{n+1}+\zeta^n)}{\partial y}+RV^{n+1}+Y=0 \qquad (2)$$
$$\frac{\zeta^{n+1}-\zeta^n}{\Delta t}+\frac{1}{2}\frac{\partial(U^{n+1}+U^n)}{\partial x}+\frac{1}{2}\frac{\partial(V^{n+1}+V^n)}{\partial y}=0$$

With this time discretization the friction term has been formulated fully implicit, X and Y fully explicit and all the other terms have been centered in time.

The spatial derivatives of the equations (2) are expressed by the finite element method, partially modified from the classic formulation, due to avoiding high numerical damping and mass conservation problems, due to the combination of the semi-implicit method with the finite element scheme (Galerkin method). With respect to the original formulation, here the water level and the velocities (transports) are described by using form functions (which have a simple form and can easily be integrated analytically over the domain) of different order, the standard linear form function for the water level but stepwise constant form function for the transports (Umgiesser et al. 2004).

Water level variable ζ anywhere in the domain can be expressed as:

$$\zeta = \zeta_{\mathrm{m}}\varphi_{\mathrm{m}}, \qquad \mathrm{m}=1,\dots,\mathrm{K}$$

where the summation over double indices is assumed, ζ_{m} is the value ζ at node m, φ_{m} the form function associated with node m and the summation runs over all K nodes of the model domain.

The form functions φ_{m} is a continuous piecewise linear functions inside the elements allowing a subdivision of the whole area of interest into small triangular elements specifying the coefficients ζ_{m} at the vertices (nodes) of the triangles. The functions φ_{m} are 1 at node m and 0 at all the other nodes and thus different from 0 only in the triangles containing the node m. An example is given in upper left part of the Figure 7 where the form function for node *i* is shown. The full circle indicates the node where the functions φ_{m} take the value 1 and the hollow circles where they are 0.

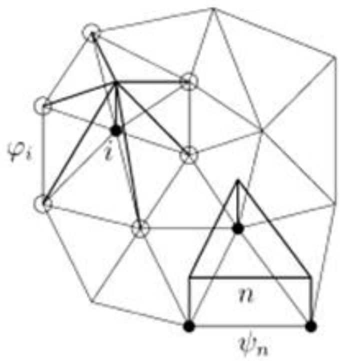

Figure 7: Form functions in the domain.

The transports are expanded over each triangle with piecewise constant (non-continuous) form functions ψ_{n} over the whole domain. The x-component of the transport can be expressed:

$$U = U_n \psi_{\mathrm{n}}, \qquad n = 1, \dots, J$$

where n is now running over all triangles and J is the total number of triangles. An example of ψ_{n} is given in the lower right part of Figure 7. The form function is constant 1 over the whole element, but outside the element – 0. Thus, it is discontinuous at the element borders. This will result in a grid that resembles more a staggered grid (where the unknowns are defined on different locations) often used in finite difference discretization. All the equations of the model, its calibration and validation is thoroughly explained in (Umgiesser et al., 2004) and its 3D implementation in (Zemlys et al., 2013).

The presence of ice is simulated by weighting the wind drag coefficient by the fractional ice concentration. This corresponds to scaling the momentum input through the surface by the area free of ice. Where ice concentration equals 1 the momentum transfer to the sea is inhibited. No ice–ocean stress is considered in the model. Ice concentration is also used to properly calculate the albedo to be used in the heat flux model. However, the model takes into account just the percentage of ice cover, not the thickness of it or the snow cover on top of it. This might be a good approach for momentum (when there is no movement under the ice) and dissolved oxygen (when the ice suspends the water interaction with the atmosphere), but this effect is too strong for light penetration, because it depends on the ice thickness and the presence of snow cover.

Shyfem and AQUABC models are combined together in the code level. The whole water quality module files start with the prefix *aquabc* and the call to it is made through a subroutine call that is done from the main program through an interface *aquabc_II_fem_interface.f*.

2.2.3. Simulation setup

The computational grid of the study area consists of 1309 nodes and 2024 triangular elements (Figure 6). The resolution is finer in the Klaipeda Strait. Also a part of Baltic Sea is included to the grid, thus preventing the disturbances of the computations of exchanges through the Klaipeda Strait area.

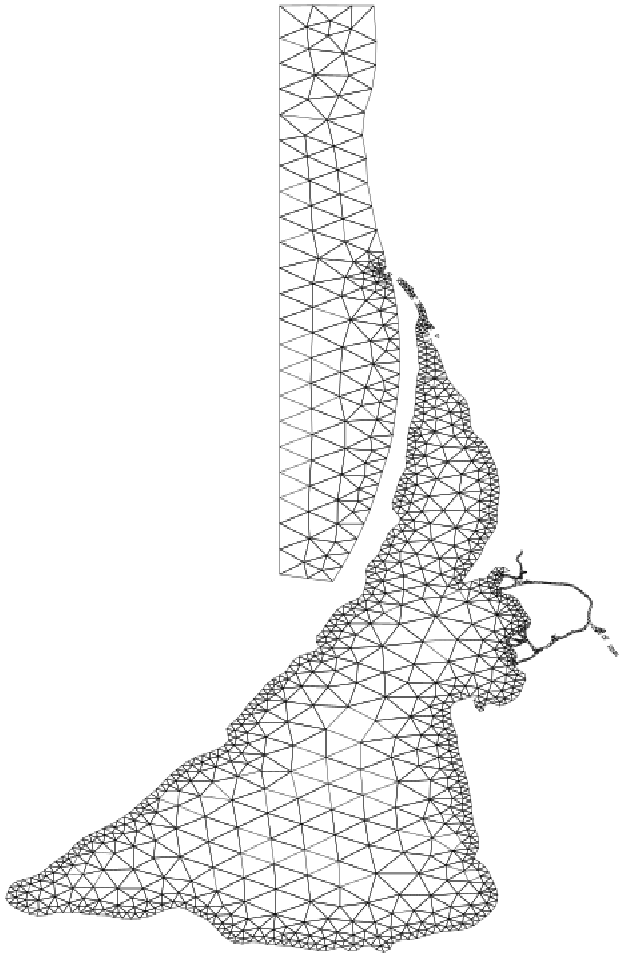

Figure 8: Computational grid.

For investigation of ice cover effect on aeration, five simulations have been carried out:

1. Reference simulation – represents the condition when no ice cover is present during winter period. This is an idealized (base) simulation for investigation of the influence of ice cover and influence of different environmental factors regarding ice. All the other simulations have been compared to it.
2. Natural ice conditions – represents simulation when ice cover is present. In this case all the environmental factors, that ice cover has an impact to (momentum, reaeration, and light), are blocked during ice cover time.
3. Ice conditions with suppressed momentum only – this simulation also has an ice cover present, however, only the momentum influence is blocked in winter, which means that there is no movement of the water due to the wind, but the light penetration and reaeration are considered to be possible.
4. Ice conditions with suppressed reaeration only – ice cover is present, but the ability to exchange gasses between the atmosphere and water is blocked in winter time. Light penetration and momentum – enabled.

5. Ice conditions with suppressed light only – ice cover is present and the ability for light to penetrate through the ice cover is blocked in winter. In this case the momentum and reaeration are considered to be possible.

For investigating the influence of separate environmental factors to dissolved oxygen variability during the ice cover period, suppression of them was achieved by adjusting the variables *aice* (for momentum) in Shyfem code, *alight* (for light) and *aair* (for reaeration) in AQUABC code. They have been set to 0 or 1 (Table 4). The model does not take into account that solar radiation is reduced during the ice cover period; this will be implemented in the new version of the model. The simulations were achieved with four sets of variables (Table 5). All simulations have been carried out for the year of 2009, with the time step of 15 min.

Table 4: Clarification of the variable values.

aice = 0	momentum is not suppressed
aice = 1	momentum is suppressed by ice cover
alight = 0	all light is transmitted
alight = 1	all light is suppressed by ice cover
aair = 0	reaeration is not suppressed by ice cover
aair = 1	reaeration is suppressed by ice cover

Table 5: Simulations' variable sets.

Reference	Suppressed all	Suppressed momentum	Suppressed light	Suppressed reaeration
aice = 0 *alight* = 0 *aair* = 0	*aice* = 1 *alight* = 1 *aair* = 1	*aice* = 1 *alight* = 0 *aair* = 0	*aice* = 0 *alight* = 1 *aair* = 0	*aice* = 0 *alight* = 0 *aair* = 1

Different scenarios of the ice cover effect allow assessing not only the ice impact, but also the influence of separate environmental factors to the variability of substances in the lagoon during ice cover period, and determine which physical effect is the most significant.

3. RESULTS

3.1. Developed visualisation system

Developed visualisation system consists of 8 modules located in files: *visualisation.m* (main program), *plotting_info.m* (module for processing data of biogeochemical model), *plotting_bio.m* (processing state and derived biogeochemical variables), *plotting_dgf.m* (processing diagnostic biogeochemical variables), *comparison.m* (comparison of simulations), *plot_t_s_wl.m* (processing hydrodynamic variables), *sec2datef.pl* (conversion of time values in seconds to dates) and *conv_levels_to_lith.m* (conversion of HIROMB reference water levels calculated by Shyfem to Lithuanian reference water levels). The modular structure of the system is shown in figure 9. The one-way arrows represent the usage of different modules, e.g. *visualisation.m* internally calls the *plotting_info.m*, *sec2datef.pl* and *plot_t_s_wl.m* modules handing them the appropriate data as parameters. The two way arrow represents the connectivity of the modules – handing and receiving appropriate data as parameters.

The visualisation system requires input files: main visualisation parameter file (**.vis* – necessary), Shyfem main configuration file (**.str* – necessary), AQUABC configuration files (**.ctrl* – necessary for visualisation of biogeochemical variables) and hydrodynamic variable and monitoring station file (**.vish* – necessary for visualisation of hydrodynamic variables).

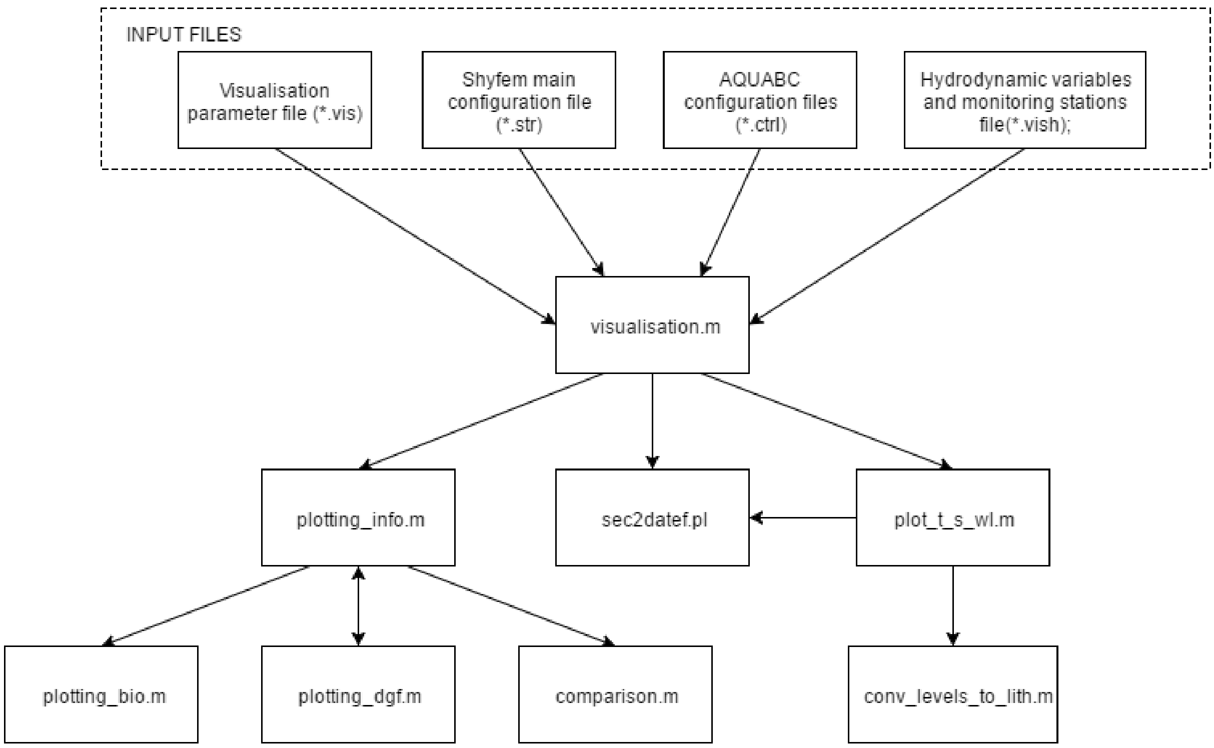

Figure 9: The modular structure of the system.

3.1.1. Execution algorithm

To start plotting graphs or calculating statistics, the visualisation system should be initiated after setting current directory to the simulation directory. After running the program it will request for simulation name, which must match the name of the main configuration Shyfem file (*.*str*) and the simulation name written in its SECTION TITLE.

The main visualisation file (script) is *visualisation.m* (Figure 10). At the beginning of this file there can be changed external program names, currently – *nosextr_node* and *splitets*. They are used for extracting interactively given node state (derived) biogeochemical variable and hydrodynamic variable time series files from model's binary output files.

When a function is called, Octave searches a list of directories for a file that contains the function declaration. This list of directories is known as the load path. By default the load path contains a list of directories distributed with Octave and additionally the current working directory. Thus the path to directory, where are stored the files of visualisation system, has to be added at the beginning of the file *visualisation.m*.

This main visualisation file reads and obtains needed information from main visualisation and Shyfem configuration files. Then there are three main sections for data processing:

1. Plotting time series and depth profiles of state (derived) biogeochemical variables, time series of diagnostic variables, comparison of simulations; computing statistics of state (derived) biogeochemical variables.
2. Plotting time series of state (derived) biogeochemical variables for interactively given nodes of the computational grid.
3. Plotting time series and depth profiles of hydrodynamic variables; computing statistics of hydrodynamic variables.

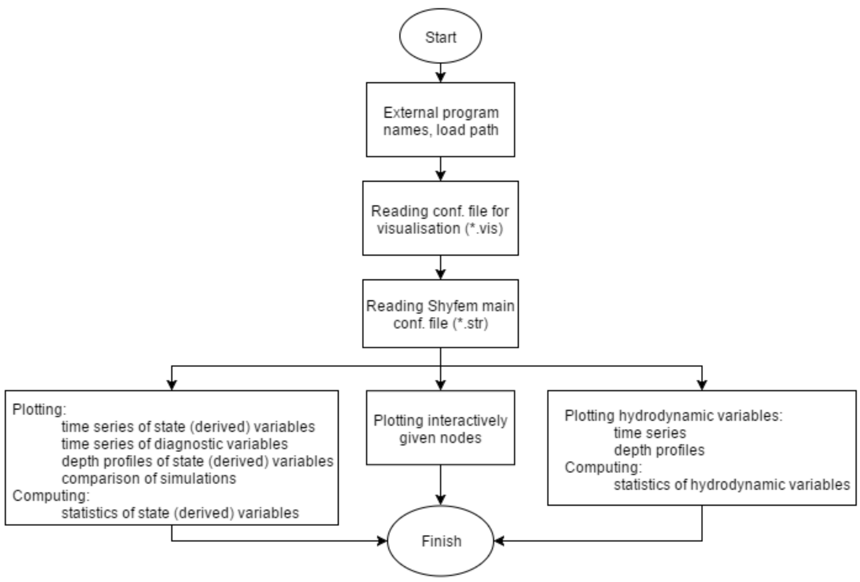

Figure 10: Structure of the file *visualisation.m*.

The first section is used by function *plotting_info.m* (Figure 11), which gathers required information for visualising biogeochemical variables. The first step in this function is reading the input file(s) – AQUABC configuration files for water column and/or sediments. There are sections containing information on state (derived) biogeochemical variable, station and diagnostic variable visualisation, and all the data file names, which are derived after the simulation of the model.

In the figure 11 there are shown two branches. One of them is for processing state (derived) biogeochemical variable data and the other is for plotting the diagnostic biogeochemical variable data. These two branches internally use additional functions for parallel plotting (or calculations of statistics).

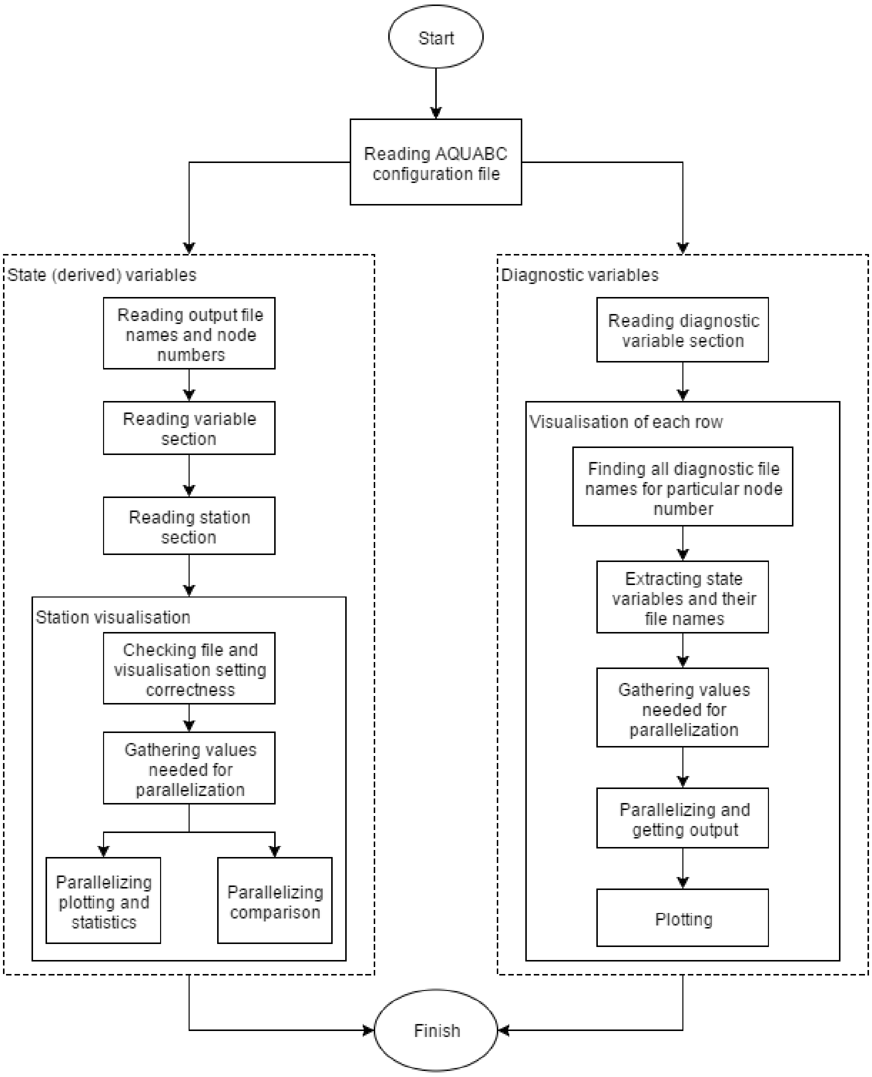

Figure 11: Structure of the file *plotting_info.m*.

In case of processing the state (derived) biogeochemical variable data – the first (left) branch is used. It requires information from AQUABC configuration input file, such as simulation output file names and their node (station) numbers, visualisation settings in variable and station sections. This information has to be stored in cell arrays for each column of each section.

After gathering the information required for visualisation, the loop is set for the cell array of stations holding the indicator for visualisation. Inside the loop there is checked the file and visualisation setting correctness – correct number of columns in the station file (compared to the number of variables defined in the variable section in the AQUABC configuration file) and correct date for depth profiles respectively. Afterwards, the additional parameters, such as figures directory, file format, picture dimensions and etc., have to be stored into cell arrays with dimensions matching the number of the variables. When all the data is gathered, it is sent to a function responsible for parallelisation of computations.

This branch has two options for parallelisation – processing state (derived) biogeochemical variables and plotting the comparison of simulations.

The first one is called *plotting_bio.m* (Figure 12). This function provides graphs and statistical analysis files of state (derived) biogeochemical variables. Depending on the simulation type (2D or 3D) the data is processed according to the visualisation parameter `vis_var` (and other variables that depend on this choice), that has been set in the main visualisation parameter file **.vis*, for state (derived) biogeochemical variables the options are: plotting time series, depth profile (in case of 3D simulation) or computation of statistics.

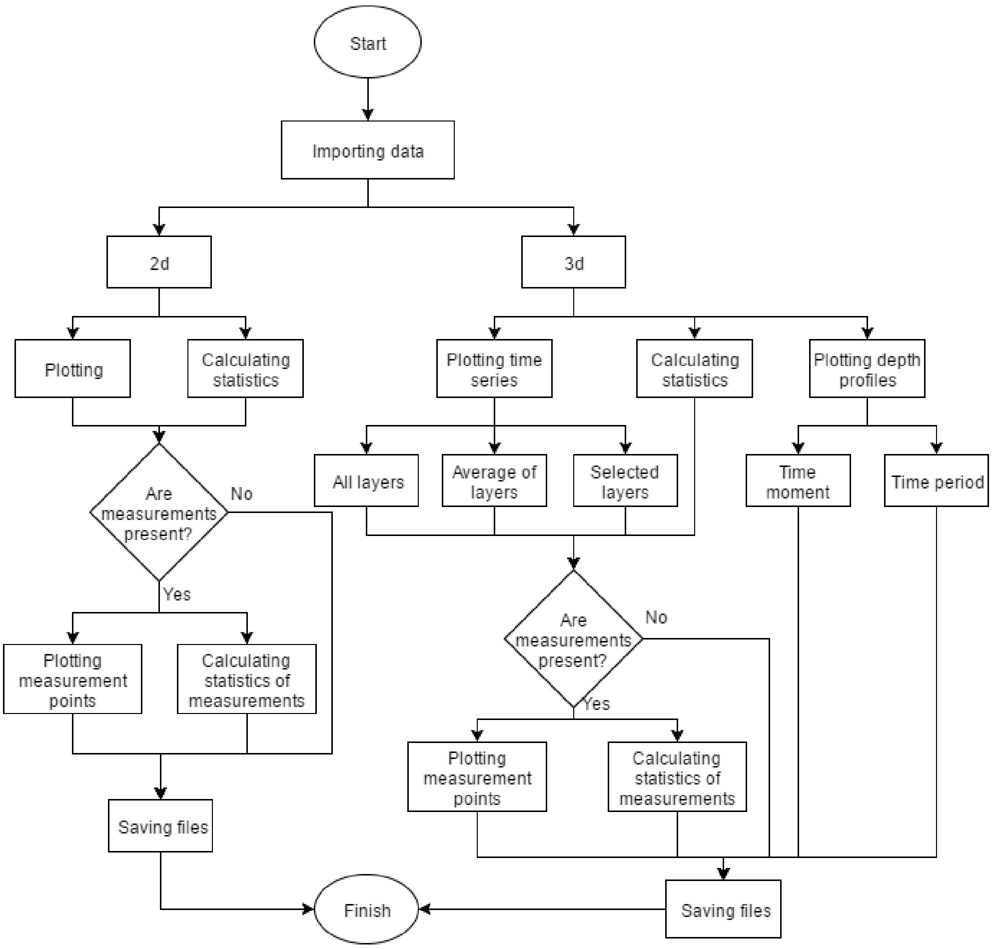

Figure 12: Structure of the file *plotting_bio.m*.

The other case in the first (left) branch (Figure 11) is responsible for parallelisation of comparisons of simulations (Figure 13). The simulations have to be specified in the parameter `comp` in the PATH SECTION of the main visualisation parameter input file (**.vis*). At first there are plotted main simulation results, according to simulation type (2D or 3D) and visualisation type (all layers, average of layers, top and bottom layers or differences of two simulations), then the comparison simulation(s) is plotted on the same graph with the same setup.

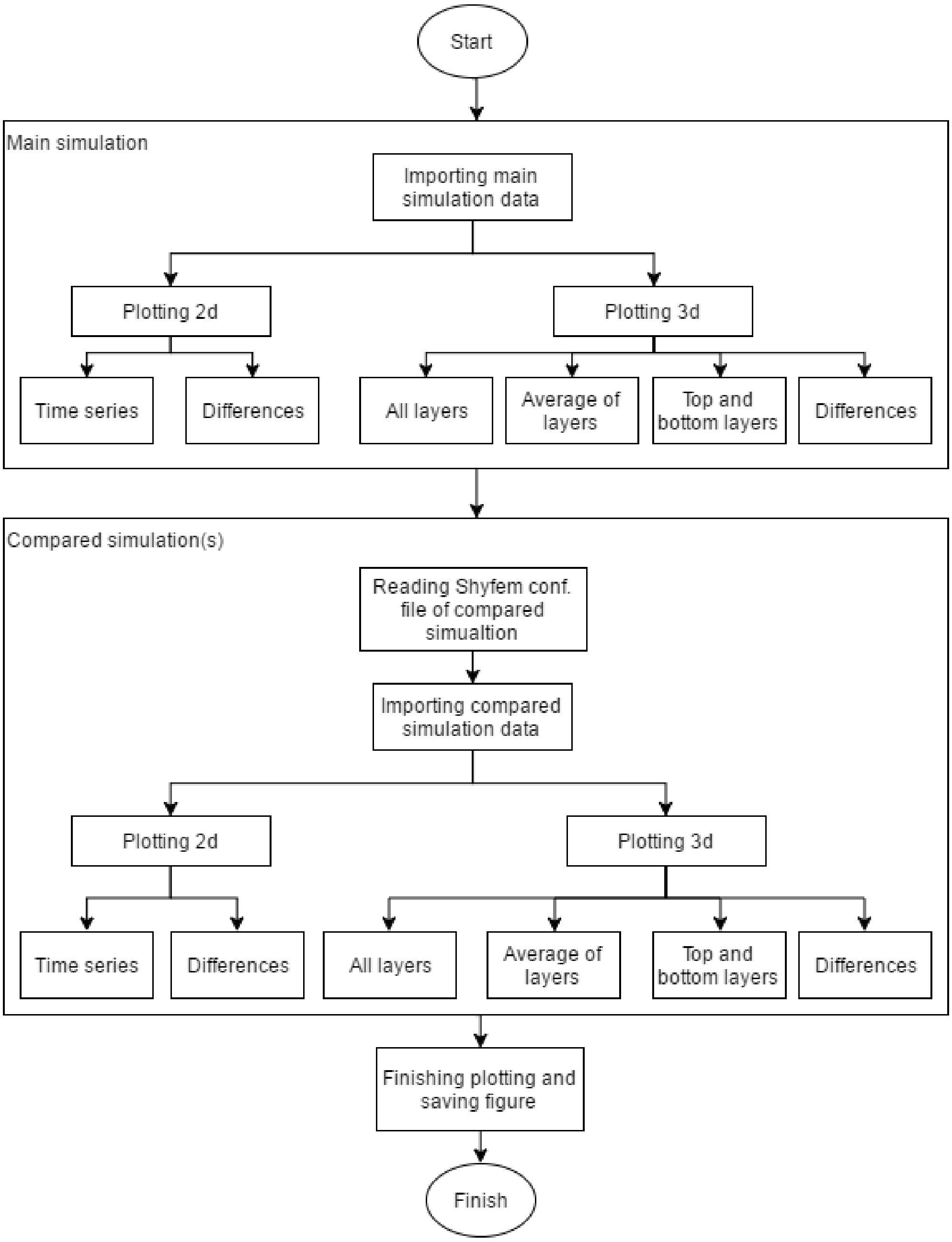

Figure 13: Structure of the file *comparison.m*.

The other branch (on the right) in the file *plotting_info.m* (Figure 11) is for plotting diagnostic variables. After gathering all the required information into cells it is sent to a function *plotting_dgf.m* (Figure 14) responsible for parallelisation of each state biogeochemical variable defined in section for plotting diagnostic variables in AQUABC configuration file. On one graph there can be plotted more than one state variable's diagnostic variable (more about this in section *3.1.2.3. AQUABC configuration files*), thus the parallelisation is set for faster generation of an output for plotting them.

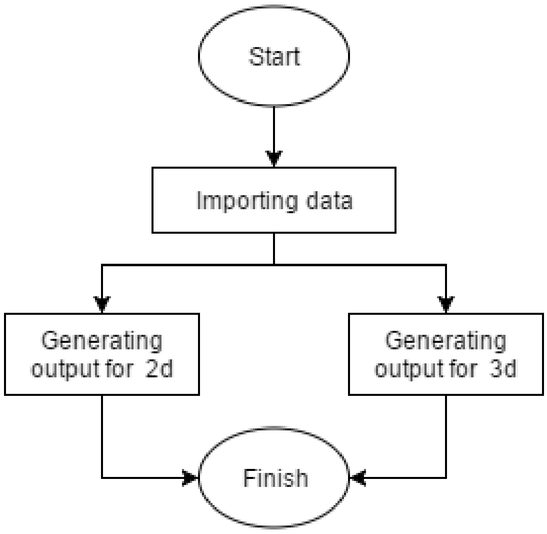

Figure 14: Structure of the file *plotting_dgf.m*.

The second section for data processing in main visualisation file (*visualisation.m*) is for plotting time series of state (derived) biogeochemical variables for interactively given nodes of the computational grid (Figure 15). When this option is chosen in visualisation parameter file **.vis* (parameter `vis_var`), then at first there are created two text files:

1. *.memory* – with simulation name and link to used computational grid,
2. *nodes.txt* – with environment (sediments or water column) and node number.

For creation of file *nodes.txt*, the system requires the user to interactively input the node number to visualise. The created text files are needed for running program *nosextr_node*, which extracts data files from the model's binary output files (**.bbs* for bottom sediments and **.bwc* for water column) for all variables (separate file for each one) of the specified node of the computational grid. After the file extraction, the system requires the user to interactively input the variable number for its visualisation, which depends on the simulation type (2D or 3D) and additional requirements that have to be set in the main visualisation parameter file.

After plotting one variable given interactively by the user, the system displays a message requiring to specify (input *yes* or *no*) if the plotting is finished or other variable of the same node has to be visualised. This message is repeated until the negative answer is received, after which the same message is presented for node visualisation – request to specify if another interactively given node has to be visualised.

When all given nodes and variables are plotted all the intermediate files are deleted, so there are no additional files left in the simulation directory.

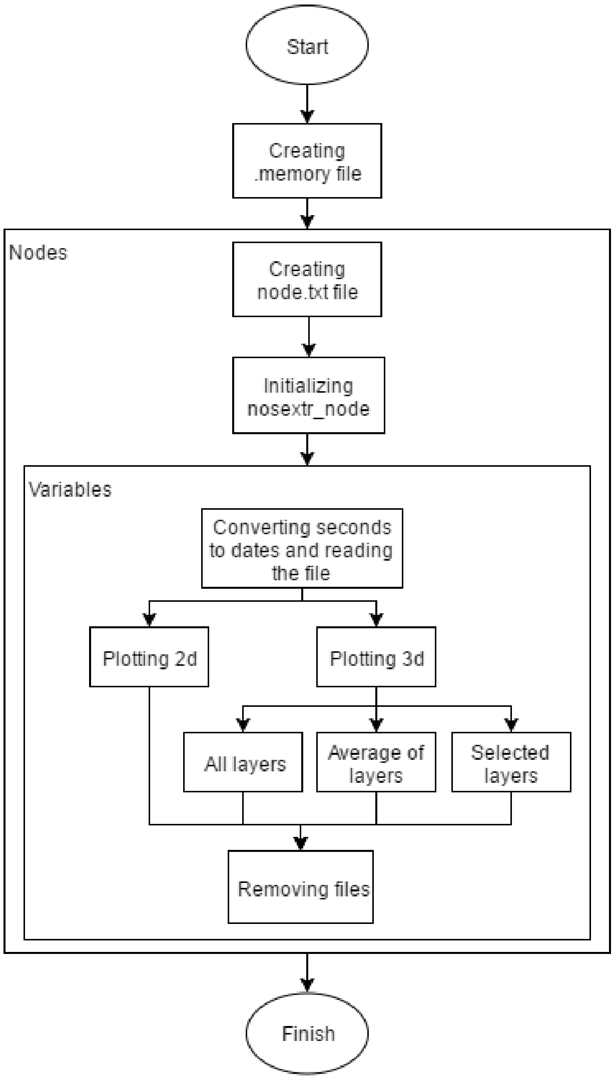

Figure 15: Section for plotting interactively given nodes.

The last data processing section in the main visualisation file (*visualisation.m*) is for plotting hydrodynamic variables' (temperature, salinity and water level) time series or depth profiles, or computing statistics of these variables (Figure 16). In this section there is also used previously mentioned program *nosextr_node*. At first there is created a *.memory* file for it. Then the hydrodynamic variable and monitoring station file (**.vish*) is read, which contains all the node numbers that have to be visualised.

There are two separate parts of this section:

1. Plotting or calculating statistics for temperature and salinity – in order the program *nosextr_node* would work there is created a text file *node.txt* (with the node number specified in the **.vish* input file). After gathering all the needed information for parallel computations, it is stored into cell arrays and then initiated parallelisation. After everything is plotted the intermediate files are removed.

2. Plotting or calculating statistics for water level – for extracting water level data, there is used a program called *splitets*, which extracts water level data files from numerical model's binary

hydrodynamic data output files (*.*ets*). After initiating it and gathering all the necessary information for parallelisation, the same procedure is done as to temperature and salinity.

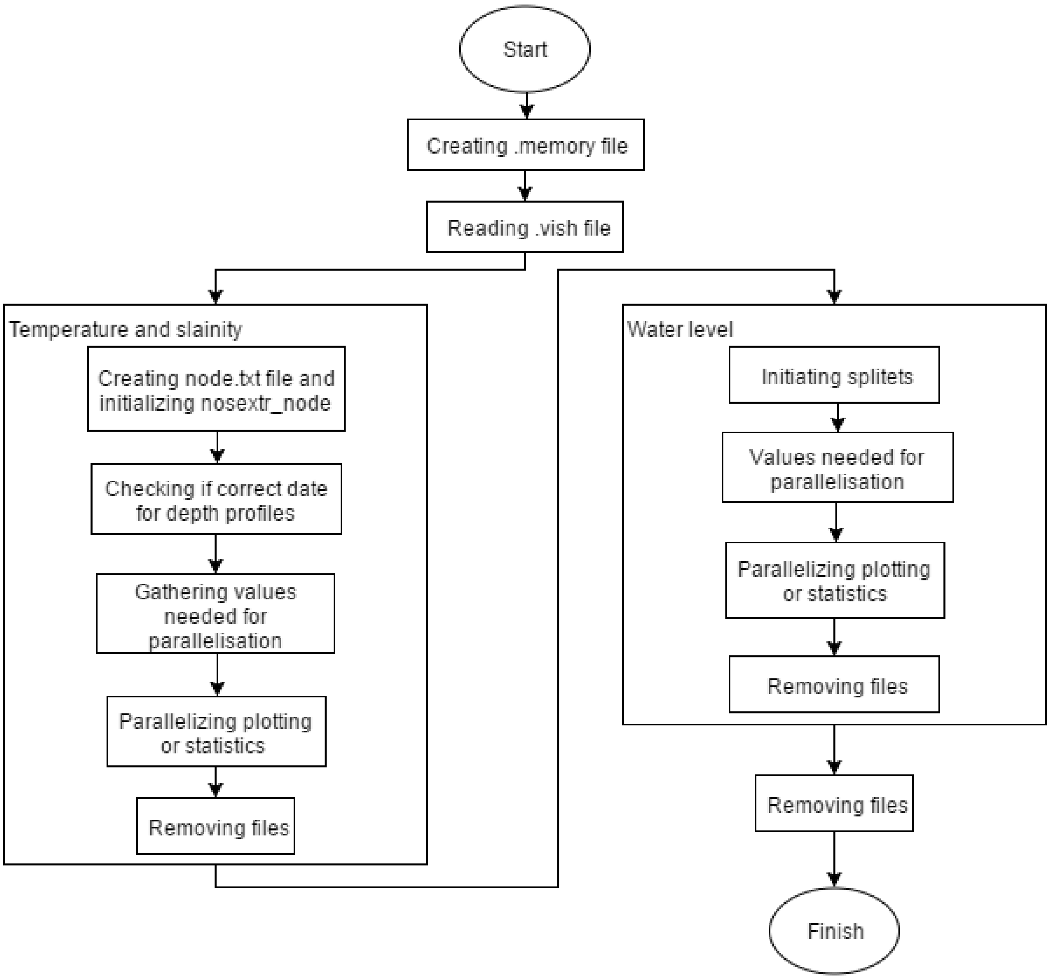

Figure 16: Section for plotting or calculating statistics for hydrodynamic variables.

Both sections (for visualising hydrodynamical variables) mentioned above use function *plot_t_s_wl.m* for parallelisation (Figure 17). The first step in this function is file conversion – the seconds' column in the data file is converted to dates. If this function is used for processing water level data then additionally the HIROMB reference levels calculated by Shyfem are converted to Lithuanian reference levels.

When the data is imported, then it can be plotted or calculated statistics of it. For plotting there are two options: time series or depth profiles (except water level), which have their own additional parameters in the main visualisation input file (*.*vis*), which define the processing.

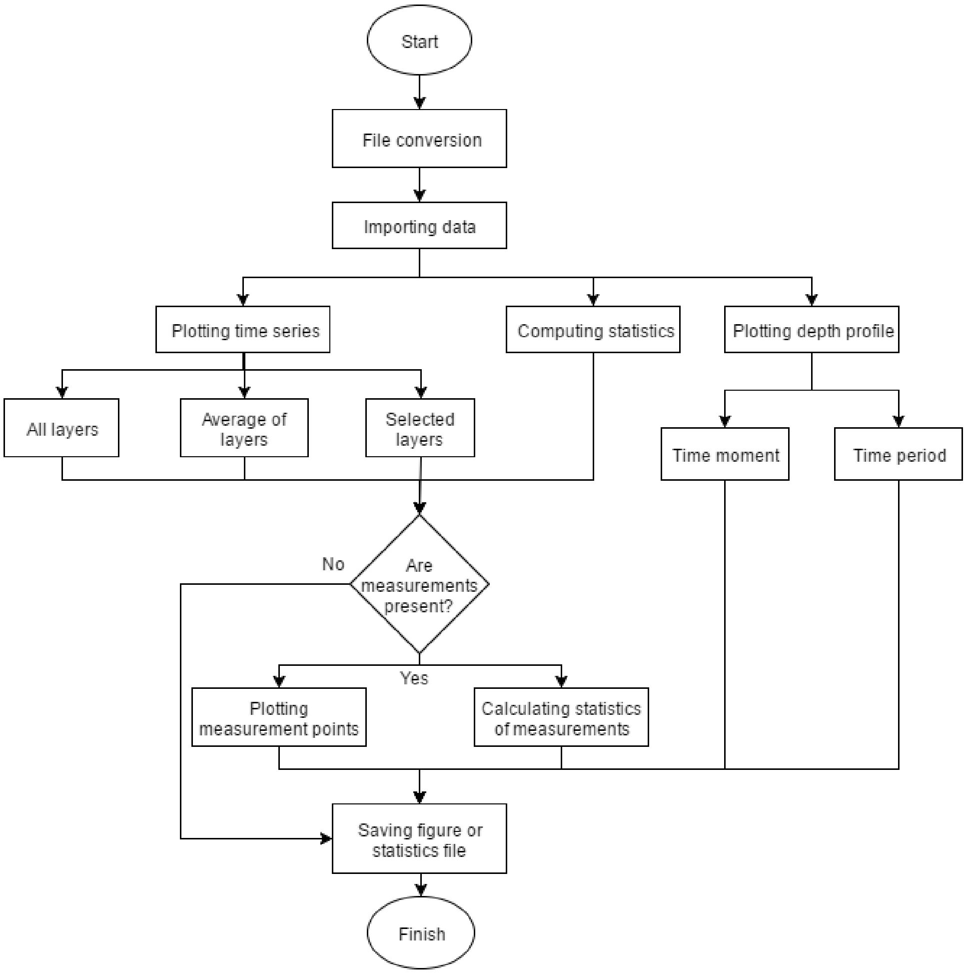

Figure 17: Structure of the file *plotting_t_s_wl.m*.

3.1.2. Input files

3.1.2.1. Visualisation parameter file

In this input file there is a wide range of parameters concerning the design of the graphs, visualisation type, directories for saving figures and performance of the program. The name of this parameter file must match the name of Shyfem main configuration file (**.str*) and must have the extension *vis*.

Visualisation parameter file has four sections: GRAPHICS, WHAT TO DO, PATH and PERFORMANCE. In these sections all of the visualisation configuration variables should be given in separate lines and their values have to be written after the equality sign as strings (in quotation marks) following by semicolon (`variable_name = 'value';`).

The set of parameters concerning the design of the graphs and etc. are in the GRAPHICS SECTION. There are four variables (three of them have set default values):

- `g_toolkit` is a variable for specifying the graphics toolkit. Currently available three toolkits: fltk, qt and gnuplot.

- `fform` defines the file format of the figure. Possible options are: png, jpg, pdf, ps2, psc, psc2, eps2, epsc2, epslatex, pdflatex, tiff, svg. If this value is not entered or it is incorrect, then the default value is set to png.
- `unit` variable defines units of picture measurements. Possible options: pixels (default), inches, centimetres, points.
- `size` is a variable for setting the size of the picture, which is the ratio between width and height. These values have to be set accordingly to units (`unit`) value. Default is set to 600:420 (pixels).

All the visualisation options are in WHAT TO DO SECTION. The main parameter of this section is '`vis_var`'. It has nine possible options (examples are available in the appendix):

1 – time series graphs of state (derived) biogeochemical variables for monitoring stations;

2 – time series graphs of diagnostic biogeochemical variables for monitoring stations;

3 – time series graphs of state (derived) biogeochemical variables for any interactively given node of the computational grid;

4 – depth profile graphs of state (derived) biogeochemical variables;

5 – time series graphs of hydrodynamic variables (temperature, salinity and water level) for monitoring stations;

6 – depth profile graphs of hydrodynamic variables (temperature and salinity) for monitoring stations;

7 – comparison graphs of time series of state (derived) biogeochemical variables for two (or more) simulations for monitoring stations;

8 – statistical analysis for state (derived) biogeochemical variables;

9 – statistical analysis for hydrodynamic variables (temperature, salinity, and water level).

Parameter '`vis`' in the WHAT TO DO SECTION gives an option to define what environment to visualise for state (derived) biogeochemical variables. By default it is '`all`', other options are to plot graphs just for sediments ('`sed`') or just for water column ('`wc`').

Parameter '`layerplot`' in this section allows to choose which layer(s) to visualise (for plotting time series). This option is applicable for both – biogeochemical and hydrodynamic variables. There are three options:

- value of ‘1’ allows visualising all the layers (this is a default value);
- value of ‘2’ enables to visualise an average of all layers;
- the third option allows to choose which layers have to be visualised. It has to start with number three (related to the third option) and a dash: 3-, then follows the numbers of layers

or an interval of layers (e.g. 1:7 means to plot layers from 1 to 7) separated by commas. For example `layerplot = '3-1,2,5:7'` means to plot layers 1, 2, and from 5 to 7.

Parameters '`from`' and '`to`' (in the same WHAT TO DO SECTION) indicates the averaging time period for plotting depth profiles. It should match the format of 'yyyymmdd HHMMSS', e.g. '20090525 200000' (date and time separated by whitespace). If a specific time moment for plotting depth profiles is needed, then these parameter values should be equal.

Parameter '`lay`' indicates type (amount) of layers for plotting the comparison of two (or more) simulations. There are four possible options:

1 – all layers (only available for comparing two simulations);

2 – average of layers (default if comparing more than two simulations);

3 – top and bottom layers;

4 – difference of simulations (only available for comparing two simulations: time series of compared simulation are subtracted from the main simulation).

All the required parameters for setting paths to directories for saving figures and specifying the list of simulations for comparison are in PATH SECTION, and they do not have any default values:

- `figuresdirw` is a parameter for setting directory to save figures for water column variables;
- `figuresdirs` is a parameter for setting directory to save figures for sediment variables;
- `figuresdird` is a parameter for setting directory to save figures for diagnostic variables;
- `figuresdirn` is a parameter for setting directory to save figures for individual nodes (entered interactively);
- `figuresdirtsl` is a parameter for setting directory to save figures for hydrodynamic variables;
- `comp` is a parameter for setting a list of simulations to compare. The number of simulations is unlimited. Here has to be written Shyfem main configuration file names with paths for each simulation to be compared except the main. All the simulations must be in quotation marks and all this list has to be in curly brackets.

To increase (or adjust) the performance of the visualisation program, the number of processors to use (parameter `nproc`) can be specified in PERFORMANCE SECTION. Default is set to eight processors.

3.1.2.2. Shyfem main configuration file

This file (*.*str*) determines the behaviour and performance of the model simulation. It contains all the necessary information for the main routine to execute the model. Nearly all parameters that can be given have a default value which is used when it is not listed in the file. The parameters, arrays and data in this file must be given in between certain sections, which have to start with the character `$` followed by a keyword and end with `$end`. The sections are described in (Umgiesser, 2016). Several parameters of four sections of this file are also required for the visualisation system. The information obtained from the Shyfem main configuration file is:

- name of the grid obtained from SECTION TITLE. Visualisation system requires it for plotting hydrodynamic variables and interactively given nodes of the computational domain;
- type of the simulation (2D or 3D) determined in the SECTION LEVEL;
- water level values obtained from SECTION LEVEL for plotting depth profiles and calculating statistics for hydrodynamic and water column biogeochemical variables;
- links to AQUABC configuration files (parameters: `bioaow`, `bioaos`) obtained from SECTION 'NAME'. They are used for plotting biogeochemical variables.
- link to file containing sediment depth values (parameter: `bbs_lev`) obtained from SECTION 'NAME'. It is used for plotting depth profiles and calculating statistics of sediment state (derived) biogeochemical variables;
- node numbers for plotting water levels specified in SECTION EXTRA.

3.1.2.3. AQUABC configuration files

There are two AQUABC configuration files – for sediments and water column. They are required for storing information necessary for saving model results in ASCII format for the defined computational grid node numbers. Additionally, in these files there has to be given all the information about state (derived) biogeochemical variable, station (node) and diagnostic variable visualisation. These three sections should follow the data describing the ASCII output (for sediments and water column).

State (derived) variable section must start with `$state_var` and end with `$end_state_var`. After starting this section in the second row should be written the names of the columns:

- `varno` indicates the number of order. In total this must match the number of the state (derived) biogeochemical variable value columns in the output data file (not including date, time and layer number in case of 3D simulation).

- variable_name column stores the names of the variables. All words of a single variable must be separated with underscore. The program will replace it with whitespace, so in the graph there will be no underscores.
- units specifies the units of the variables. The same underscore rule applies to this as to variable names. If the variable does not have measurement units, then in the units column there has to be placed a dash.
- visualize is an indicator for visualisation (1 – yes, 0 – no). Here it can be chosen which variables have to be visualised.
- min is a minimum value. The data lower than this value will not be present in the graph. If there is no minimum value required, then a dash has to be placed in this column.
- max is a maximum value. The data higher than this value will not be present in the graph. The same dash rule applies to maximum value as to minimum value.

Each row of these columns (apart from $state_var and $end_state_var) should start (or end) with at least one whitespace, because this character is a delimiter of the columns. If the whitespace is not present in any of these required locations, then the data will be merged and the values will be distorted. The same rule of column separation applies for all of the visualisation sections in AQUABC configuration files. An example of model variable section is presented below:

```
$state_var
   no    variable_name      units       visualize     min       max
   1      nutr_NH4_N        mg_N/l          1         0.008     0.073
   2      nutr_NO3_N        mg_N/l          0         0.5        -
   3      nutr_PO4_P        mg_P/l          1          -        0.09
   4      pH                -               1          -         -
$end_state_var
```

The second section that is needed for visualisation of state (derived) biogeochemical variables is stations section. It has to start with $stations and end with $end_stations. After starting this section in the second row there must be written the names of the columns:

- nodes are the node numbers of the computational domain. They have to match simulation time series output information specified in the beginning of AQUABC configuration file.
- station_names are the names of the stations, same underscore rule applies as to names in variable section.
- visualize is an indicator for visualisation (1 – yes, 0 – no). Here it can be chosen which stations have to be visualised.

- `measurements` is an indicator for plotting observed data (1 – yes, 0 – no). If the station does not have it, then this indicator should be 0. Zero should also be when the observed data is present, but it does not have to be visualised.
- `measurement_files` column has links to measurement data files.

An example of model station section is presented below:

```
$stations
   nodes   station_names  visualize   measurements   measurement_files
   2691       STA1S          1            1          /link/to/measurements/file
   2256       STA2N          0            0          /link/to/measurements/file
   2040       STA3V          1            1          /link/to/measurements/file
   2152       STA5J          0            0            -
   2652       STA6J          1            0            -
$end_stations
```

The last section in AQUABC configuration files is for plotting diagnostic variable data. It has to start with `$diagn_var` and end with `$end_diagn_var`. After starting this section in the second row should be written the names of the columns:

- `station_node` is a column for node numbers. They have to match simulation time series output information specified in the beginning of AQUABC configuration file.
- `state_var_layer_and_diagn_var_number` – state variable number, layer number(s) and diagnostic variable number(s), all separated by semicolon. If the simulation is 3D, then several layers can be plotted; their numbers have to be separated by comma or with dash (or a colon), which indicates an interval. For instance 1-3,5 (or 1:3,5) means that there will be plotted layers 1,2,3 and 5. The same principal applies to diagnostic variable numbers. If the simulation is 2D, then it means that there is just one layer, so in the layer part of the column there should be written a number 1. This column can be composed of multiple columns (separated by whitespace), which means that on the same graph there can be plotted more than one state variable. Overall, data on one row will be plotted on one graph.

An example of diagnostic variable section is presented below:

```
$diagn_var
  station_node     state_var_layer_and_diagn_var_numbers
     2691              2;1;6,7
     2691              1;1;3,4             2;1;3,4
     2691              1;1-3,5;10          1;1-3,5;20:22
$end_diagn_var
```

3.1.2.4. Hydrodynamic variables and monitoring stations file

The visualisation system provides graphs for three hydrodynamic variables – salinity, temperature and water level. A separate input file is required for the visualisation of these variables. Its name has to match simulation name with the extension *vish*. In this file there must be two sections. The first one has to start with `$variables` and end with `$end_variables`. This section contains information about the hydrodynamic variables. After starting this section in the second row should be names of the columns:

- `variable` is a variable indicator: 11 – salinity, 12 – temperature, and z – water level;
- `var_name` represents the column with the names of the variables;
- `units` are the units of the variables.

```
$variables
   variable      var_name       units
      11         Salinity        PSU
      12         Temperature     C
      z          Water_level     cm
$end_variables
```

The second section in **.vish* file has to start with `$stations` and end with `$end_stations`. This section contains information about station visualisation. After starting this section in the second row there must be names of the columns:

- `variable` is a variable indicator: 11 – salinity, 12 – temperature, and z – water level;
- `nodes` are the node numbers. For processing water level data they must match node numbers in Shyfem main configuration file SECTION EXTRA.
- `station_names` are the names of the stations (separated with underscore);
- `visualise` is an indicator for visualisation (1 – yes, 0 – no). Here can be chosen which stations have to be visualised;
- `measurements` is an indicator for plotting measurements data (1 – yes, 0 – no). If the station does not have it, then this indicator should be 0. Zero should also be when there are measurement data, but it does not have to be visualised.
- `measurements_file` column has links to measurement data files.

An example of station section for plotting hydrodynamic variables is presented below:

```
$stations
  variable  nodes  station_names    visualise  measurements    measurements_file
    11      1823   Klaipeda_strait      1           1         /link/to/measurements/file
    12      1657   Juodkrante           0           0         -
    z       1692   Nida_KM              1           0         -
$end_stations
```

If the water level station does not have observed measurements data, then the graph will not be plotted even if it's indicated to be visualised.

Column separation and underscore (for separate words of the variables, station names and etc.) rules apply the same as to visualisation sections in AQUABC configuration files.

3.2. Simulation results and analysis

Five scenarios were performed due to thorough investigation of the ice cover effect on temperature, salinity, and aeration. The study of ice cover effect on aeration is divided into two parts: (1) individual factor importance to dissolved oxygen concentration, and (2) study of oxygen saturation for determining hypoxic conditions. The results and findings of the analysis are presented in this chapter of the thesis.

3.2.1. Ice cover effect on temperature and salinity

In the model ice has an impact just to the momentum on the water surface. In reality the solar radiation is reduced during the ice cover period, however this version of the model does not take it into account. Analysed ice cover situation showed that temperature and salinity behaves differently.

Since the ice cover in the Klaipėda Strait is present in the model, during that time the temperature variations are the most noticeable in that area (Figure 18, this and all the other figures of the analysed nodes (stations) can be found in the appendix), because it is a transitional area, where sea water meats the water from the lagoon. In other stations the difference is negligible. During the summer time the difference of simulations with natural ice cover and reference simulation (ice free) is equals to zero, which proves that model simulates temperature correctly – there is no ice in summer, thus the temperatures are the same (Figure 19).

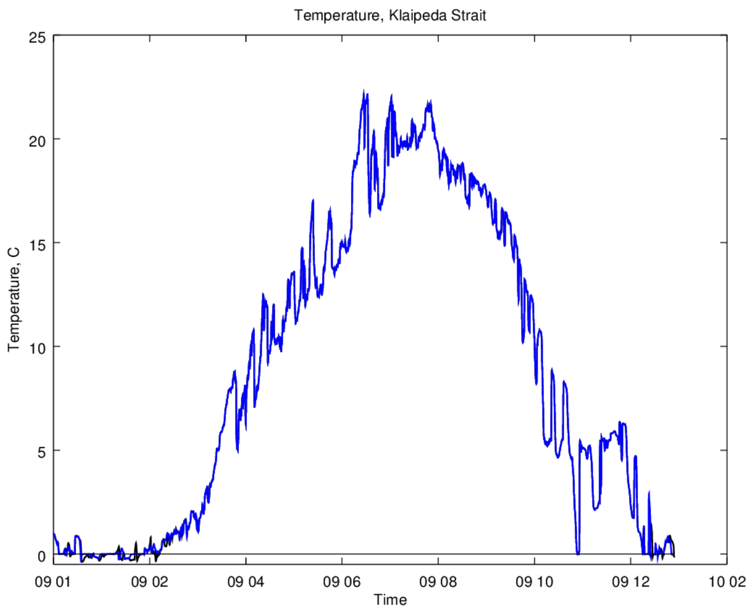

Figure 18: Water temperature in Klaipėda Strait. Without ice (black) and with ice cover (blue).

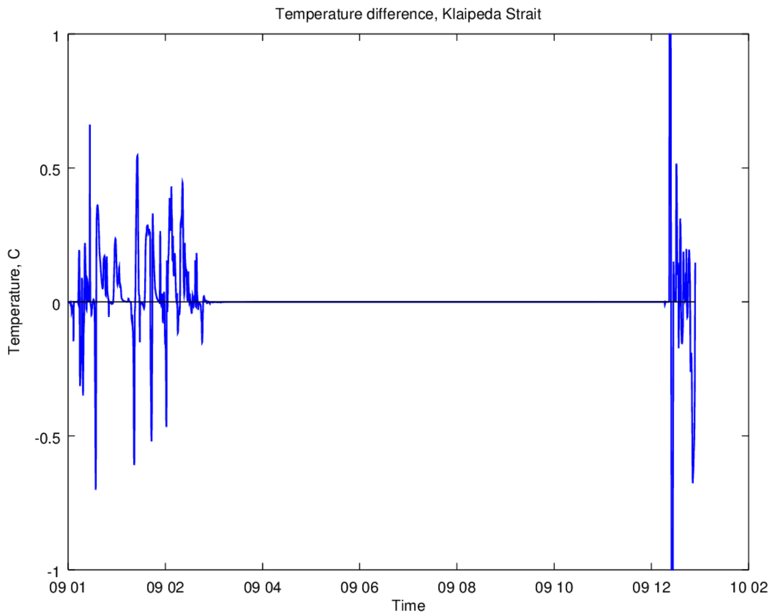

Figure 19: Difference of temperature – simulation of natural ice conditions subtracted from the reference simulation.

In the ice cover period salinity is preconditioning and thus the changes are visible in the summer time (Figure 20), although it is very small. This is due to the slow water renewal, which is more noticeable in the southern, south-western part of the lagoon, where the water renewal time is longer, than in the parts of the lagoon, which are closer to more turbid, water discharge areas (Klaipėda Strait, Ventė, South East - Matrosovka). However, in the South East of the lagoon, there is an opposite reaction – salinity slightly increases during the ice cover period (Figure 21), this accumulation of saline water might be due to the prevailing stronger south-easterly winds (Figure 22).

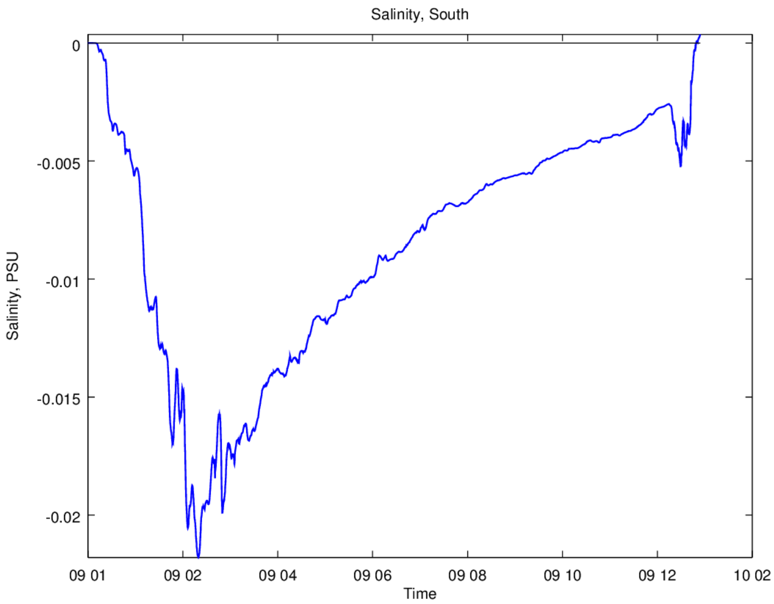

Figure 20: Difference of salinity – simulation of natural ice conditions subtracted from the reference simulation.

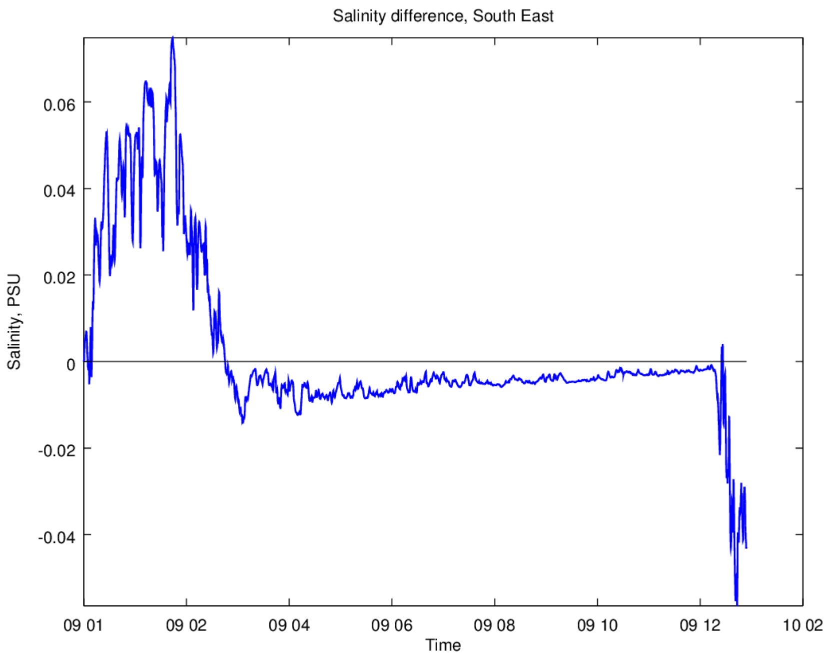

Figure 21: Difference of salinity in South East of the lagoon– simulation of natural ice conditions subtracted from the reference simulation.

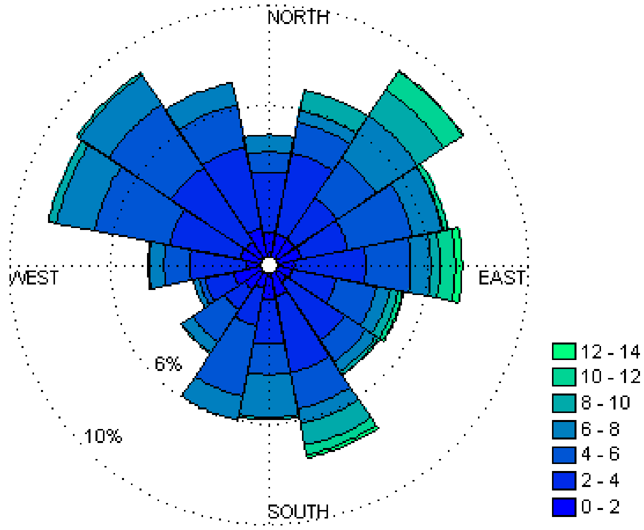

Figure 22: Wind rose diagram of station in the south east of the lagoon during ice cover period.

3.2.2. Ice cover effect on dissolved oxygen

The magnitude of different physical processes suppressed by ice cover is studied in this section of work. When reaeration, light and momentum are suppressed by ice cover, the superposition of their effects can be observed. The concentration of dissolved oxygen severely decreases during the ice cover period (winter time) and shifts (or slight increases) in spring and summer time (Figure 23). In the difference graph (simulation when ice cover is present subtracted from the reference simulation) the variations in the spring and summer time are more noticeable

(Figure 24). However the changes should be seen only in the winter time when the ice cover is present, thus to understand this situation in the ice free period it is required to investigate each physical factor's effect on the concentration of DO.

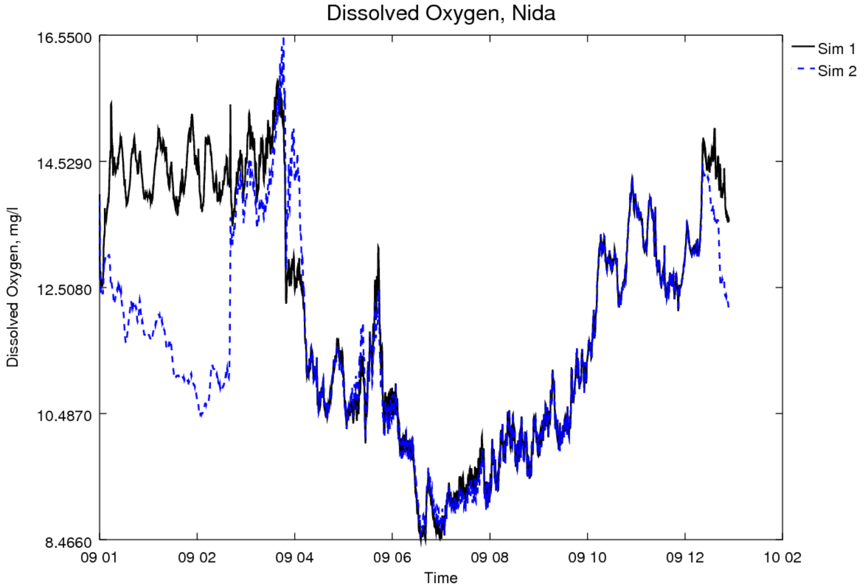

Figure 23: Comparison of dissolved oxygen concentrations – without ice cover (Sim 1) and with ice cover (Sim 2).

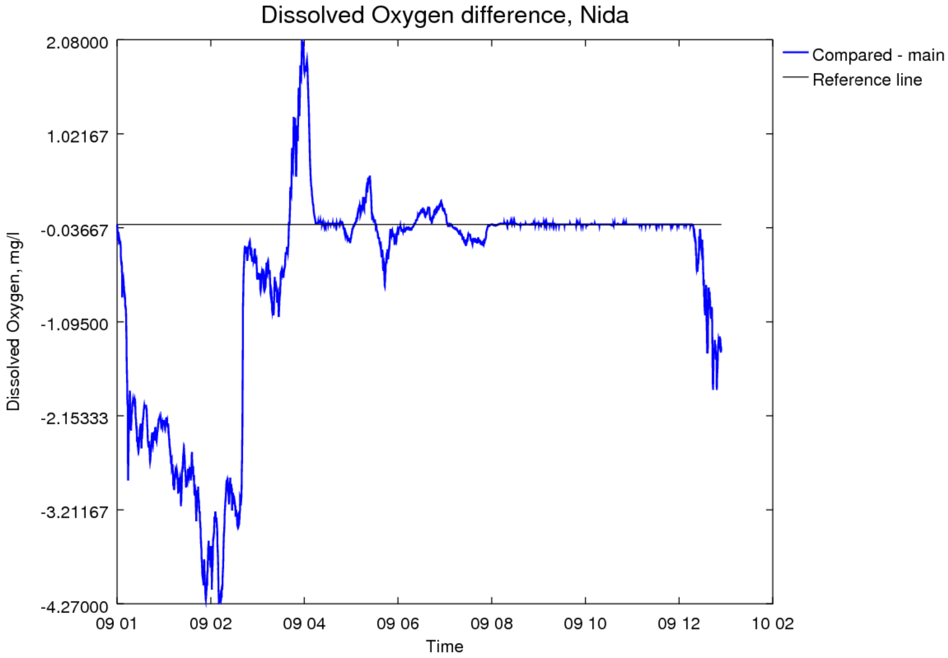

Figure 24: Difference of simulations – simulation of natural ice conditions subtracted from the reference simulation.

The RMSE analysis of the whole year (Figure 25), when the ice cover was present in winter time, shows that the greatest impact on DO has suppressed reaeration. Then (in second place) in Klaipėda Strait, Ventė, and South East the impact of suppressed momentum is bigger than suppressed light, because these locations are in the area of intensive movement (from Baltic Sea, Nemunas watershed, and Matrosovka River). The opposite is visible in Nida, South, and South West – the impact of suppressed light is greater than of suppressed momentum, because the flow there is not as intensive. But this is valid just for comparison of the data of the whole year.

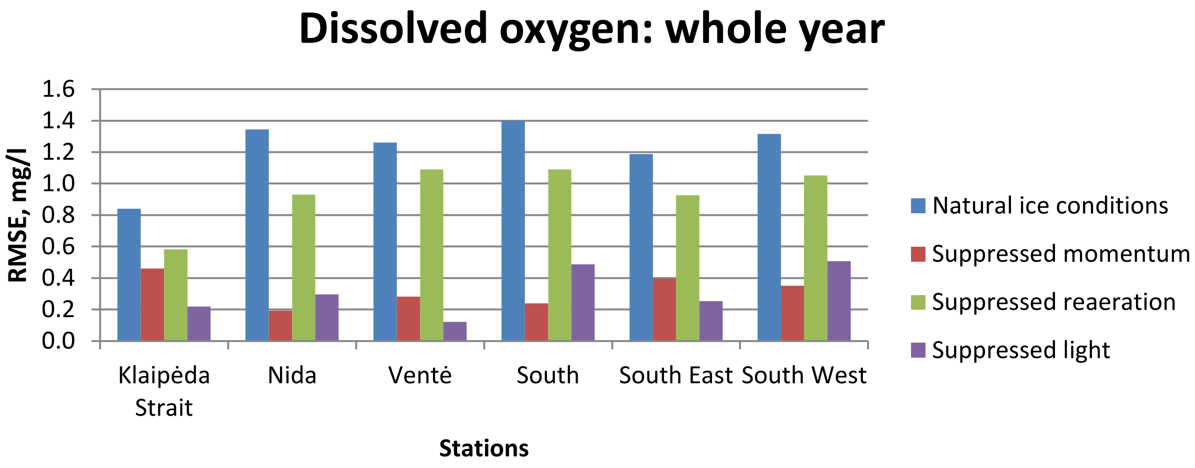

Figure 25: RMSE of DO concentration for the whole year.

During the ice cover period (Figure 26) everywhere (in the 6 analysed stations) suppressed momentum has bigger impact than suppressed light, although the difference is greater in more turbid areas (Klaipėda Strait, Ventė, and South East).

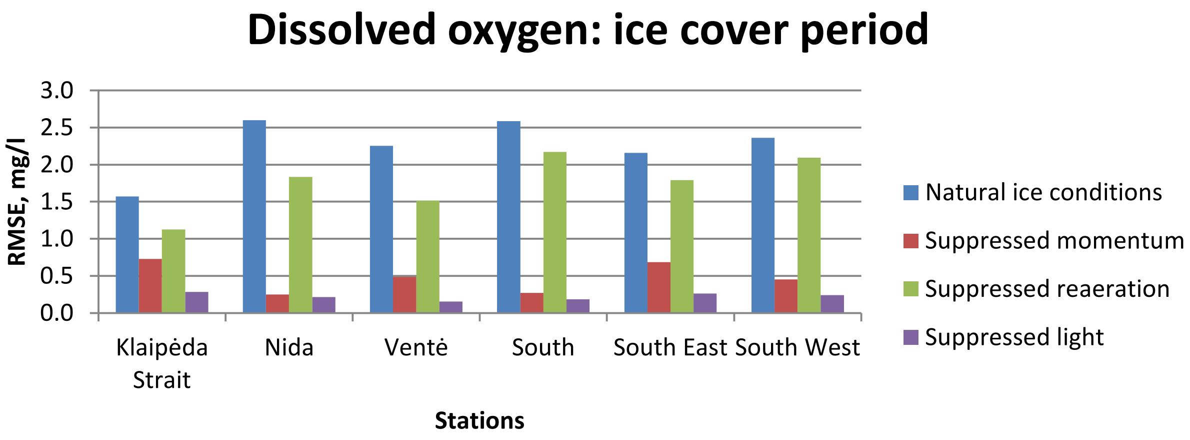

Figure 26: RMSE of DO concentration for the winter period (January-March).

The greatest impact on dissolved oxygen concentration during the ice cover period has suppressed reaeration (Figure 27). When the ice cover blocks the air from the atmosphere, the wind induced mixing (momentum) and light induced photosynthesis will not outweigh the impact of reaeration, thus the concentration of dissolved oxygen decreases. Oxygen produced by photosynthesis is relatively small compared to oxygen gained from the atmosphere, and mixing this amount into deeper levels or spreading it further in the water body will not increase it.

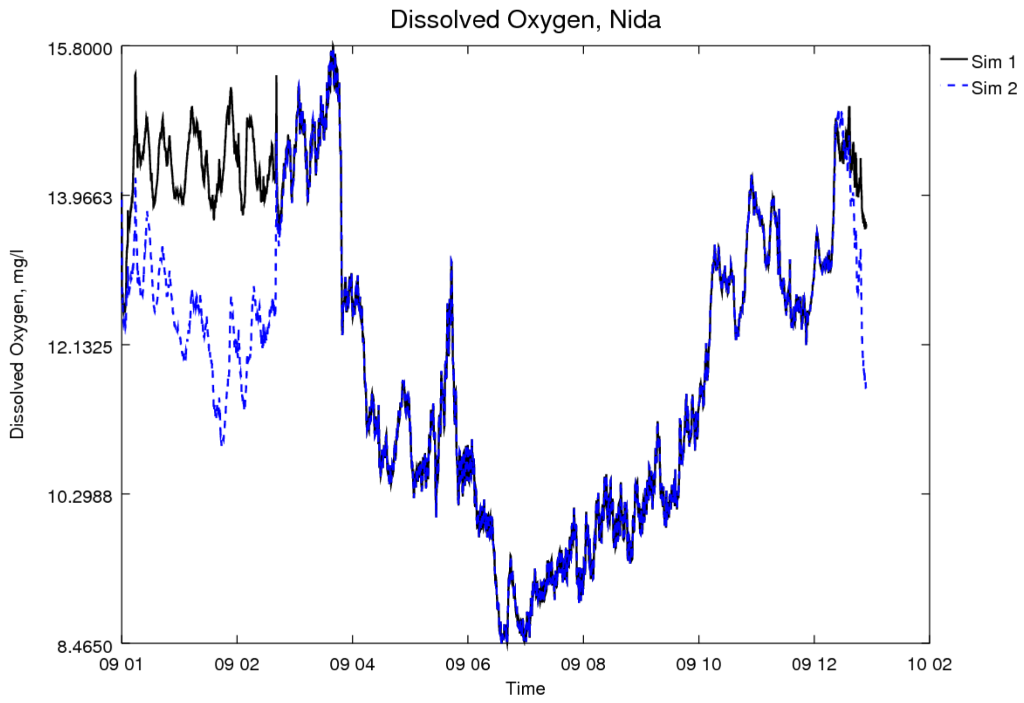

Figure 27: Comparison of dissolved oxygen concentrations – without ice cover (Sim 1) and with ice cover, when only the reaeration is suppressed (Sim 2).

During the summer period (Figure 28), when the ice cover is not present and its affect should not be visible at all, there is an opposite situation – the effect of ice cover drags into the summer time and the greatest impact of it has suppressed light and momentum.

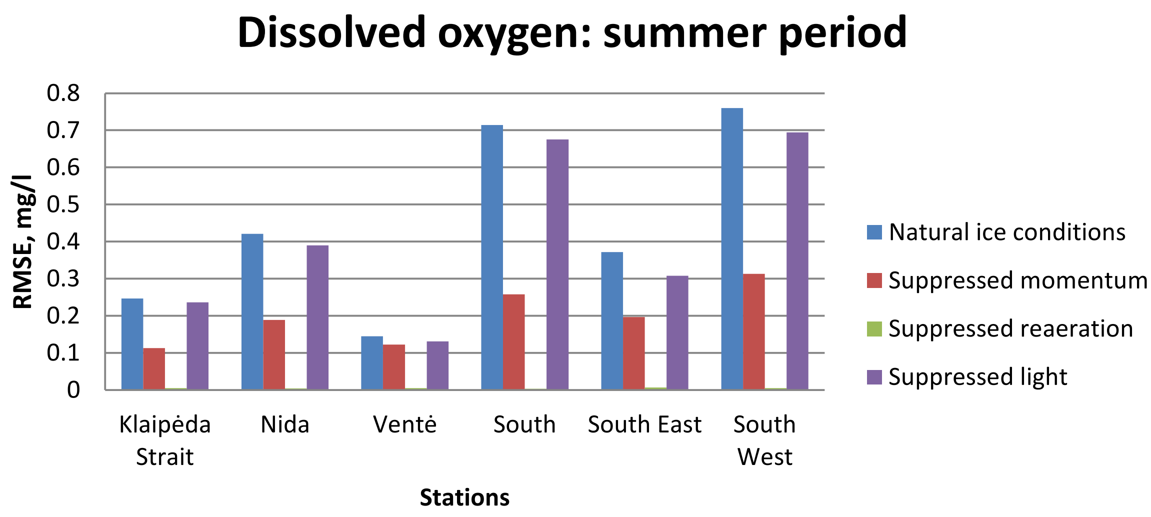

Figure 28: RMSE of DO concentration for the summer period (April-October).

When the light is blocked the greatest effect can be seen on the photosynthesis and concentration of phytoplankton. Differences graphs (Figure 29) of oxygen and phytoplankton display the similar pattern of fluctuations, two peaks in the end of April-beginning of May (true to every station) and July (not as much in South East and South West for oxygen concentration).

a) b)

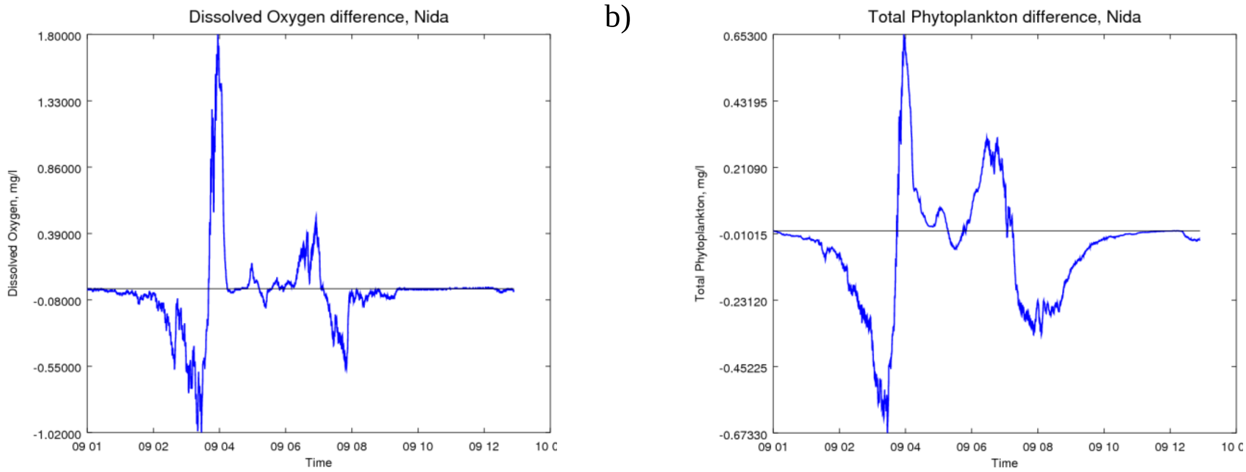

Figure 29: Differences of oxygen (a) and phytoplankton (b) – simulation of ice cover (when only the light is suppressed) subtracted from the reference simulation.

Succession in phytoplankton communities is basically initiated by physical and hydrographical events, e.g. light, turbulence, internal and surface waves, and temperature (Adrian et al., 1999). Blocked light in the Curonian lagoon affects the succession pattern over the entire year – the start of the growing is slightly shifted starting from spring (April-May) and continuing further in the year.

In (Pełechata et al., 2015) was studied two winter cases (mild and severe) and their effect on phytoplankton concentration in the shallow lake. The results showed that highest phytoplankton numbers occurred in the growing seasons after severe winters. In the Curonian lagoon case, the severe winter could be with ice and mild winter – without ice. Another study of shallow, highly eutrophic, polymictic (too shallow to develop thermal stratification), flushed lake (Adrian et al., 1999) showed that a one day increase in ice duration corresponded to a 0.4-day delay in the development of maximal total algal biomass. The delay of the phytoplankton succession in spring is also noticeable in the Curonian lagoon (Figure 30). The shifts of phytoplankton concentration are not uncommon (Winder et al., 2010). Due to the shift in phytoplankton concentration the oxygen produced by it also is shifted in spring and summer.

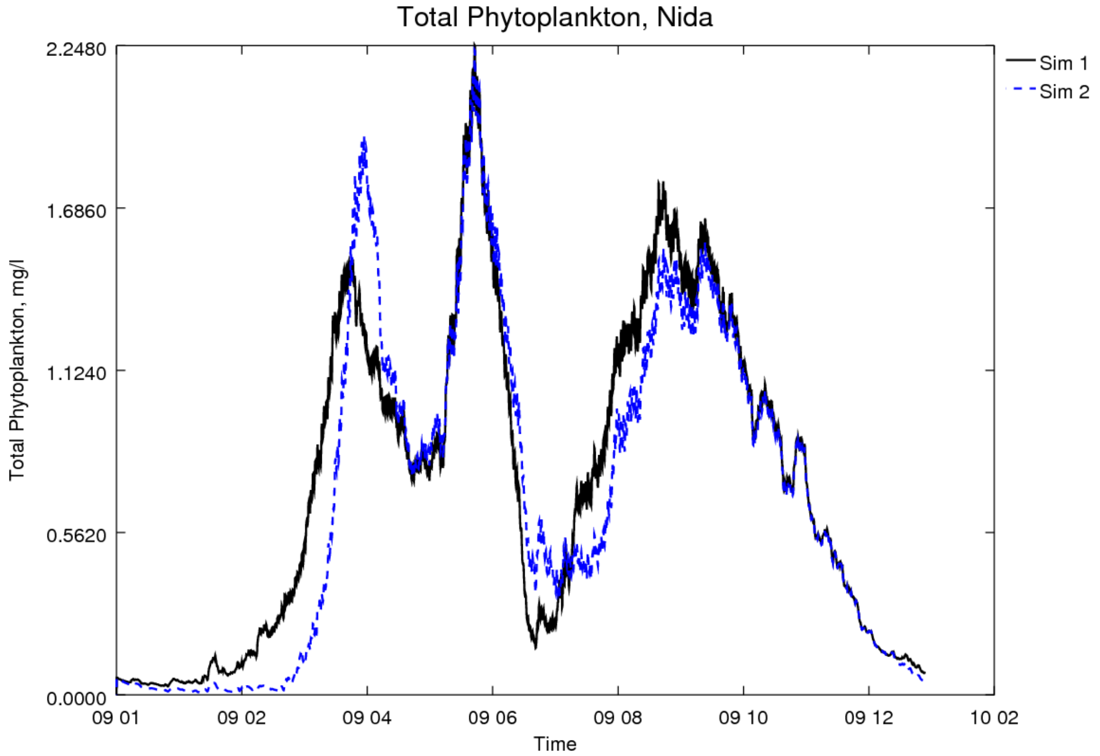

Figure 30: The delay of the phytoplankton growth – without ice cover (Sim 1) and with ice cover, when only the light is suppressed (Sim 2).

During the ice cover period in more turbid areas (Klaipėda Strait, Ventė, South East) the concentration of phytoplankton increases, because it is not flushed out further from the water discharge areas into the lagoon, thus it can produce oxygen in a processes of photosynthesis. However the effect of momentum is more useful for dissolving oxygen from the atmosphere (re-aeration) by creating waves (it creates more surface area, so more diffusion can occur) and mixing the DO into the deeper layers of the water body, thus in the winter time when momentum is suppressed the dissolved oxygen more or less decreases, or the amplitude of the fluctuations is smaller, except Klaipėda Strait, where the dissolved oxygen concentration slightly increases. The fluctuations of the DO and phytoplankton in summer time have the same pattern. However the shifts of peaks of phytoplankton concentration in summer (phytoplankton increases earlier) has an effect on oxygen, thus there are earlier increase (shift) of dissolved oxygen concentration in summer (Figure 31).

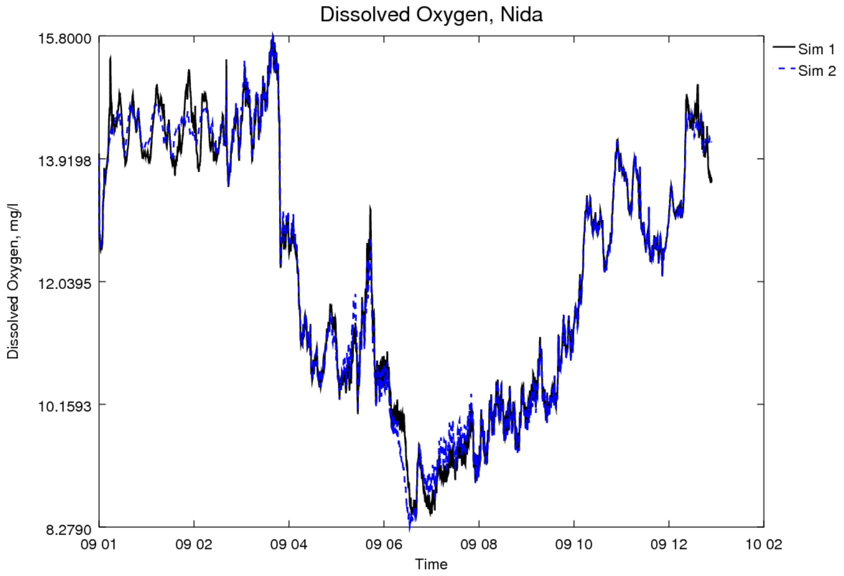

Figure 31: Comparison of dissolved oxygen concentrations – without ice cover (Sim 1) and with ice cover, when only the momentum is suppressed (Sim 2).

3.2.3. Ice cover effect on oxygen saturation

The minimum oxygen saturation (in the whole territory of the lagoon) in 2009 was affected by the ice cover; however hypoxia has not been reached (Figure 32). Additionally, there is a noticeable decrease in the end of the ice cover period. The not so sudden drop of the values (not from the beginning of the year) might be due to the time required for model to spin up, which means that the time taken for the model to reach a state of statistical equilibrium under the applied forcing is too long and the initial conditions might need adjustment. Since the model is run in 2D, the absence of hypoxia might be due to the stratification of the water column, e.g. lower concentrations might occur in the bottom levels.

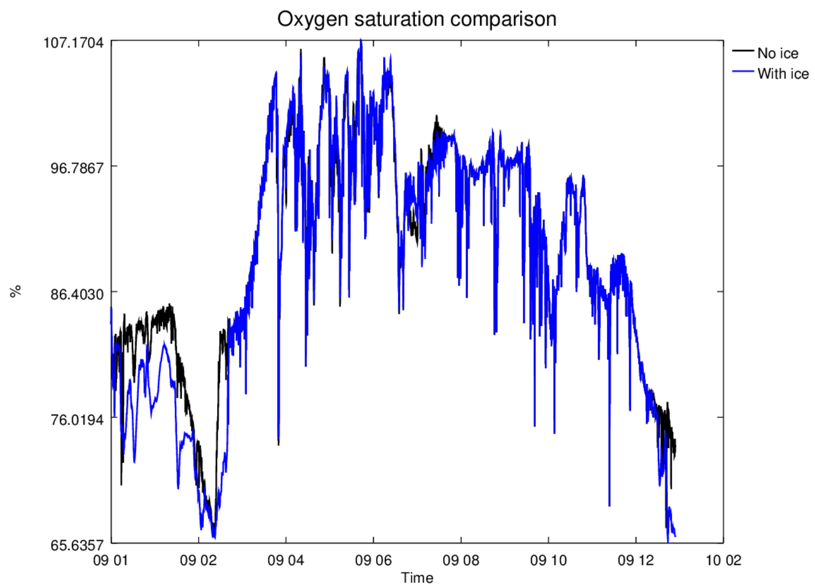

Figure 32: The minimum oxygen saturation in the entire lagoon.

The same situation of decreased oxygen saturation can be observed in separate stations (Figure 33) – it is clear that the percentage does not decrease lower than 30% (hypoxia does not occur) during the ice cover period. Additionally, oxygen saturation increase is noticeable during the spring phytoplankton bloom.

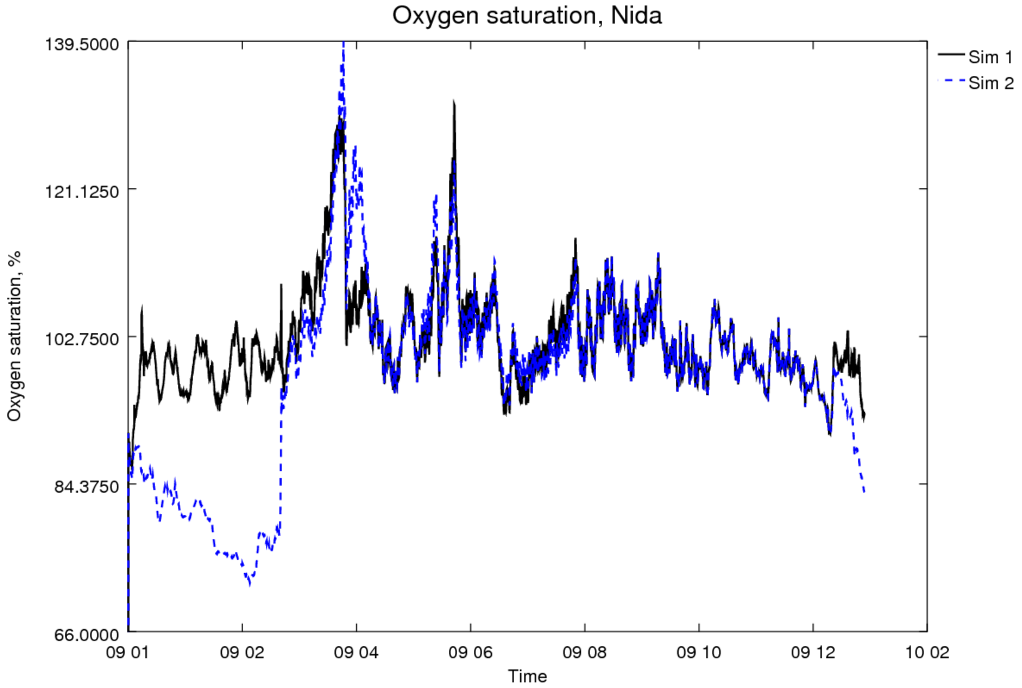

Figure 33: Oxygen saturation in Nida, without ice cover (Sim 1) and with ice cover (Sim 2).

CONCLUSIONS AND RECOMENDATIONS

The benefits of a numerical model are indisputable. Numerical approach enables to get an insight and solution of a complex problem. By coupling two models (hydrodynamic and biogeochemical) together the comprehension of their interactions can be achieved. Work with the numerical model is complicated (complex) itself; it requires a great precision and thoroughness. The set-up of the model and processing of its output can have a great impact on the knowledge derived from it by the researchers.

Hydrodynamic finite element model Shyfem was developed for modelling shallow water bodies. It was successfully applied to studying hydrodynamic processes of numerous lagoons as well as the Curonian lagoon. Ecological model AQUABC is relatively new and still under development, thus the calibration, validation of this model, interpretation of the derived results and their fast depiction are of great importance.

The developed visualisation system consists of 8 different modules responsible for reading input files and parallelisation of the computations, processing biogeochemical and hydrodynamic variable data, and data conversion if needed. The system requires input files, in which the visualisation parameters, and station and variable visualisation information are specified. The high speed of the system can be adjusted by the user – specifying the amount of processors to use in the main visualisation parameter file. Analysis showed that the speed increases with the increased number of processors and reaches the maximum speed, when each variable is computed (plotted) on a separate core.

The system allows user to quickly and easily obtain time series and depth profiles (3D case) graphs of biogeochemical and hydrodynamic variables, time series graphs of diagnostic biogeochemical variables, time series graphs of biogeochemical state and derived variables data comparison of several model simulations, and files with statistical estimates.

A few recommendations are suggested for the improvement of visualisation system:

- the visualisation sections in AQUABC configuration files should be transferred to a separate file (as is done with the hydrodynamic variables);
- the option of choosing the environment to visualise (parameter `'vis'` in main visualisation parameter file) should be expanded with inclusion of hydrodynamic variables. This would allow the visualisation of separate hydrodynamic variables (not all together);
- the ability to plot velocities should be included in the hydrodynamic variable visualisation;
- the comparison of hydrodynamic variables of several simulations should be included, as well as the comparison of interactively given nodes of several simulations.

- the number of directories for saving the figures should be reduced to three – removing the diagnostic variable and interactively given node directories. These figures could be saved in the water column and sediment directories.

The developed visualisation system was applied for studying the ice cover effect on natural aeration in the Curonian lagoon. Five simulations have been carried out for studying the variations of dissolved oxygen: reference (ice free), natural ice conditions, only the reaeration suppressed, only the momentum suppressed, and only the light suppressed. The analysis showed that during the ice cover period the greatest impact on dissolved oxygen concentration has the suppressed reaeration. Additionally there are noticeable concentration shifts in the summer time (ice cover effect on DO drags into the summer), this is due to the shift of phytoplankton growth, which also adds oxygen to the water in a process of photosynthesis.

The analysis of oxygen saturation showed a noticeable decrease during the ice cover period, however the level of hypoxia (<30%) was not reached. The results of minimum oxygen saturation in the entire lagoon showed the decrease of values in the end of ice period, this might occur due to the long model spin up time, which might be resolved by adjusting initial conditions. The absence of hypoxia might be due to the dimensionality of the simulations (2D). Analysis of 3D model results should be done to investigate oxygen saturation in lower levels of the water column.

The model takes into account just the percentage of ice cover, not the thickness of it or the snow cover on top of it. Additionally it does not take into account that solar radiation is reduced during the ice cover period. The ice cover was interpolated over the entire lagoon from the data of just four monitoring stations. The use of satellite data could give a better representation of ice cover conditions in the lagoon. Overall, an improved model would improve the knowledge of ice cover effect on the physical and biogeochemical processes in the water body.

LITERATURE

Adrian R., Walz N., Hintze T. et al. 1999. Effects of ice duration on plankton succession during spring in a shallow polymictic lake. Freshwater biology 41, 621-632.

Aleksandrov S. V. 2010. Biological production and eutrophication of Baltic Sea estuarine ecosystems: The Curonian and Vistula Lagoons. Marine Pollution Bulletin 61 (2010) 205–210.

Antonopoulos V. Z., Gianniou S. K. 2003. Simulation of water temperature and dissolved oxygen distribution in Lake Vegoritis, Greece. Ecological Modelling, Vol. 160, Issues 1–2, 1 Feb. 2003, p. 39–53.

Ateljevich E., Colella P., Graves D. T. et al. 2009. CFD modeling in the San Francisco Bay and Delta. Proceedings of the fourth SIAM conference on mathematics for industry, pp. 99–107.

Atkinson K. E. Numerical analysis. Encyclopædia Britannica Online. Encyclopædia Britannica Inc. Web. 31 Mar. 2016 <http://www.britannica.com/topic/numerical-analysis>.

Bajo M., Ferrarin C., Dinu I. et al. 2014. The water circulation near the Danube Delta and the Romanian coast modelled with finite elements. Continental Shelf Research 78 (2014) 62–74.

Balevičienė J., Balevičius A., Stanevičius V. et al. 2007. Kuršių marių pakrantės augmenijos pjovimo, siekiant iš marių pašalinti dalį biogeninių medžiagų, galimybių studija. Vilnius.

Basos N. 2013. GIS as a tool to aid pre- and post-processing of hydrodynamic models. Application to the Guadiana Estuary. Universidade do Algarve.

Bellafiore D., Umgiesser G. 2009. Hydrodynamic coastal processes in the North Adriatic investigated with a 3D finite element model. Ocean Dynamics (2010) 60:255–273.

Blazek I. 2005. Computational Fluid Dynamics: Principles and Applications. Third edition, Elsevier, UK.

Bukantis A., Šinkūnas P., Taločkaitė E. 2007. Klimato kaita: prisitaikymas prie jos poveikio Lietuvos pajūryje. Geologijos ir geografijos institutas, 2007.

Cataudella S., Crosetti D., Massa F. 2015. Mediterranean coastal lagoons: sustainable management and interactions among aquaculture, capture fisheries and the environment. Food and agriculture organization of the united nations, Rome.

Chatzinikolaou E. 2012. Use and limitations of ecological models. Transitional Waters Bulletin n. 2, p.34-41.

Chen C., Beardsley R. C., Cowles G. 2006. An unstructured grid, finite volume coastal ocean model (FVCOM) system. Oceanography Vol. 19, No. 1, Mar. 2006.

Chikita K. A., Uyehara H., Mamun A. A. et al. 2015. Water and Heat Budgets of a Coastal Lagoon Controlled by Groundwater Outflow to the Ocean. Limnology, 16 :149–157.

Church I. 2008. Developing a nested finite-element hydrodynamic model to predict phase and amplitude modification of the tide within narrow fjords. University of New Brunswick.

Collins R. 2011. Hazardous substances in Europe's fresh and marine waters. EEA, Copenhagen.

Cucco A., Sorgente R., Sinerchia M. et al. 2013. Operational oceanography, innovative technologies and applications, III National Meeting of the National Group of Operational Oceanography.

Dailidienė I. 2007. Kuršių marių hidrologinio režimo pokyčiai. GEOGRAFIJA. 2007. T. 43. Nr. 1. P. 36–43.

Davulienė L., Trinkūnas G. 2003. Circulation dynamics in the curonian lagoon waters. Lithuanian Journal of Physics, Vol. 44, No. 1, pp. 67–73.

De Martin F., Modaressi H., Aochi H. 2007. Coupling of FDM and FEM in seismic wave propagation. 4th International Conference on Earthquake Geotechnical Engineering, June 25-28, 2007, Paper No. 1743.

De Pascalis F., Perez-Ruzafa A., Gilabert J. et al. 2011. Climate change response of the Mar Menor coastal lagoon (Spain) using a hydrodynamic finite element model. Estuarine Coastal Shelf Sci., 114, 118–129.

Desai Y. M., Eldho T. I., Shah A. H. 2011. Finite element method with applications in engineering. Pearson.

Eilola K., Almroth-Rosell E., Edman M. et al. 2015. Model set-up at COCOA study sites. OCEANOGRAFI Nr. 117.

Ertürk A., Razinkovas A., Zemlys P. et al. 2008. Linking NPZD and Foodweb Models of an Estuarine Lagoon Ecosystem. Computational Science and Techniques 09/2015; 3(1).

Fernandez F. A., Kulas L. 2004. A simple finite difference approach using unstructured meshes from FEM mesh generators. 15th International Conference on Microwaves, Radar and Wireless Communications.

Ferrarin C., Razinkovas A., Gulbinskas S. et al. 2008. Hydraulic regime-based zonation scheme of the Curonian Lagoon. Hydrobiologia (2008) 611:133–146.

Ferrarin C., Umgiesser G., Bajo M. et al. 2010. Hydraulic zonation of the lagoons of Marano and Grado, Italy. A modelling approach, Estuarine Coastal and Shelf Sciences, 87(4), 561-572.

Ferrarin, C., Umgiesser G. 2005. Hydrodynamic modeling of a coastal lagoon: The Cabras lagoon in Sardinia, Italy. Ecological Modelling, Vol. 188, 340-357.

Filgueira R., Grant J., Bacher C. et al. 2012. A physical–biogeochemical coupling scheme for modeling marine coastal ecosystems. Ecological Informatics, Volume 7, Issue 1, Pages 71–80.

Ganju N. K., Brush M. J., Rashleigh B. et al. 2015. Progress and Challenges in Coupled Hydrodynamic-Ecological Estuarine Modeling. Estuaries and Coasts.

Gasiūnaitė Z. R., Olenina I. 1998. Zooplankton-phytoplankton interactions: a possible explanation of the seasonal succession in the Kuršių Marios lagoon. Hydrobiologia 363: p. 333-339.

Ghorbani M. A., Khiavi M. P. 2011. Hydrodynamic Modeling of Infinite Reservoir using Finite Element Method. International Journal of Civil, Environmental, Structural, Construction and Architectural Engineering Vol:5, No:8, 2011.

Gonenc I. E., Wolflin J. P. 2004. Coastal Lagoons: Ecosystem Processes and Modeling for Sustainable Use and Development. CRC Press.

Gulbinskas S., Mileriene R. 2012. Evaluation of the sea-floor integrity in lithuanian baltic sea waters. Book of Abstracts. International Conference Littoral 2012: Coasts of Tomorrow. VLIZ Special Publication 61.

Hadaś E. 2014. GIS system for 3d visualization of hydrodynamic modeling of flood flows in river valleys. JUNIORSTAV 2014, 6.3 Cartography and GIS.

Henshaw W. D. 1996. Automatic Grid Generation. Acta Numerica (1996), pp. 1–28.

Hinkelmann R. 2005. Efficient Numerical Methods and Information-Processing Techniques for Modeling Hydro- and Environmental Systems. Springer.

Holleman R., Fringer O., Stacey M. 2013. Numerical diffusion for flow-aligned unstructured grids with application to estuarine modelling. International journal for numerical methods in fluids.

James I. D. 2001. Modelling pollution dispersion, the ecosystem and water quality in coastal waters: a review. Environmental Modelling & Software 17 (2002) 363–385.

Jensen T. G. 1998. Open boundary conditions in stratified ocean models. Journal of Marine Systems 16 1998 297–322.

Jørgensen S. E. 2011. Handbook of Ecological Models used in Ecosystem and Environmental Management. CRC Press, Taylor & Francis Group.

Jørgensen S.E. 2009. Ecological Modelling: An Introduction. University of Copenhagen, Denmark.

Jørgensen S.E., Bendoricchio G. 2001. Fundamentals of Ecological Modelling. Elsevier science Ltd.

Kangping L., Changhong L. 2012. A coupled FDM–FEM method for free surface flow interaction with thin elastic plate. Journal of Marine Science and Technology (2013) 18:1–11.

Kelin H., Ding P., Wang Z. et al. 2008. A 2D/3D hydrodynamic and sediment transport model for the Yangtze Estuary, China. Journal of Marine Systems 77 (2009) p. 114–136.

Kemker C. 2013. Dissolved Oxygen. Fundamentals of Environmental Measurements. Fondriest Environmental, Inc. 19 November 2013. Web. < http://www.fondriest.com/environmental-measurements/parameters/water-quality/dissolved-oxygen/ >.

Kress N., Herut B. 2001. Spatial and seasonal evolution of dissolved oxygen and nutrients in the Southern Levantine Basin (Eastern Mediterranean Sea): chemical characterization of the water masses and inferences on the N : P ratios. Deep Sea Research Part I: Oceanographic Research Papers, Volume 48, Issue 11, November 2001, Pages 2347–2372.

Likens G. E. 2009. Biogeochemistry of Inland Waters. Encyclopedia of of inland waters. Elsevier. The Netherlands.

Liungman O., Moreno-Arancibia P. 2010. Developing a 3D coupled hydrodynamic and ecological model to be used in coastal management.

Ma P., Madsen O. S. 2011. An Open Boundary Condition for Numerical Coastal Circulation Models. Journal of Physical Oceanography, 41, 2363–2380.

MacWilliams M. L., Bever A. J., Gross E. S. et al. 2015. Three-Dimensional Modeling of Hydrodynamics and Salinity in the San Francisco Estuary: An Evaluation of Model Accuracy, X2, and the Low–Salinity Zone. San Francisco Estuary and Watershed Science, 13(1).

MacWilliams M. L., Gross E. S., DeGeorge J. F. et al. 2007. Three-dimensional hydrodynamic modeling of the San Francisco estuary on an unstructured grid. 32nd Congress, Venice Italy.

Martin J. L., McCutcheon S. C. 1999. Hydrodynamics and Transport for Water Quality Modeling. Lewis Publishers, CRC Press.

Martin, T., Steele M., Zhang J. 2014. Arctic Ocean Sea Ice Loss: Modeling the effect on Wind-to-Ocean Momentum Transfer. Witness the Arctic, Fall 2014 issue 3.

Mazzotti F. J., Vinci J. J. 2007. Validation, Verification, and Calibration: Using Standardized Terminology When Describing Ecological Models. Wildlife Ecology and Conservation Department, UF/IFAS Extension.

Nezlin N. P., Kamer K., Hyde J. et al. 2009. Dissolved oxygen dynamics in a eutrophic estuary, Upper Newport Bay, California. Estuarine, Coastal and Shelf Science, Vol 82, Issue 1, 20 March 2009, P. 139–151.

Nobre A. M., Ferreira J. G., Nunes J. P. et al. 2010. Assessment of coastal management options by means of multilayered ecosystem models. Estuarine, Coastal and Shelf Science 87 (2010) 43–62.

O'Boyle S., McDermott G., Wilkes R. 2009. Dissolved oxygen levels in estuarine and coastal waters around Ireland. Marine Pollution Bulletin Volume 58, Issue 11, November 2009, Pages 1657–1663.

Ogunniye O. S. 2015. Some selected numerical methods for solving stiff ordinary differential equation. Adekunle Ajasin University.

Oshana R. 2016. Multicore Software Development Techniques: Applications, Tips, and Tricks. Elsevier.

Pan Q., Gamma M. C., Popescu I. 2014. An Open Visualization Tool (openVT) For Mesh Based Water Models. CUNY Academic Works.

Parallel package documentation. Previewed at 4th of May 2016. Available at: <http://octave.sourceforge.net/parallel/package_doc/index.html>.

Park Y. S., Lek S., Baehr C. et al. 2015. Advanced Modelling Techniques Studying Global Changes in Environmental Sciences. Elsevier.

Pełechata A., Pełechaty M., Pukacz A. 2015. Winter temperature and shifts in phytoplankton assemblages in a small Chara-lake. Aquatic Botany 124 (2015) 10–18.

Pilkaitytė R., Razinkovas A. 2006. Factors controlling phytoplankton blooms in a temperate estuary: nutrient limitation and physical forcing. Marine Biodiversity: Patterns and Processes, Assessment, Threats, Management and Conservation, Developments in Hydrobiology, 2006.)

Raškauskienė A. 2008. Hidroekosistemų įvairovė ir apsauga. Previewed at 6th of May 2016. Available at: <http://vhost.asu.lt/nm/l-projektas/el-kursai.html>.

Razinkovas A., Gasiūnaitė Z., Viaroli P. et al. 2008. Preface: European lagoons—need for further comparison across spatial and temporal scales. Hydrobiologia (2008) 611:1–4.

Rykiel E. J. 1996. Testing ecological models: the meaning of validation. Ecological Modelling 90, 229-244.

Roland A., Cucco A., Ferrarin C. et al. 2009. On the development and verification of a 2-D coupled wave-current model on unstructured meshes. Journal of Marine Systems, Vol. 78 (Suppl. 1), 244-254.

Rukšėnienė V., Dailidienė I., Myrberg K. et al. 2015. A simple approach for statistical modelling of ice phenomena in the Curonian Lagoon, the south-eastern Baltic Sea. BALTICA Vol. 28 No 1 June 2015, 11-18.

Schiewer U. 2008. Ecology of Baltic Coastal Waters. Springer.

Sheng J. Yang B. 2009. A Nested-Grid Ocean Circulation Model for Simulating Three-Dimensional Circulation and Hydrography over Canadian Atlantic Coastal Waters. Terrestrial, Atmospheric and Oceanic Sciences, 21, p. 27-44.

Sheng J., Rao Y. R. 2006. Circulation and thermal structure in Lake Huron and GeorgianBay: Application of a nested-grid hydrodynamic model. Continental Shelf Research 26 (2006) 1496–1518.

Singh V. P., Singh P., Karitashia U. K. 2011. Encyclopedia of snow, ice and glaciers. Springer.

Sonntag S., Hense I. 2011. Phytoplankton behavior affects ocean mixed layer dynamics through biological-physical feedback mechanisms. Geophys. Res. Lett., 38, L15610.

Umgiesser G. 2016. SHYFEM - Finite Element Model for Coastal Seas: User Manual. Version 7.5.6.

Umgiesser G., Canu D. M., Cucco A. et al. 2004. A finite element model for the Venice Lagoon. Development, set up, calibration and validation. Journal of Marine Systems 51 (2004) 123 – 145.

Umgiesser G., Tu T. A., De Pascalis F. et al. 2007. Hydrodynamic modelling of the Tam Giang-Cau Hai lagoon, Vietnam.

Umgiesser G., Zemlys P., Ertürk A. et al. 2015. Seasonal renewal time variability in the Curonian Lagooncaused by atmospheric and hydrographical forcing. Ocean Sci., 12, 391–402.

Wehmeyer L. L., Wagner C. R. 2011. Relation between Flows and Dissolved Oxygen in the Roanoke River between Roanoke Rapids Dam and Jamesville, North Carolina, 2005–2009. Scientific Investigations Report 2011–5040, U.S. Geological Survey, Reston, Virginia.

Winder M., Cloern J. E. 2010. The annual cycles of phytoplankton biomass. Philos Trans R Soc Lond B Biol Sci. 2010 Oct 12; 365(1555): 3215–3226.

Zemlys P., Ertürk A., Razinkovas A. 2008. 2D finite element ecological model for the Curonian lagoon. Hydrobiologia (2008) 611:167–179.

Zemlys P., Paškauskas R., Umgiesser G. et al. 2011. Technical report 3: Water quality modelling system. Klaipėda.

Zemlys, P., Ferrarin, C., Umgiesser G. et al. 2013. Investigation of saline water intrusions into the Curonian Lagoon (Lithuania) and two-layer flow in the Klaipėda Strait using finite element hydrodynamic model. Ocean Sci., 9, 573-584.

Zhai X., Sheng J., Greatbatch R. 2003. A new two-way nested-grid ocean modelling technique applied to the scotian shelf and slope. Estuarine and Coastal Modeling - Proceedings of the Eighth International Conference. 342-357.

Zhang H. J., Zhou J. Z., Bi S. et al. 2012. Two-dimensional shallow hydrodynamic model based an adaptive structured grid. Journal of Hydrodynamics (Ser.A).

Zhang X., Davidson E. A., Mauzerall D. L. et al. 2015. Managing nitrogen for sustainable development. Nature 528, p. 51–59.

Zhen-Gang J. 2008. Hydrodynamics and Water Quality: Modeling Rivers, Lakes, and Estuaries. A John Wiley & Sons, Inc., Publication.

Zilius M., Bartoli M., Bresciani M. et al. 2013. Feedback Mechanisms Between Cyanobacterial Blooms, Transient Hypoxia, and Benthic Phosphorus Regeneration in Shallow Coastal Environments. Estuaries and Coasts DOI 10.1007/s12237-013-9717-x.

Žilinskas G., Jarmalavičius D., Pupienis D. et al. 2012. Kuršių marių akvatorijos gamtinių, ypatumų, esamos Kuršių marių krantų būklės ir jos kaitos tendencijų analizė. Vilnius.

APPENDIX

Examples of applications of visualisation system

For all examples the parameters in GRAPHICS SECTION were set to:

```
g_toolkit = 'fltk';
fform = 'png';
unit = 'pixels';
size = '600:420';
```

An example of state variable (concentration of zooplankton) time series and observed data points graph is shown in figure 1. Parameter `vis_var` set to `'1'`. Since the performed simulation was 2D, no other parameters require adjustment.

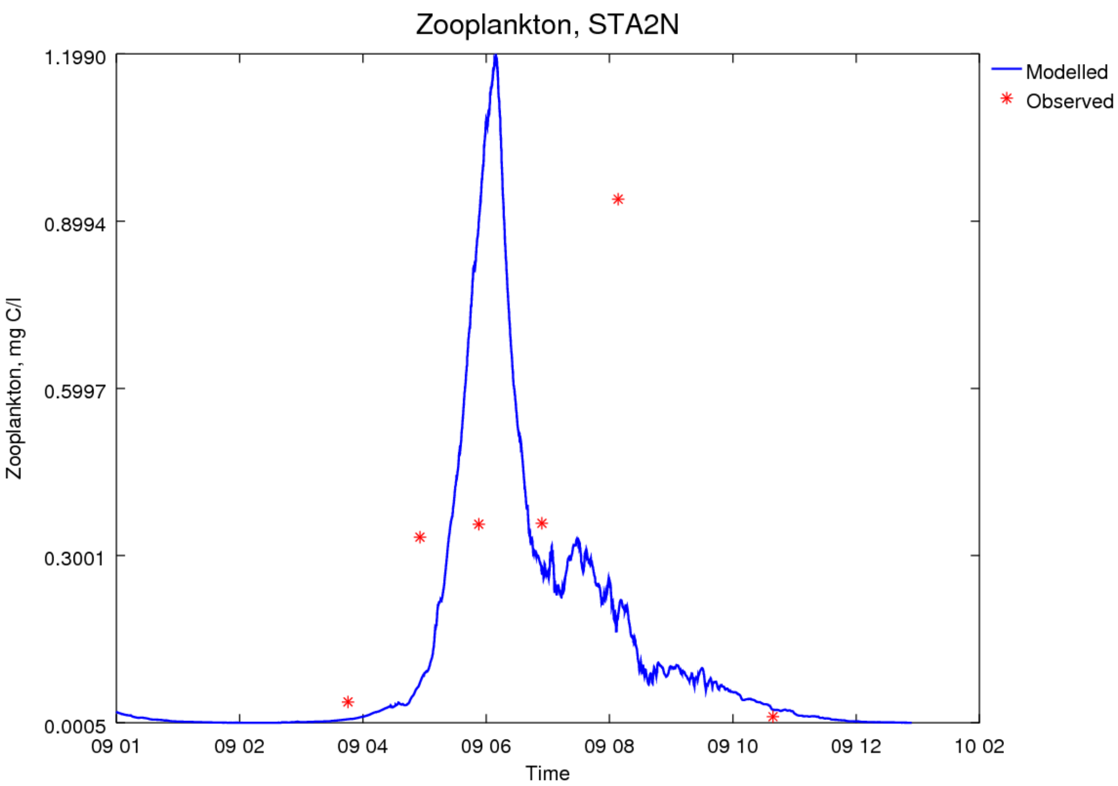

Figure 1: Concentration of zooplankton, simulation – 2D.

When the performed simulation is 3D, then there is required adjustment of additional parameter `layerplot`. It can be set to:

- 1 – plot all layers (Figure 2);
- 2 – plot average of layers (Figure 3);
- 3 – plot only layers with given numbers (Figure 4). In the example the variable is set to: `layerplot = '3-1,3,5'`.

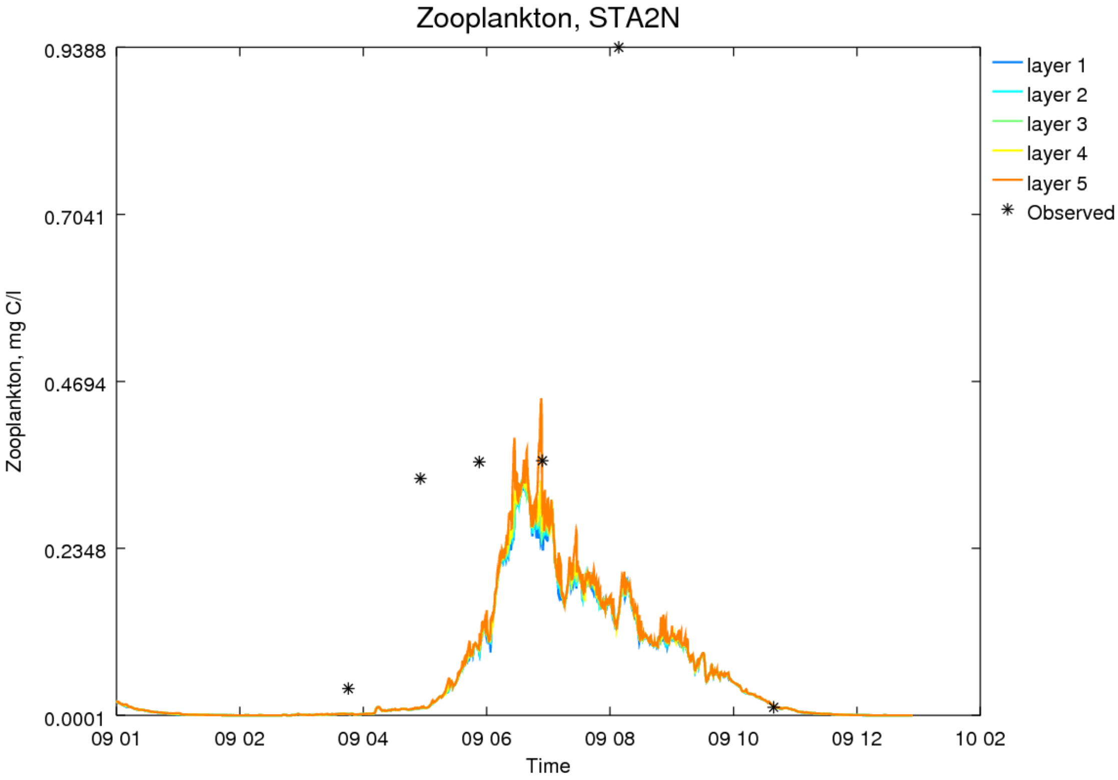

Figure 2: Concentration of zooplankton, simulation – 3D, all layers.

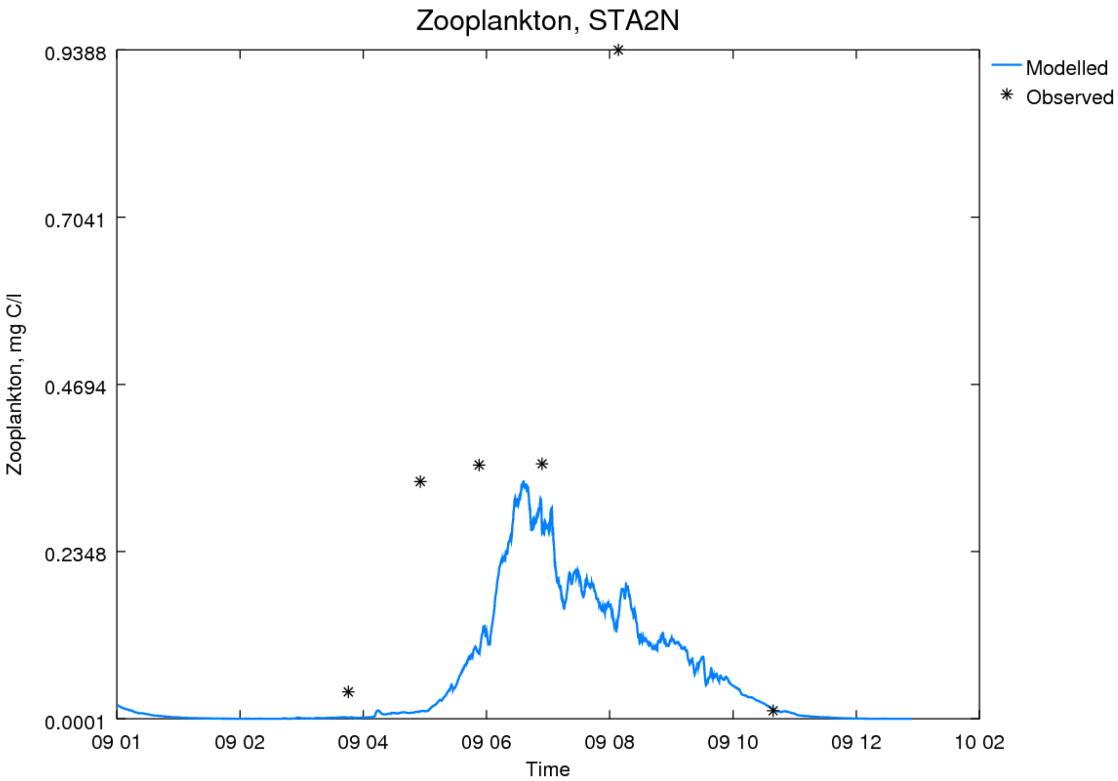

Figure 3: Concentration of zooplankton, simulation – 3D, average of layers.

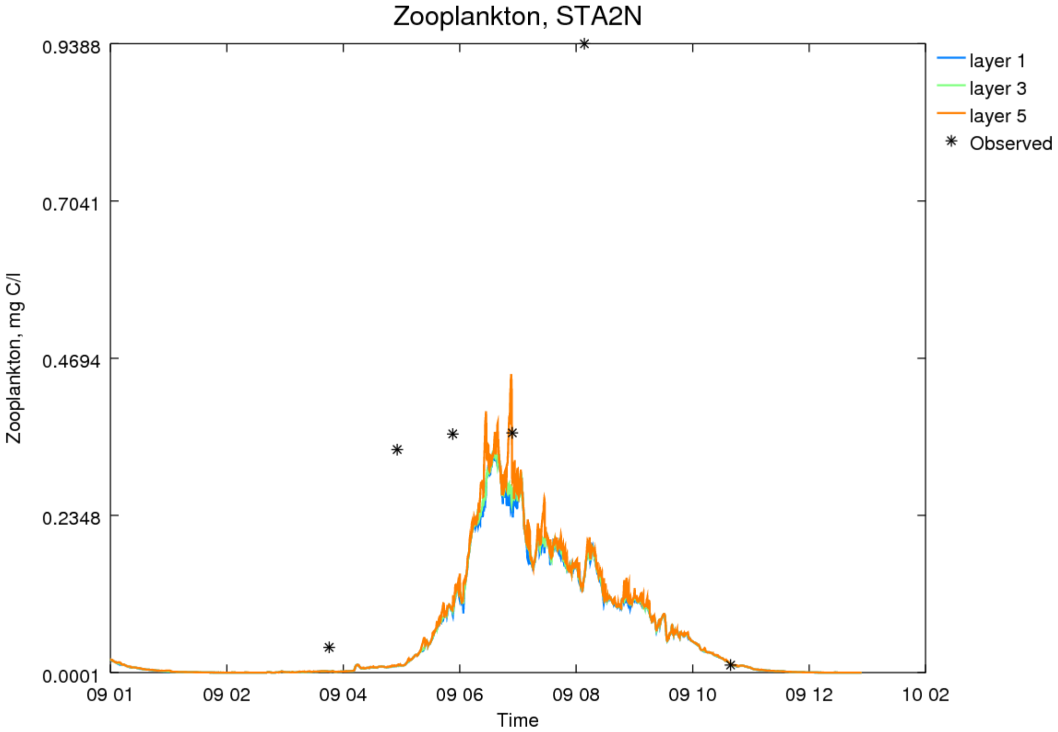

Figure 4: Concentration of zooplankton, simulation – 3D, selected layers.

Depth profile of the same variable can be plotted when `vis_var = '4'` (Figure 5). For this example there is required an averaging time period and the values were set to:

```
from = '20090101 060000';
to   = '20091231 200000';
```

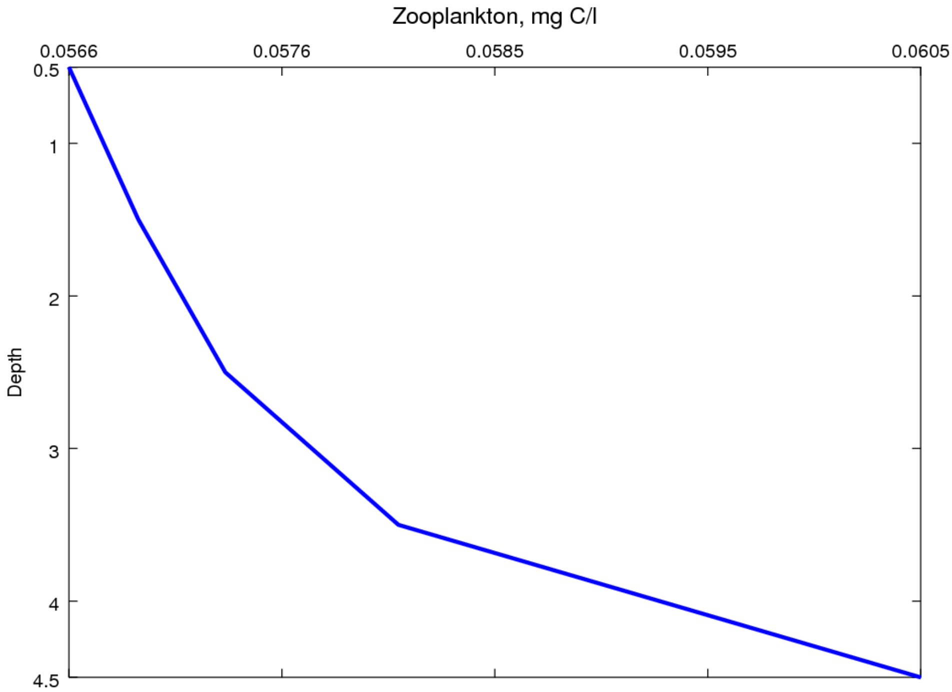

Figure 5: Depth profile of zooplankton concentration.

These examples were of the water column variable, but the exact same procedures (visualisation parameters adjustments) have to be applied when visualising sediment state (derived) variables.

Example of diagnostic variable visualisation is shown in figure 6. For this the diagnostic variable visualisation section is required in AQUABC configuration file:

```
$diagn_var
      station_node     state_var_nr_layer_and_diagn_var_number
      2691               1;1-3,5;10         1;1-3,5;22
$end_diagn_var
```

These values mean that for station node 2691 there will be plotted 1st state variable's layers 1,2,3,5 of diagnostic variable 10 and 1st state variable's layers 1,2,3,5 of diagnostic variable 22. All these values are plotted on the same graph.

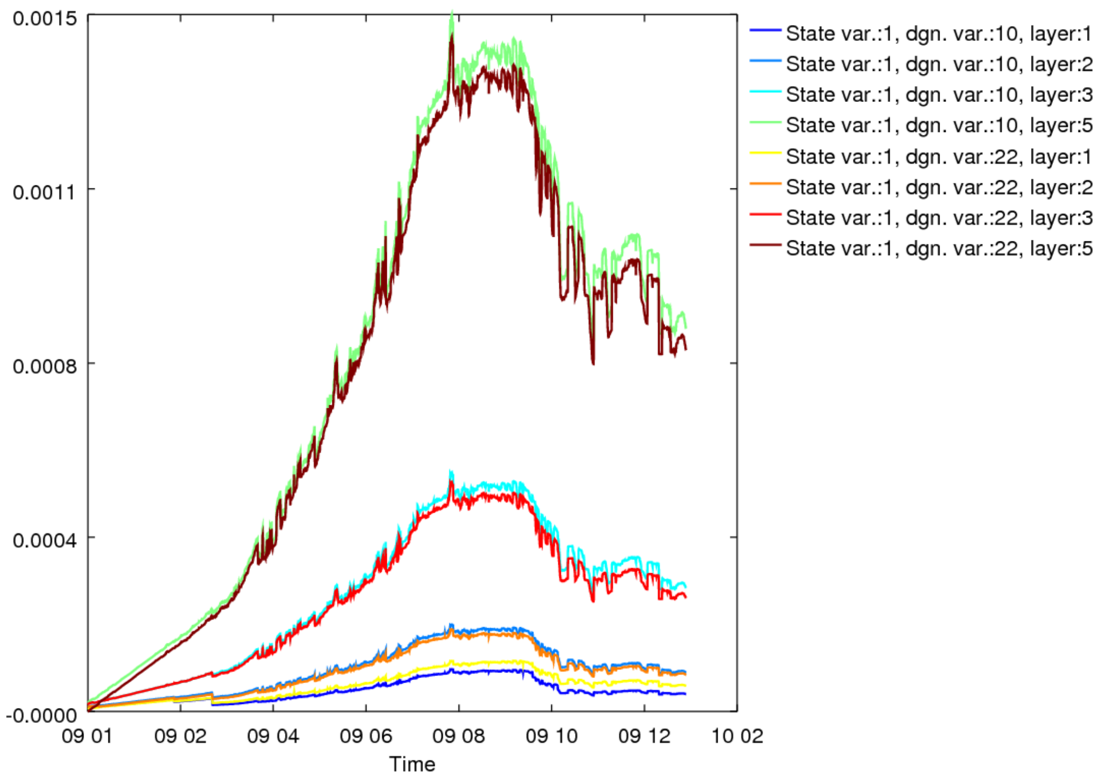

Figure 6: Selected diagnostic variables and layers of water column variable, simulation – 3D.

An example of modelled hydrodynamic variable (temperature) and its observed values is shown in figure 7. Parameter `vis_var` is set to `'5'`. Since the simulation is 2D, no additional parameters need adjustment.

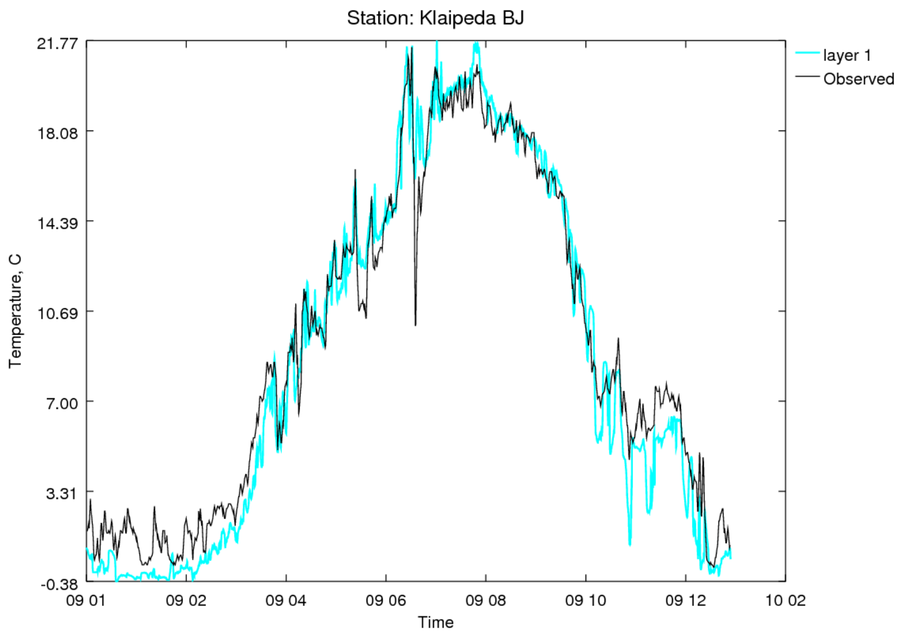

Figure 7: Temperature, simulation – 2D.

When the performed simulation is 3D, then there is required to adjust an additional parameter `layerplot`. It can be set to:

- 1 – plot all layers (Figure 8);
- 2 – plot average of layers (Figure 9);
- 3 – plot only layers with given numbers (Figure 10). In the example the variable is set to: `layerplot = '3-1,3:5'`, which means that there will be plotted layers 1,3,4 and 5.

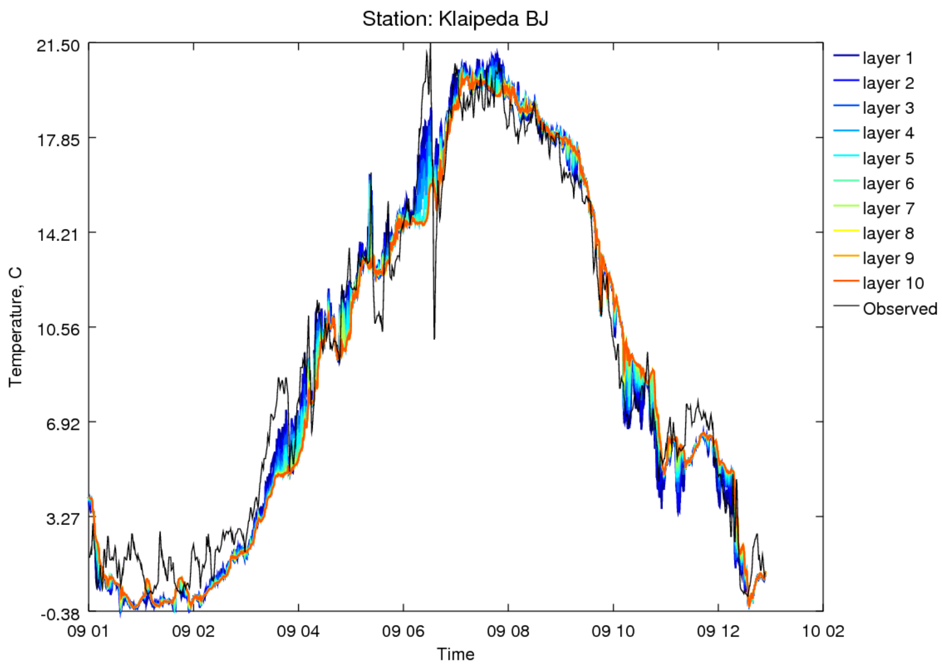

Figure 8: Temperature, simulation – 3D, all layers.

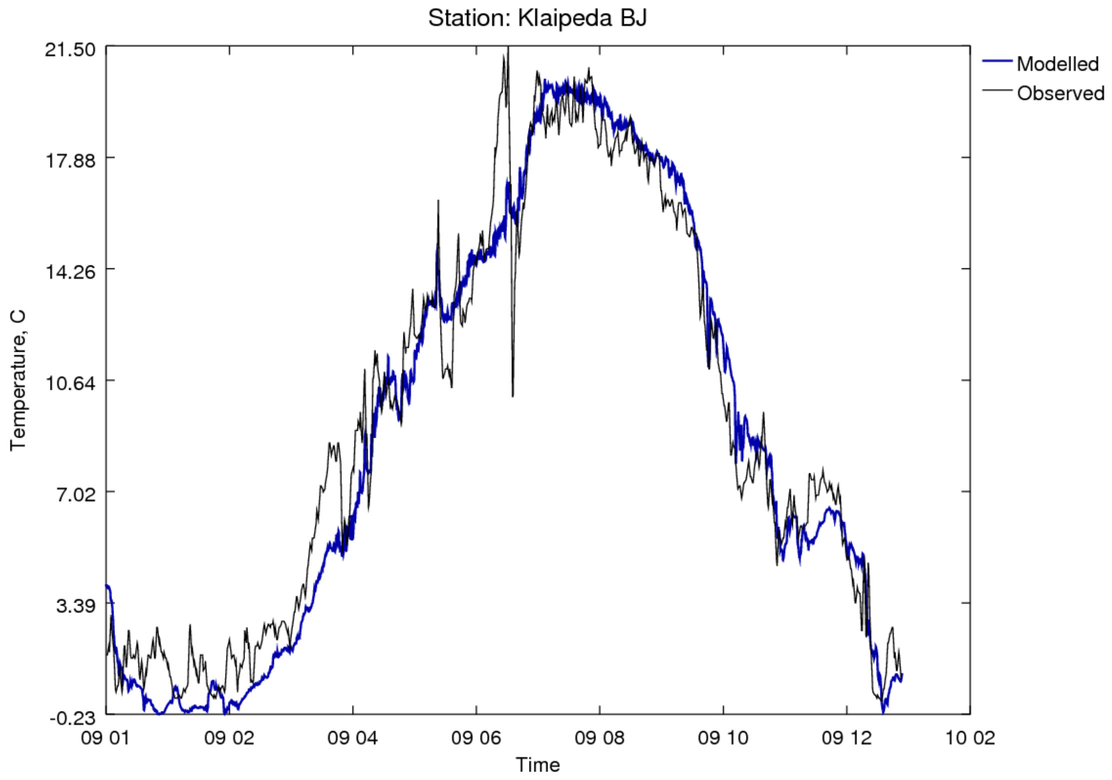

Figure 9: Temperature, simulation – 3D, average of layers.

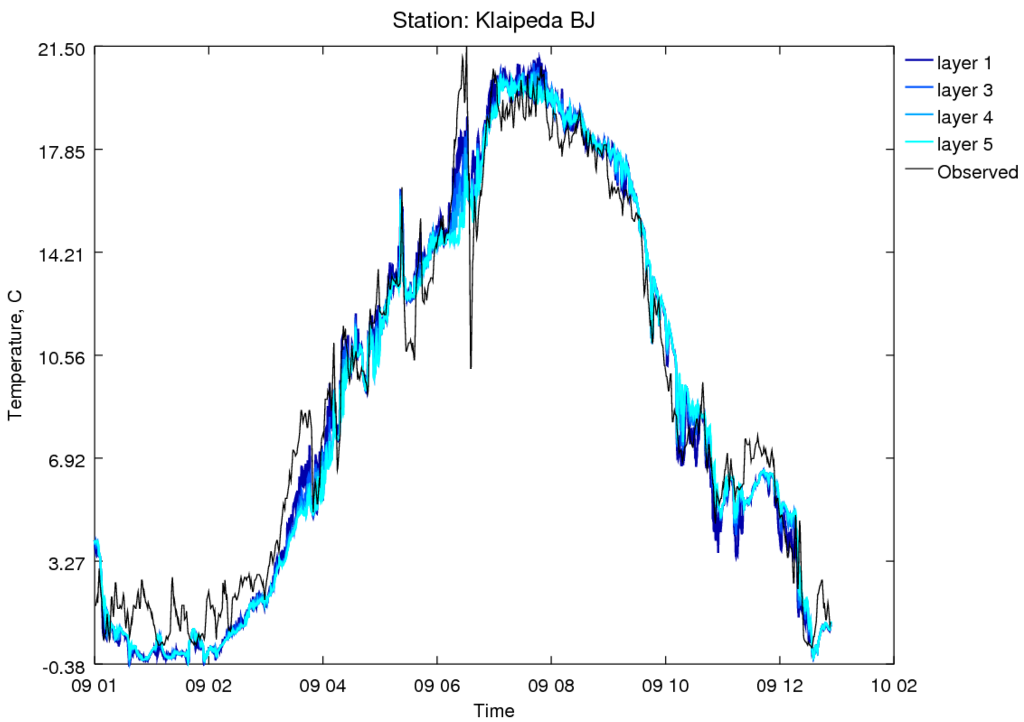

Figure 10: Temperature, simulation – 3D, selected layers.

Depth profile of the same hydrodynamic variable can be plotted when `vis_var = '6'` (Figure 11). For the depth profiles there is required an averaging time period and the values were set to:

```
from = '20090101 060000';
to   = '20091231 200000';
```

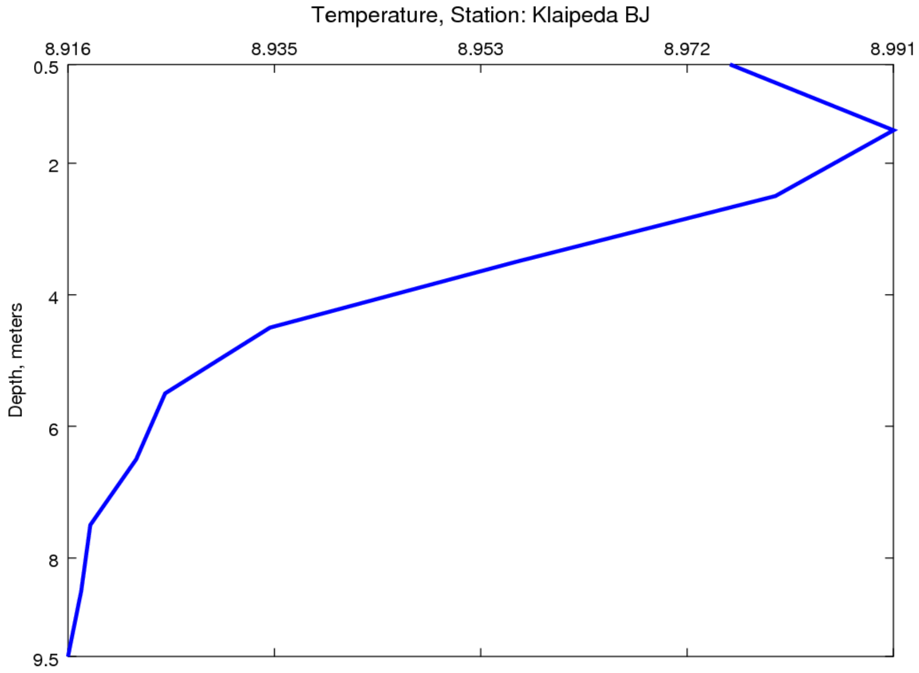

Figure 11: Depth profile of temperature.

When comparing two or more simulations the visualisation parameter `vis_var` has to be set to `'7'`. This option requires adjusting additional parameter `lay`, which is responsible for layers visualisation type. It has three possible options:

- 1 – plot all layers (only available for comparing 2 simulations). An example of comparison of two simulations is shown in figure 12. The main simulation is 3D (5 layers) and it is compared with 2D simulation (1 layer).
- 2 – plot average of layers. An example of this option is shown in figure 13. There are compared three simulations: the main one is 3D and it is compared with two 2D simulations.
- 3 – plot top and bottom layers. Figure 14 shows another example of comparing three simulations. The simulations are the same as previously mentioned (3D, 2D and 2D), just the top and bottom layers were plotted of the 3D simulation.

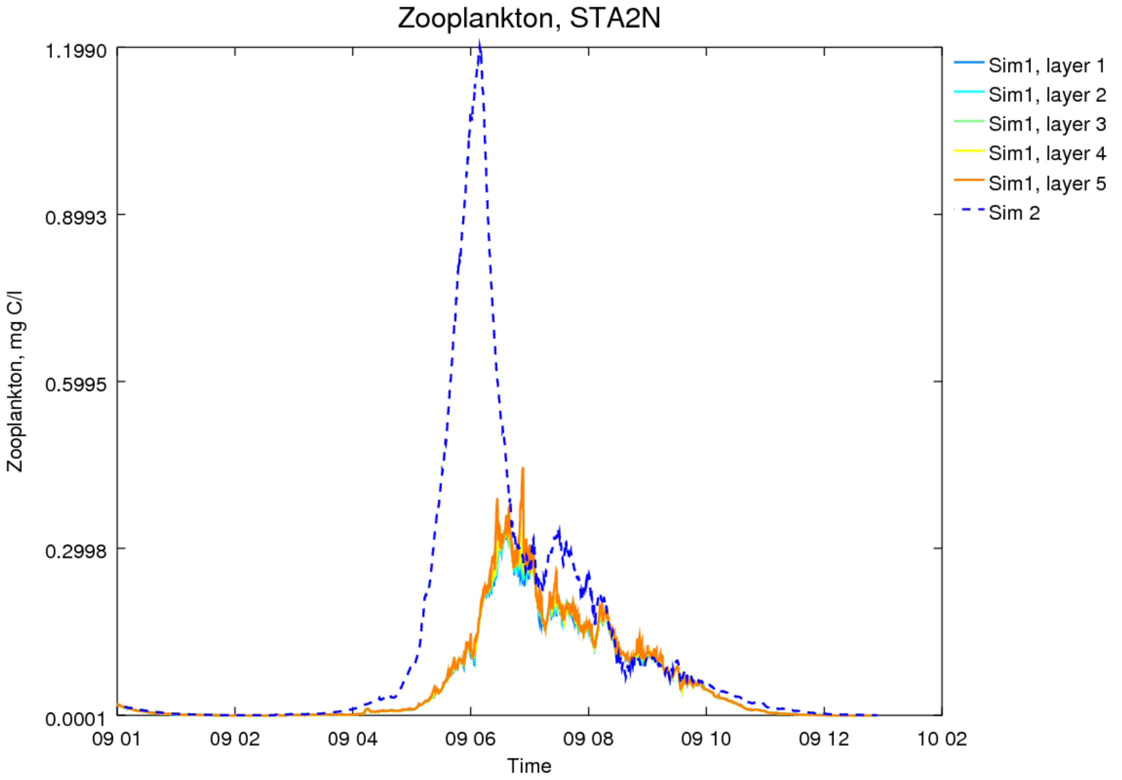

Figure 12: Comparison of two simulations (3D and 2D), all layers.

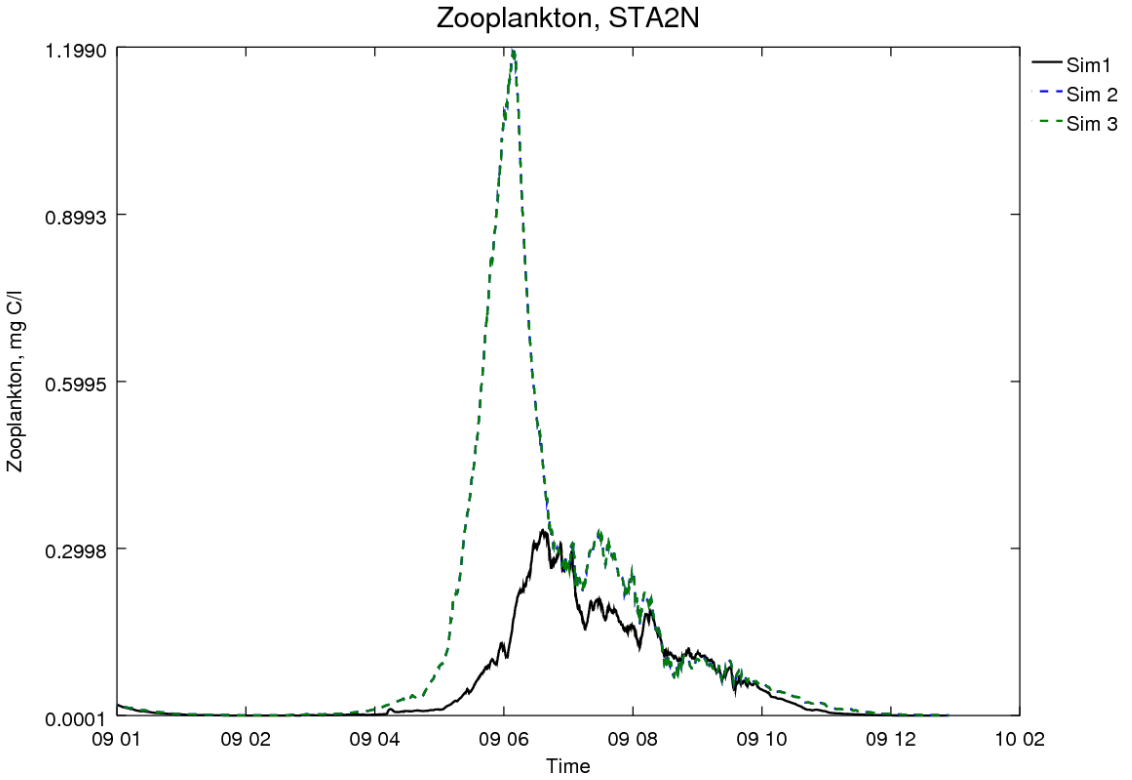

Figure 13: Comparison of three simulations (3D, 2D and 2D), average of layers.

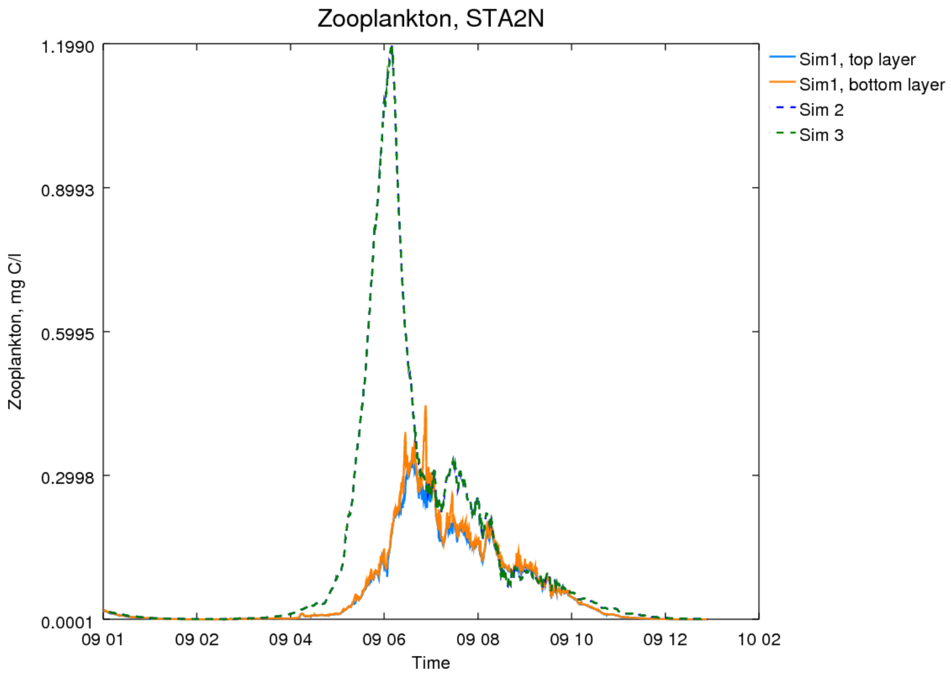

Figure 14: Comparison of three simulations (3D, 2D and 2D), top and bottom layers of 3D simulation.

When the visualisation parameter is set to calculate statistics (`vis_var = '8'` for state (derived) biogeochemical variables or `vis_var= '9'` for hydrodynamic variables), then there is derived an output statistics file, which has the name of the variable (for hydrodynamic variables) or the environment (for biogeochemical variables). An example of one station's hydrodynamic variable (temperature) in such file is presented below. On the left there are statistics when the performed simulation is 2D and on the right – when the simulation is 3D. The difference is that when the simulation is 3D, then there are additionally computed statistics for each layer.

```
Station: Vente, node: 1947

   Modelled (all):
    min = -0.01949
    max = 23.03
    mean = 8.7728
    std = 7.804

Measured mean = 9.7082
Measured std = 7.8931

RMSE = 1.5572
R squared = 0.9764
```

```
Station: Vente, node: 1947, units: C

Modelled layer 1
   min = -0.005757
   max = 23.93
   mean = 9.2426
   std = 7.9726

Modelled layer 2
   min = -0.005757
   max = 23.94
   mean = 9.2486
   std = 7.9684

Modelled (all):
   min = -0.005757
   max = 23.94
   mean = 9.2456
   std = 7.9701

Measured mean = 9.7082
Measured std = 7.8931

RMSE = 1.2576
R squared = 0.97895
```

In one statistics file of state (derived) biogeochemical variables (water column or sediments) there are stored all calculations of all stations and all variables that were specified to be processed (in AQUABC configuration files). When it is set to calculate statistics for hydrodynamic variables, then there are created files for each variable; in those files there are stored all calculations of all stations that were specified to be processed (in **.vish* file). The same statistics output structure (above) is for both – state (derived) biogeochemical and hydrodynamical variables, the only difference is in the first row – in state variables output instead of node number there is written a variable name.

Temperature (with and without natural ice cover conditions)

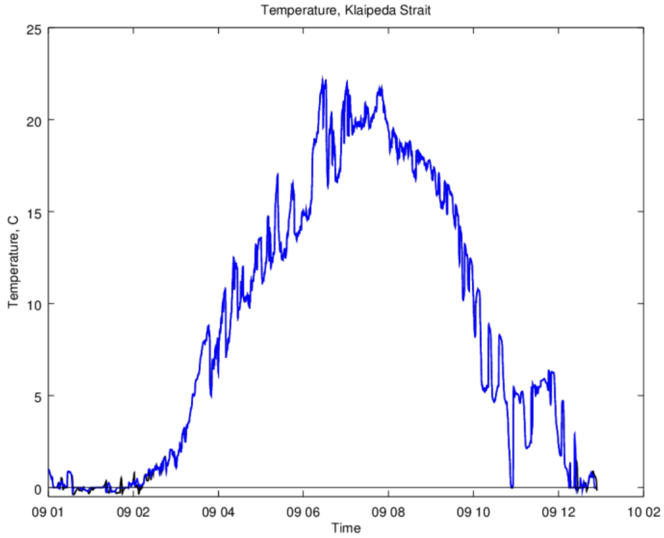

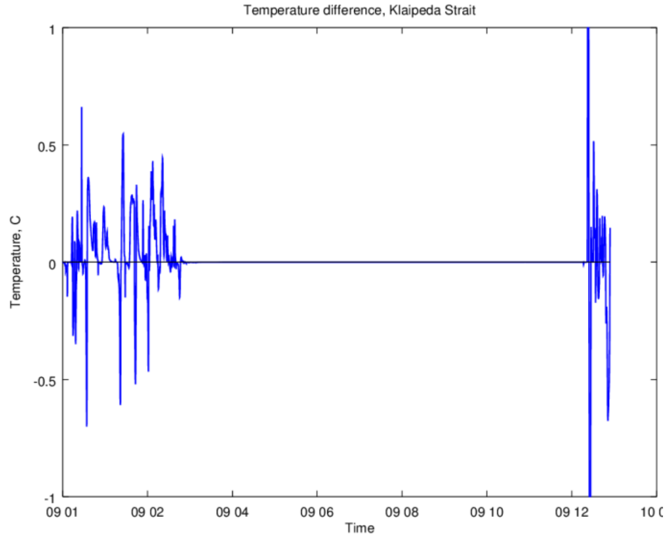

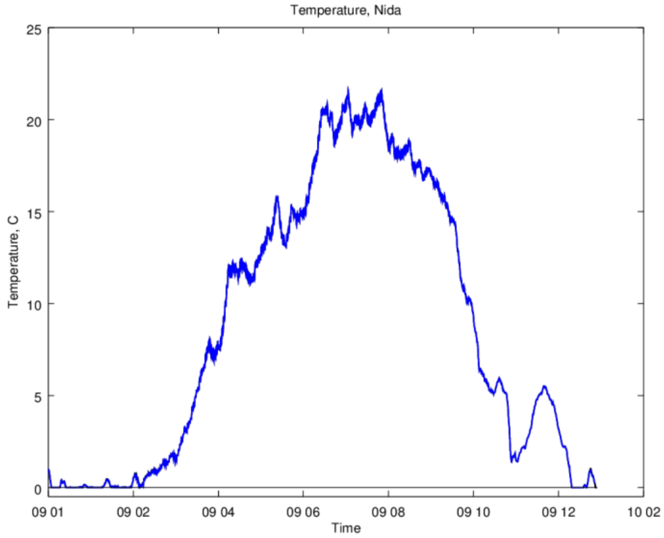

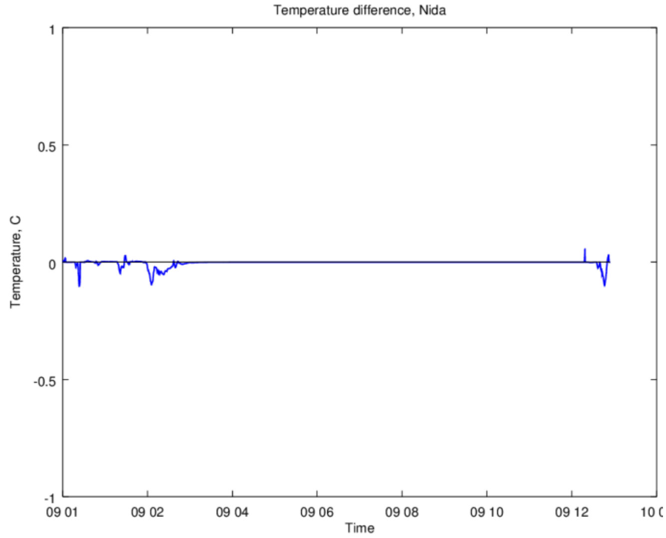

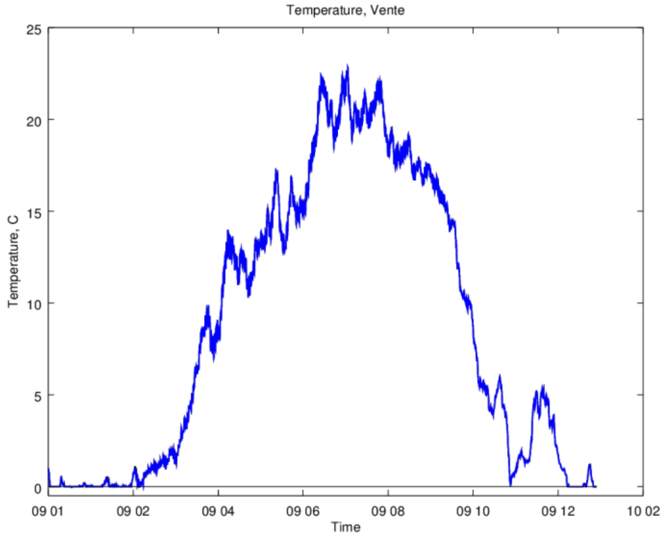

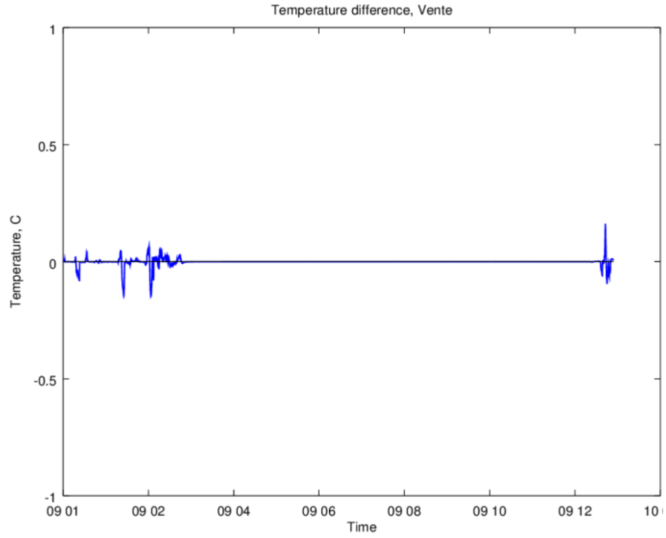

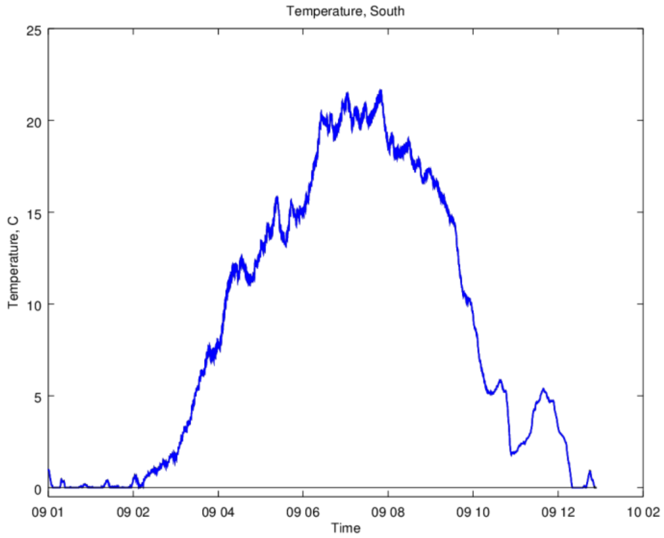
Temperature, South
Temperature, C
25
20
15
10
5
0
09 01
09 02
09 04
09 06
09 08
09 10
09 12
10 02
Time

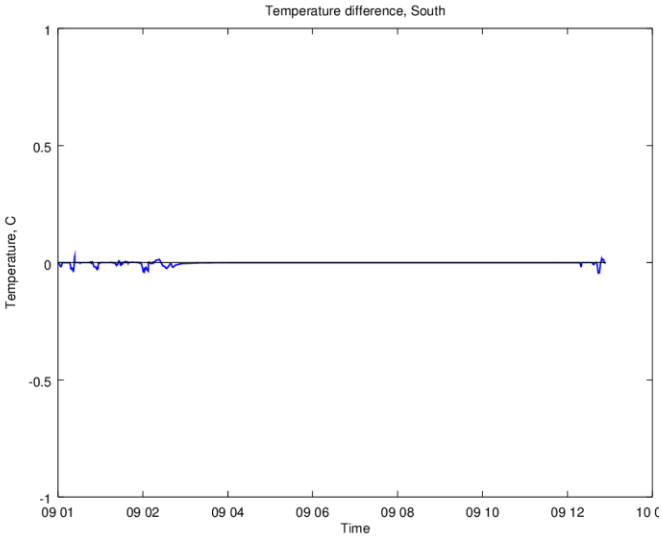
Temperature difference, South
Temperature, C
1
0.5
0
-0.5
-1
09 01
09 02
09 04
09 06
09 08
09 10
09 12
Time

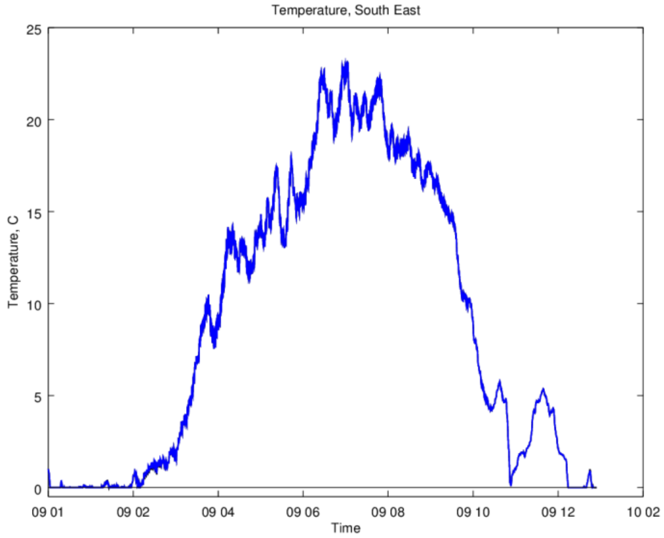
Temperature, South East
Temperature, C
25
20
15
10
5
0
09 01
09 02
09 04
09 06
09 08
09 10
09 12
10 02
Time

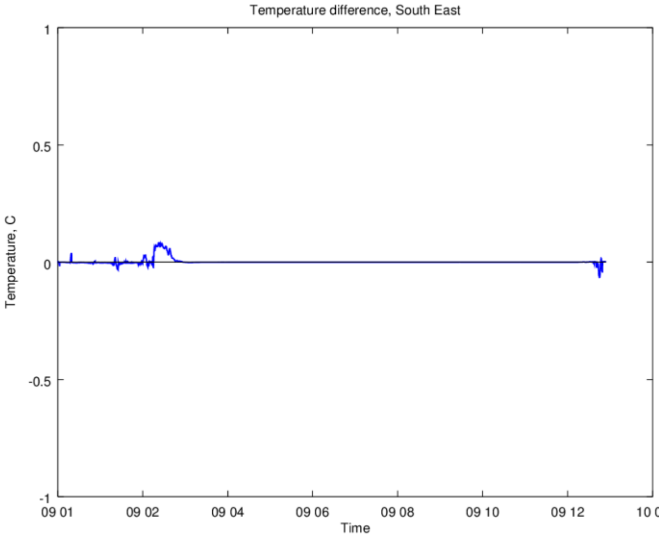
Temperature difference, South East
Temperature, C
1
0.5
0
-0.5
-1
09 01
09 02
09 04
09 06
09 08
09 10
09 12
Time

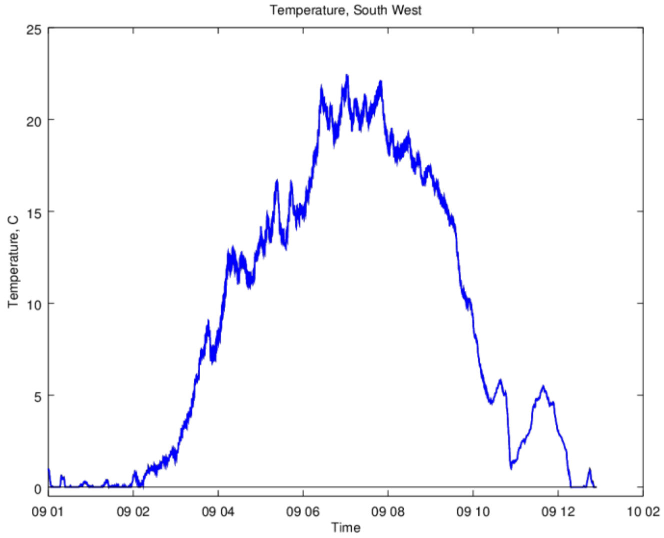
Temperature, South West
Temperature, C
25
20
15
10
5
0
09 01
09 02
09 04
09 06
09 08
09 10
09 12
10 02
Time

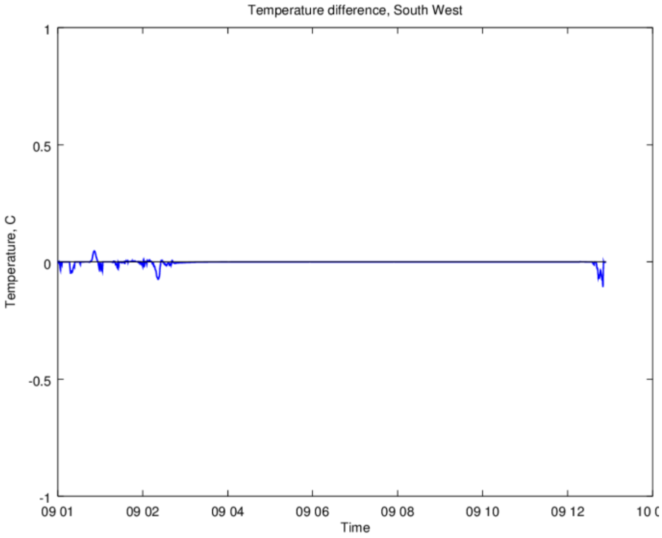
Temperature difference, South West
Temperature, C
1
0.5
0
-0.5
-1
09 01
09 02
09 04
09 06
09 08
09 10
09 12
Time

Salinity (with and without natural ice cover conditions)

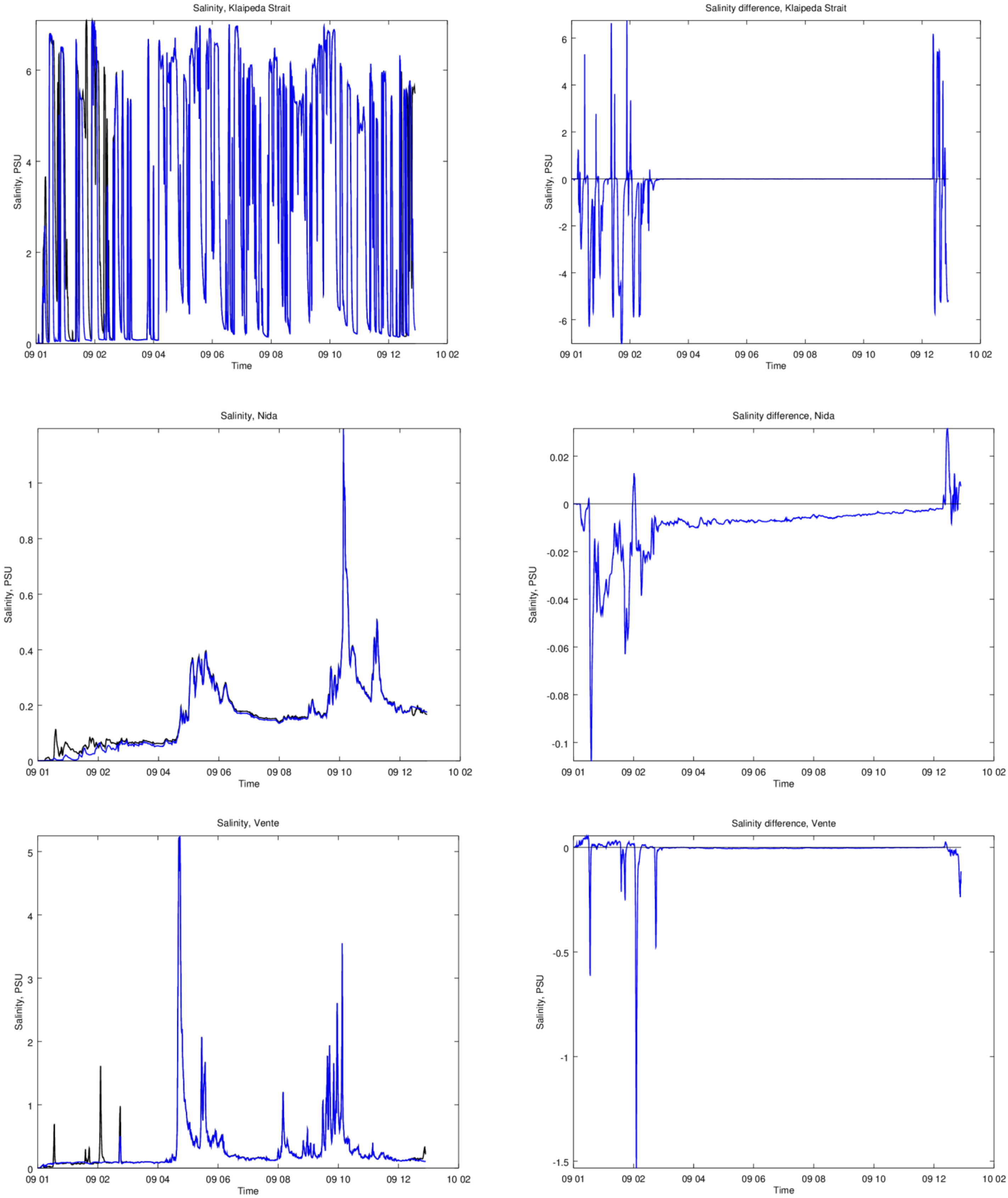

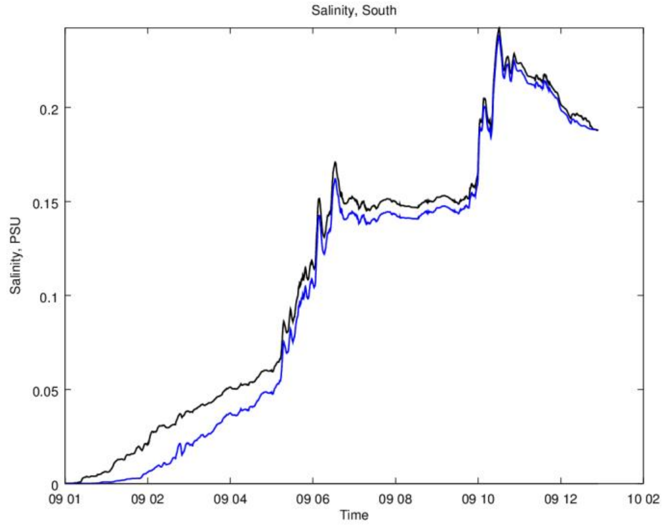
Salinity, South
Salinity, PSU
Time
0.2
0.15
0.1
0.05
0
09 01
09 02
09 04
09 06
09 08
09 10
09 12
10 02

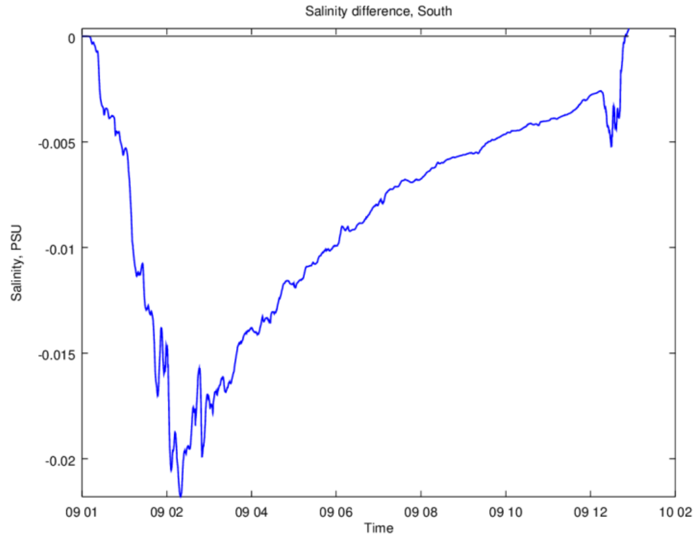
Salinity difference, South
Salinity, PSU
Time
0
-0.005
-0.01
-0.015
-0.02
09 01
09 02
09 04
09 06
09 08
09 10
09 12
10 02

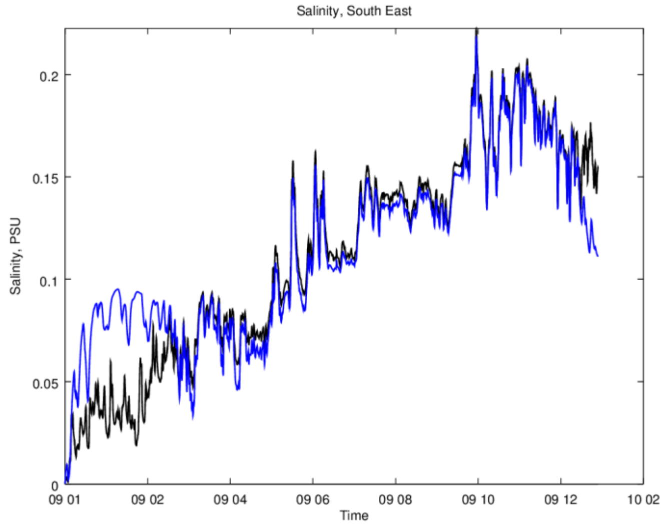
Salinity, South East
Salinity, PSU
Time
0.2
0.15
0.1
0.05
0
09 01
09 02
09 04
09 06
09 08
09 10
09 12
10 02

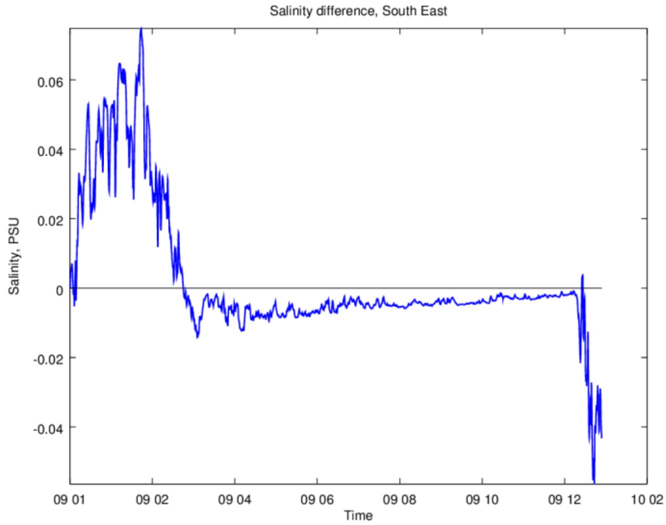
Salinity difference, South East
Salinity, PSU
Time
0.06
0.04
0.02
0
-0.02
-0.04
09 01
09 02
09 04
09 06
09 08
09 10
09 12
10 02

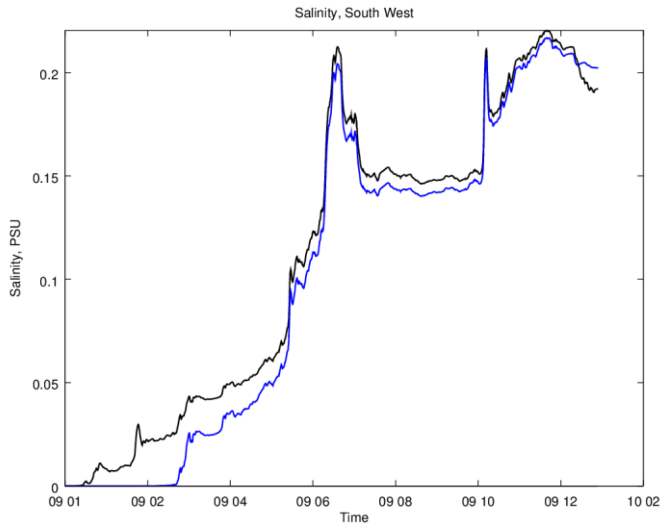
Salinity, South West
Salinity, PSU
Time
0.2
0.15
0.1
0.05
0
09 01
09 02
09 04
09 06
09 08
09 10
09 12
10 02

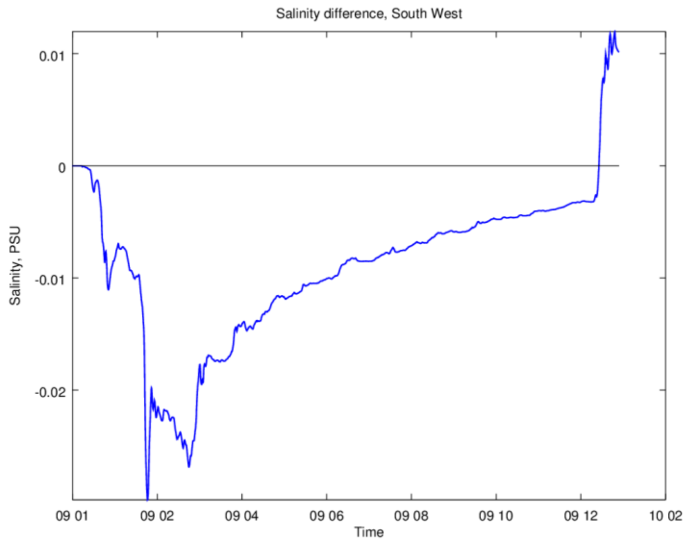
Salinity difference, South West
Salinity, PSU
Time
0.01
0
-0.01
-0.02
09 01
09 02
09 04
09 06
09 08
09 10
09 12
10 02

Dissolved oxygen (with and without natural ice cover conditions)

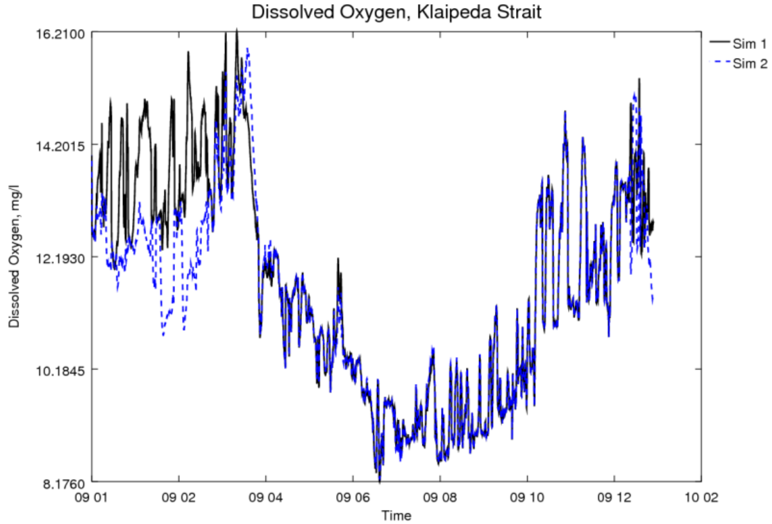

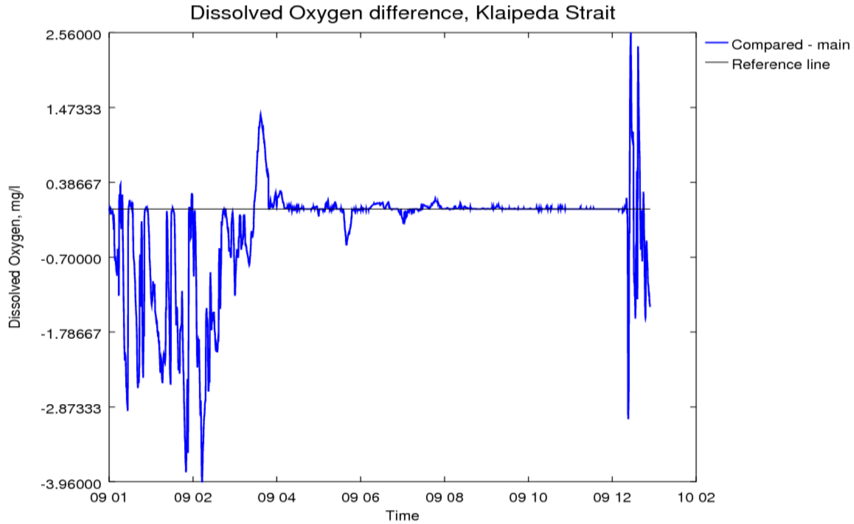

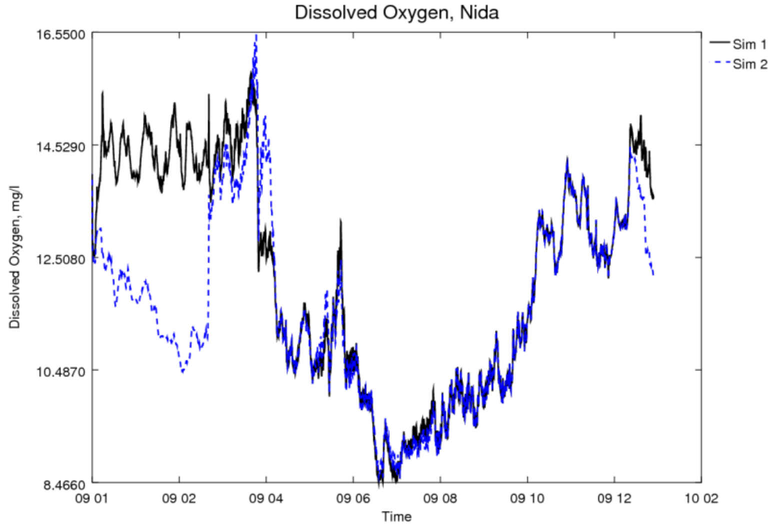

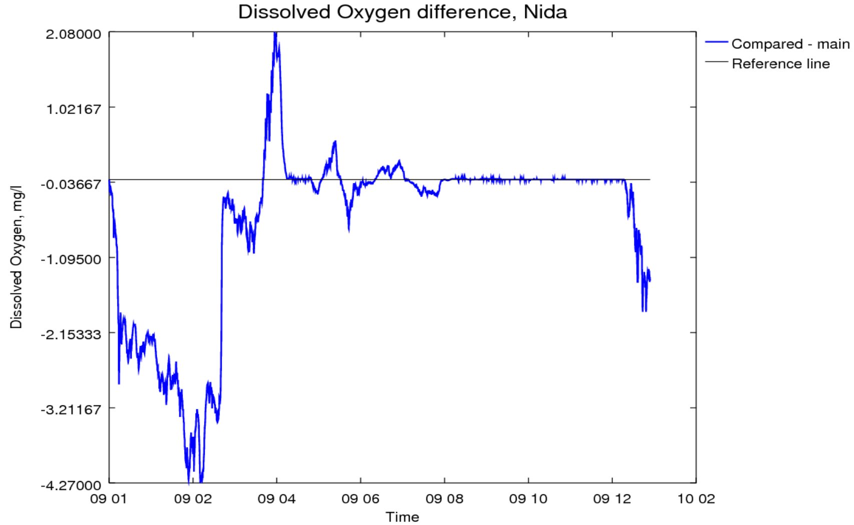

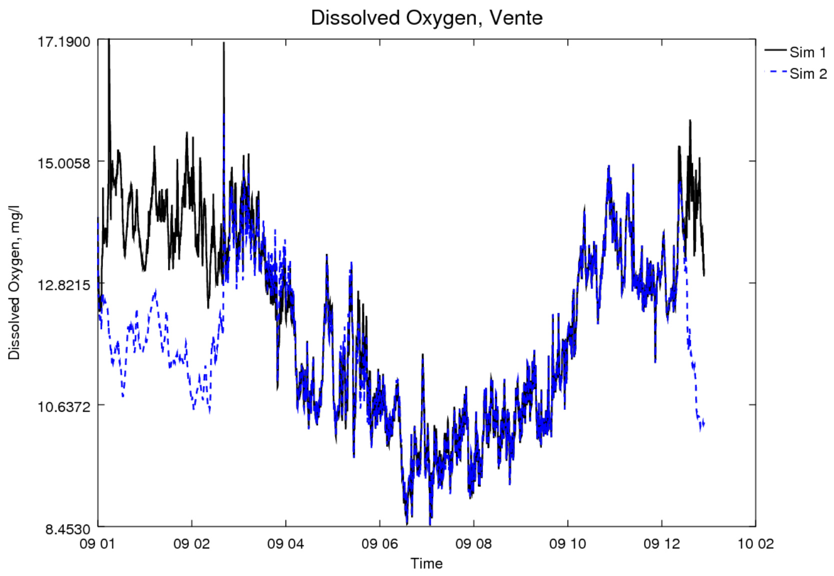
Dissolved Oxygen, Vente
Sim 1
Sim 2
17.1900
15.0058
12.8215
10.6372
8.4530
Dissolved Oxygen, mg/l
09 01
09 02
09 04
09 06
09 08
09 10
09 12
10 02
Time

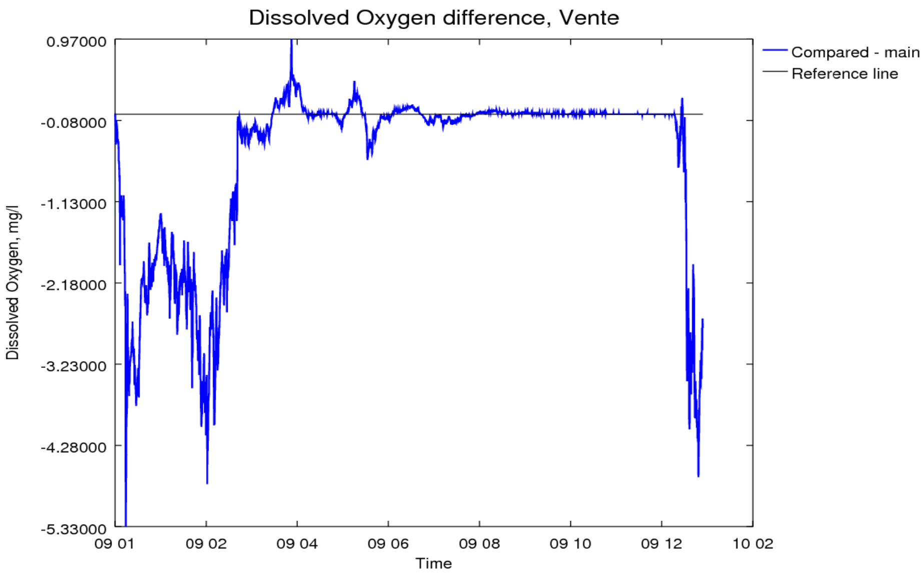
Dissolved Oxygen difference, Vente
Compared - main
Reference line
0.97000
-0.08000
-1.13000
-2.18000
-3.23000
-4.28000
-5.33000
Dissolved Oxygen, mg/l
09 01
09 02
09 04
09 06
09 08
09 10
09 12
10 02
Time

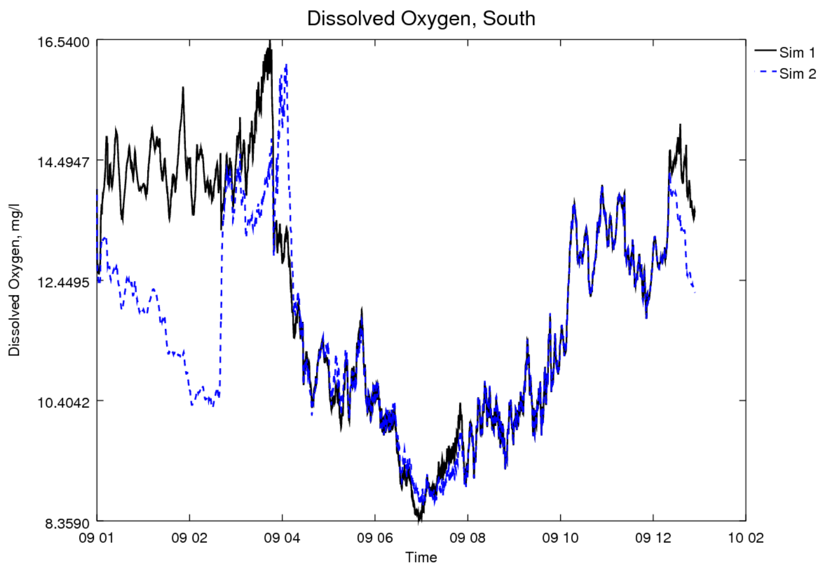
Dissolved Oxygen, South
Sim 1
Sim 2
16.5400
14.4947
12.4495
10.4042
8.3590
Dissolved Oxygen, mg/l
09 01
09 02
09 04
09 06
09 08
09 10
09 12
10 02
Time

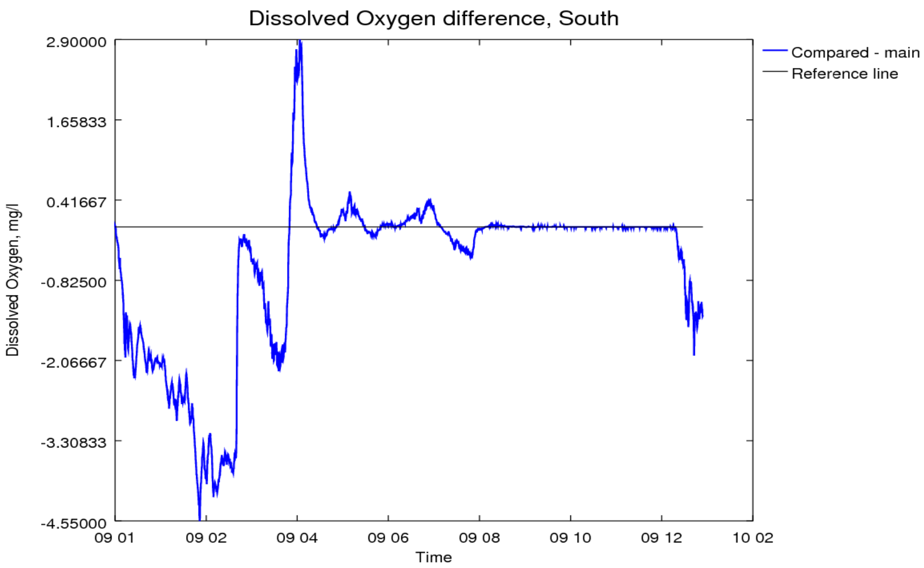
Dissolved Oxygen difference, South
Compared - main
Reference line
2.90000
1.65833
0.41667
-0.82500
-2.06667
-3.30833
-4.55000
Dissolved Oxygen, mg/l
09 01
09 02
09 04
09 06
09 08
09 10
09 12
10 02
Time

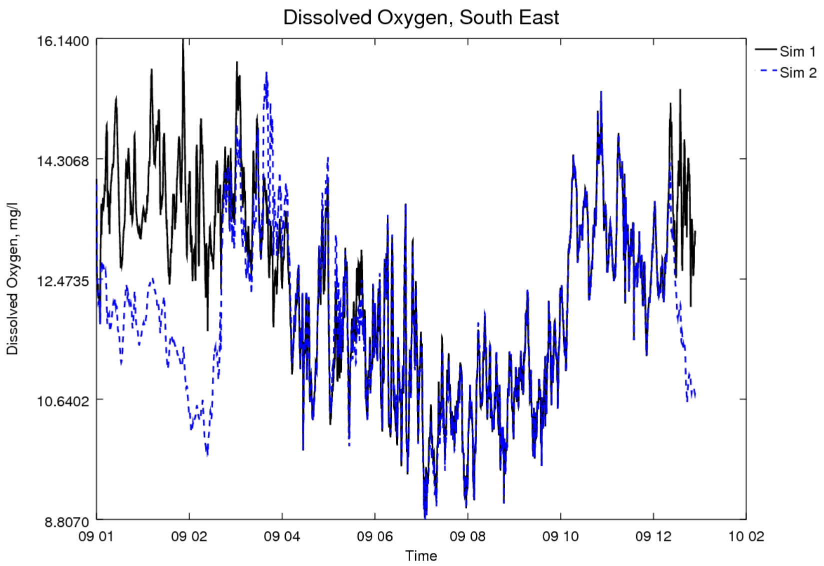
Dissolved Oxygen, South East
16.1400
14.3068
12.4735
10.6402
8.8070
Dissolved Oxygen, mg/l
09 01
09 02
09 04
09 06
09 08
09 10
09 12
10 02
Time
Sim 1
Sim 2

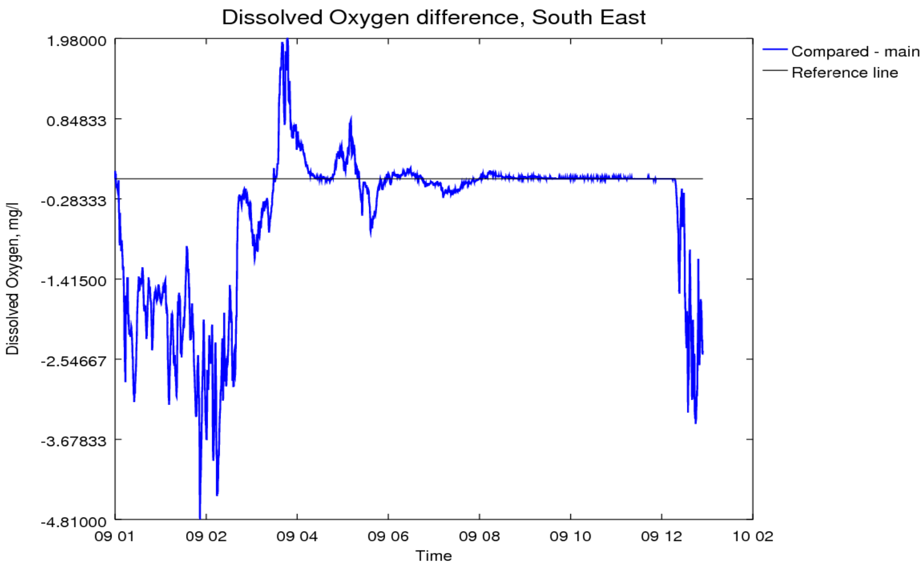
Dissolved Oxygen difference, South East
1.98000
0.84833
-0.28333
-1.41500
-2.54667
-3.67833
-4.81000
Dissolved Oxygen, mg/l
09 01
09 02
09 04
09 06
09 08
09 10
09 12
10 02
Time
Compared - main
Reference line

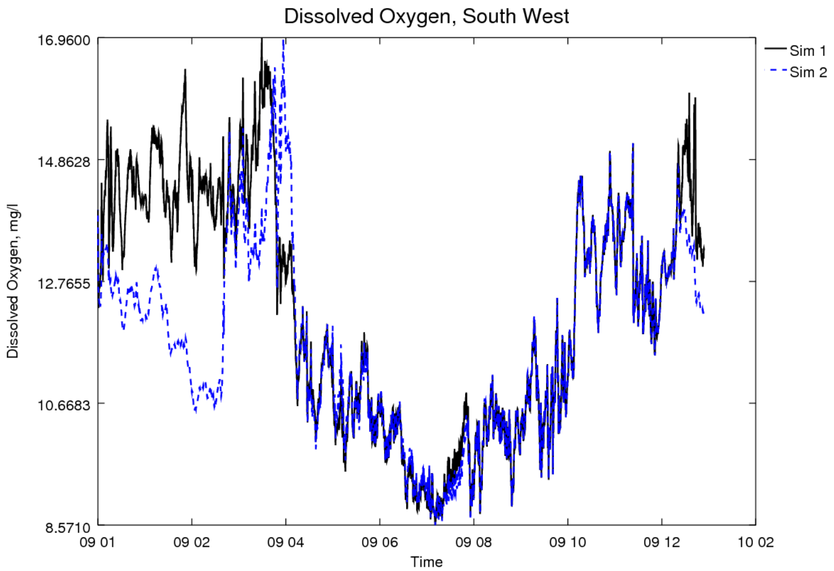
Dissolved Oxygen, South West
16.9600
14.8628
12.7655
10.6683
8.5710
Dissolved Oxygen, mg/l
09 01
09 02
09 04
09 06
09 08
09 10
09 12
10 02
Time
Sim 1
Sim 2

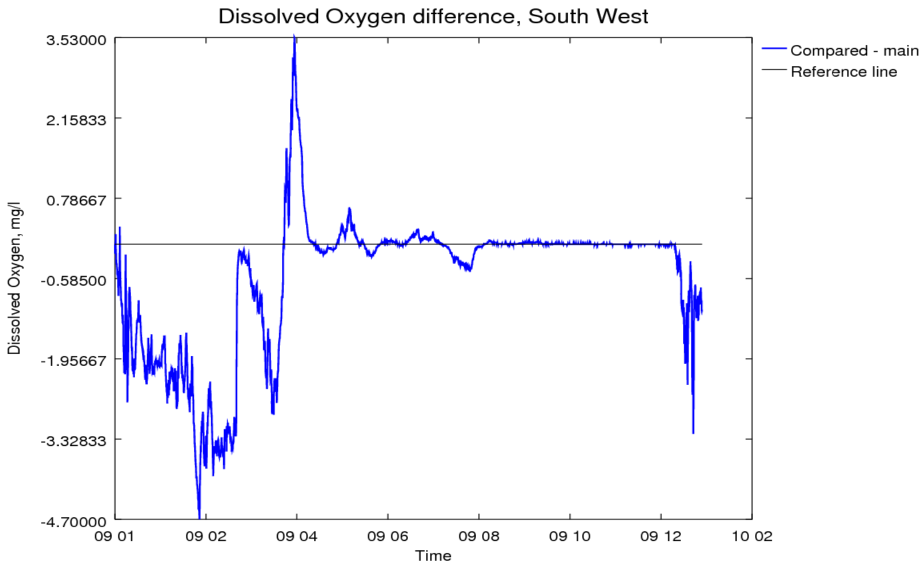
Dissolved Oxygen difference, South West
3.53000
2.15833
0.78667
-0.58500
-1.95667
-3.32833
-4.70000
Dissolved Oxygen, mg/l
09 01
09 02
09 04
09 06
09 08
09 10
09 12
10 02
Time
Compared - main
Reference line

Dissolved oxygen concentrations (reference with only reaeration suppressed)

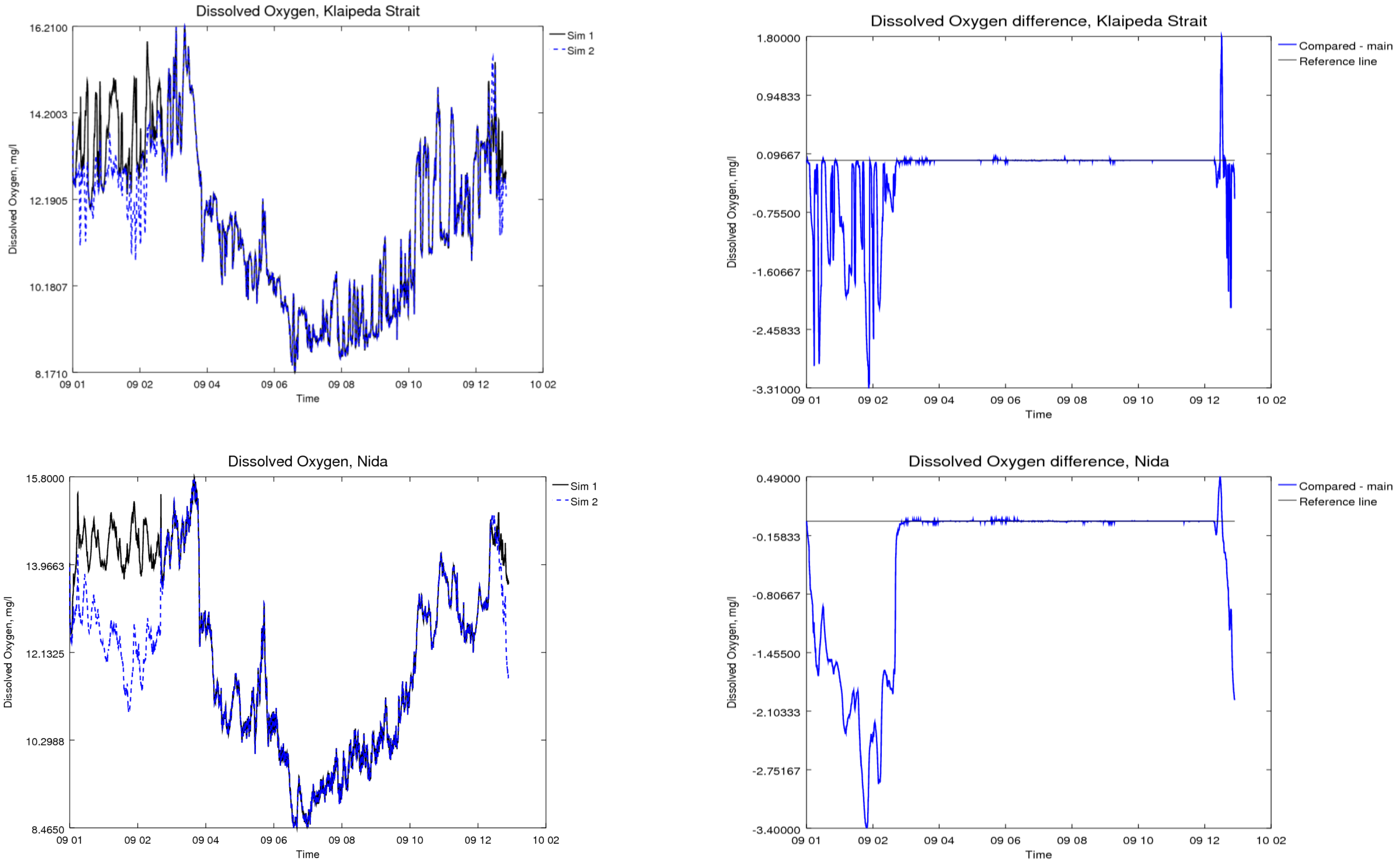

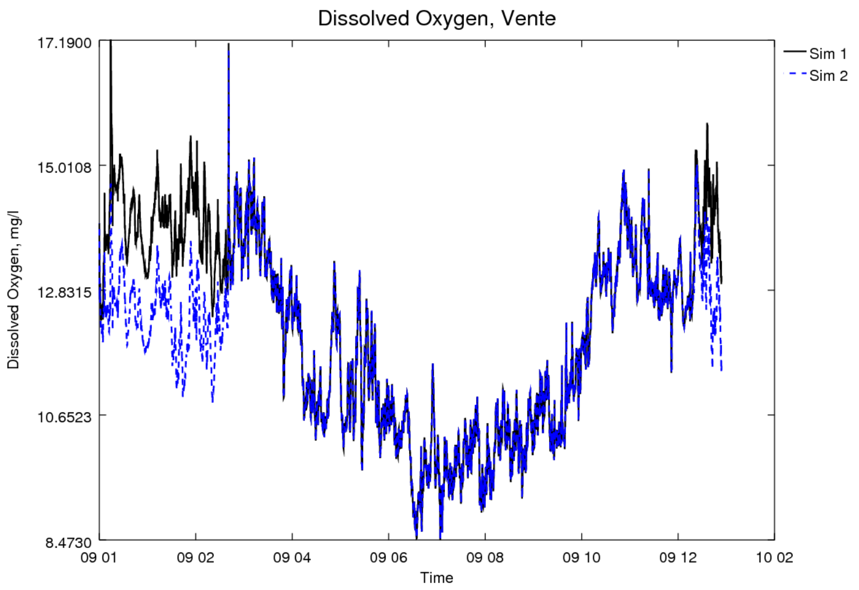
Dissolved Oxygen, Vente
17.1900
15.0108
12.8315
10.6523
8.4730
Dissolved Oxygen, mg/l
09 01
09 02
09 04
09 06
09 08
09 10
09 12
10 02
Time
Sim 1
Sim 2

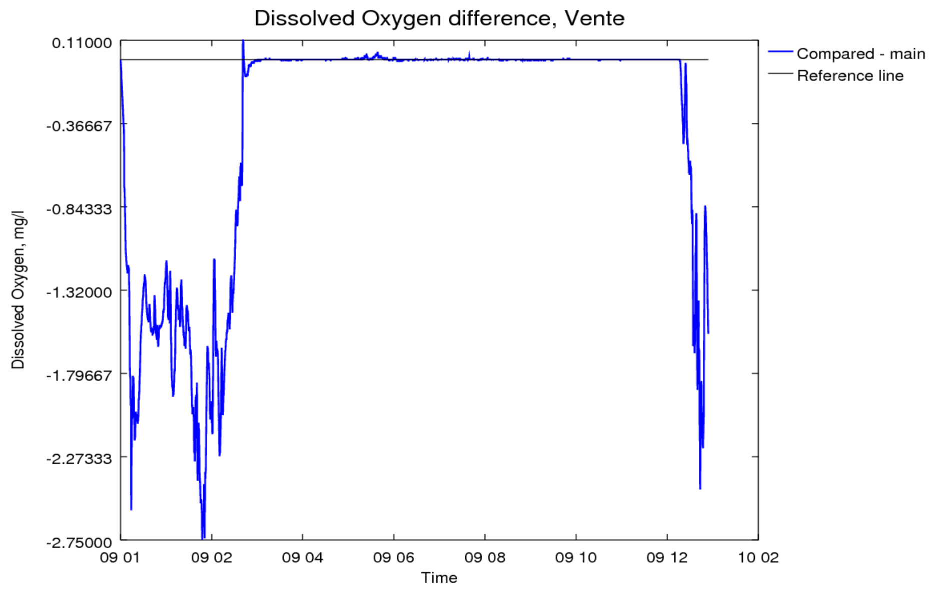
Dissolved Oxygen difference, Vente
0.11000
-0.36667
-0.84333
-1.32000
-1.79667
-2.27333
-2.75000
Dissolved Oxygen, mg/l
09 01
09 02
09 04
09 06
09 08
09 10
09 12
10 02
Time
Compared - main
Reference line

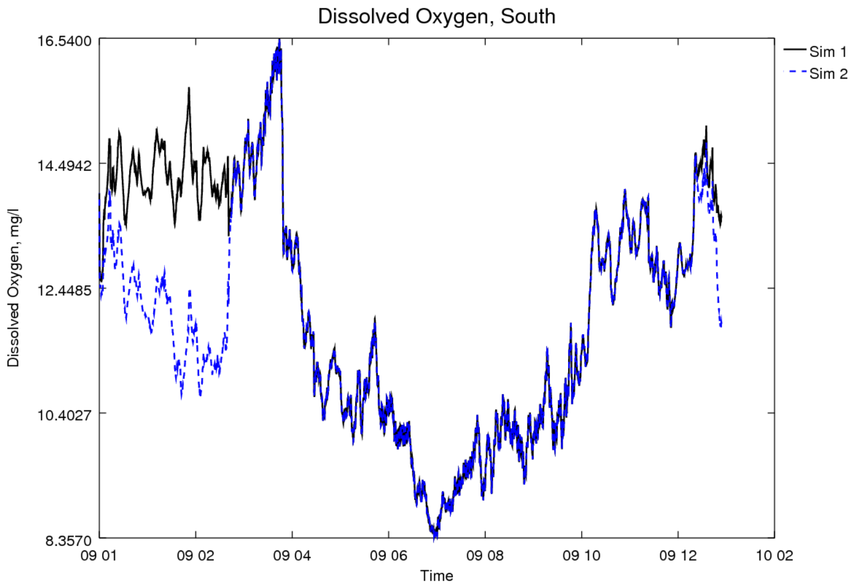
Dissolved Oxygen, South
16.5400
14.4942
12.4485
10.4027
8.3570
Dissolved Oxygen, mg/l
09 01
09 02
09 04
09 06
09 08
09 10
09 12
10 02
Time
Sim 1
Sim 2

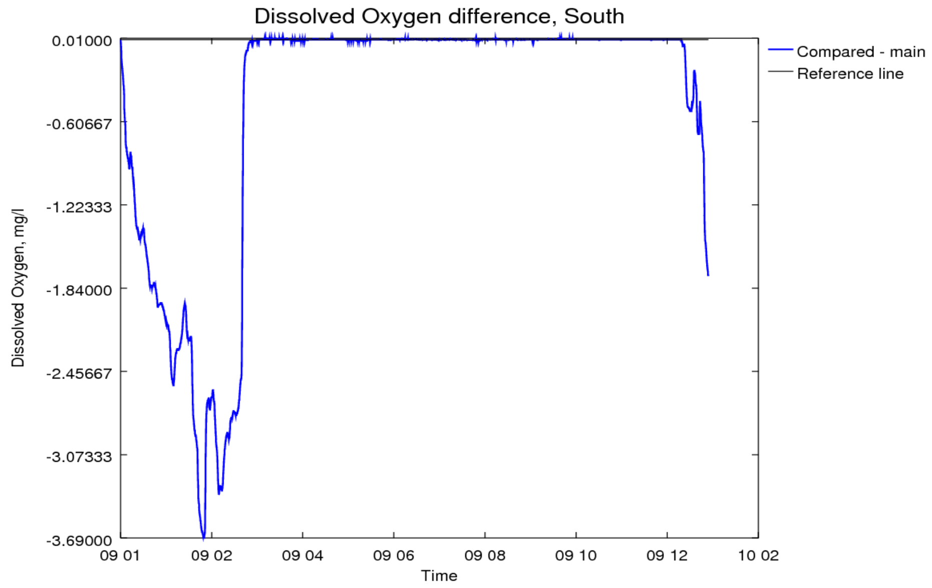
Dissolved Oxygen difference, South
0.01000
-0.60667
-1.22333
-1.84000
-2.45667
-3.07333
-3.69000
Dissolved Oxygen, mg/l
09 01
09 02
09 04
09 06
09 08
09 10
09 12
10 02
Time
Compared - main
Reference line

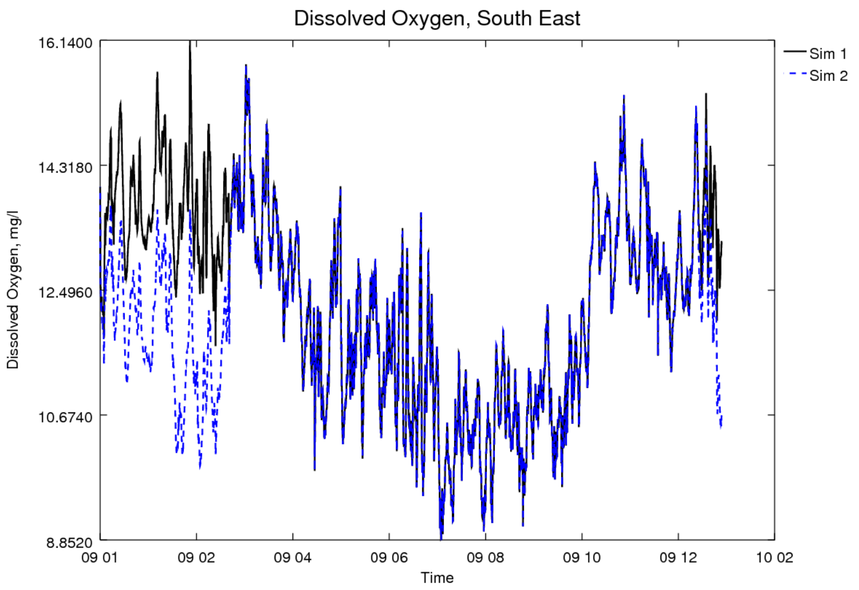
Dissolved Oxygen, South East
Sim 1
Sim 2
16.1400
14.3180
12.4960
10.6740
8.8520
Dissolved Oxygen, mg/l
09 01
09 02
09 04
09 06
09 08
09 10
09 12
10 02
Time

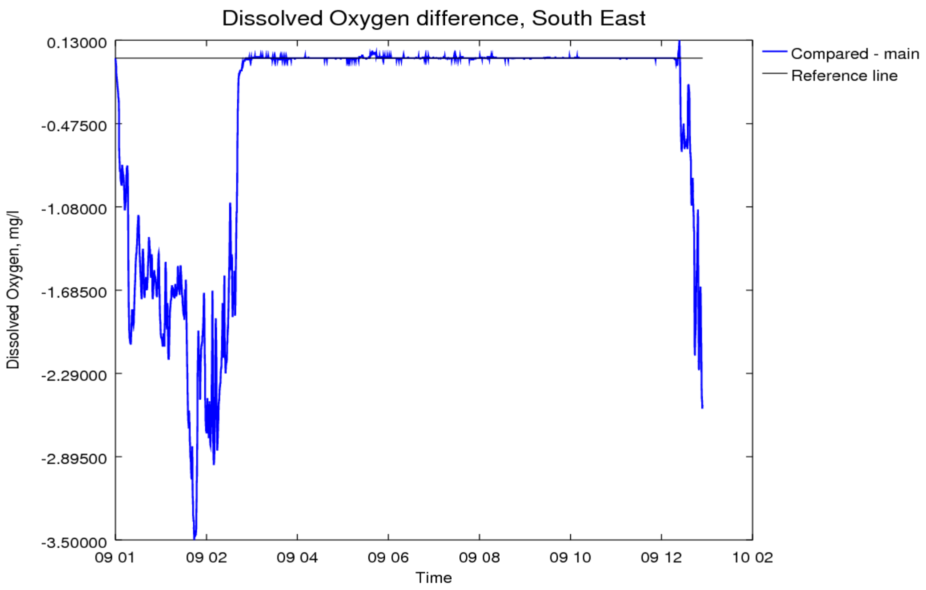
Dissolved Oxygen difference, South East
Compared - main
Reference line
0.13000
-0.47500
-1.08000
-1.68500
-2.29000
-2.89500
-3.50000
Dissolved Oxygen, mg/l
09 01
09 02
09 04
09 06
09 08
09 10
09 12
10 02
Time

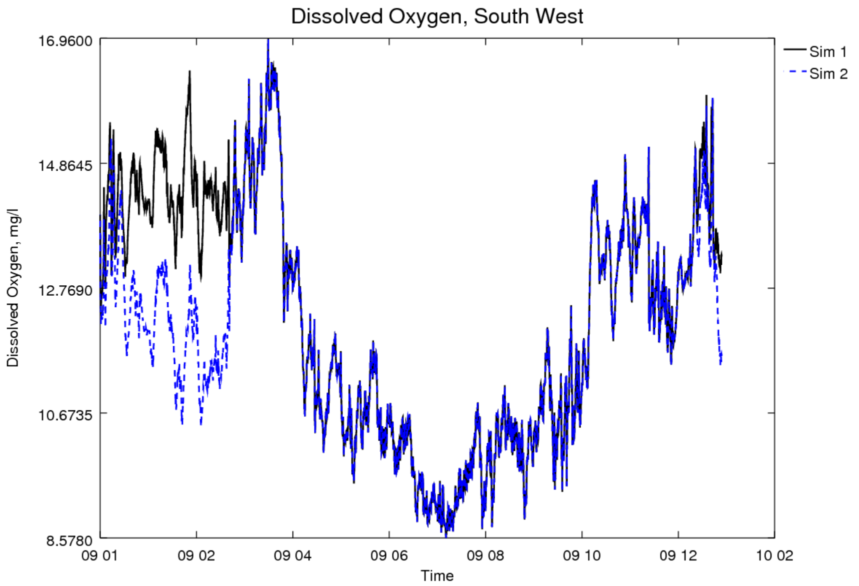
Dissolved Oxygen, South West
Sim 1
Sim 2
16.9600
14.8645
12.7690
10.6735
8.5780
Dissolved Oxygen, mg/l
09 01
09 02
09 04
09 06
09 08
09 10
09 12
10 02
Time

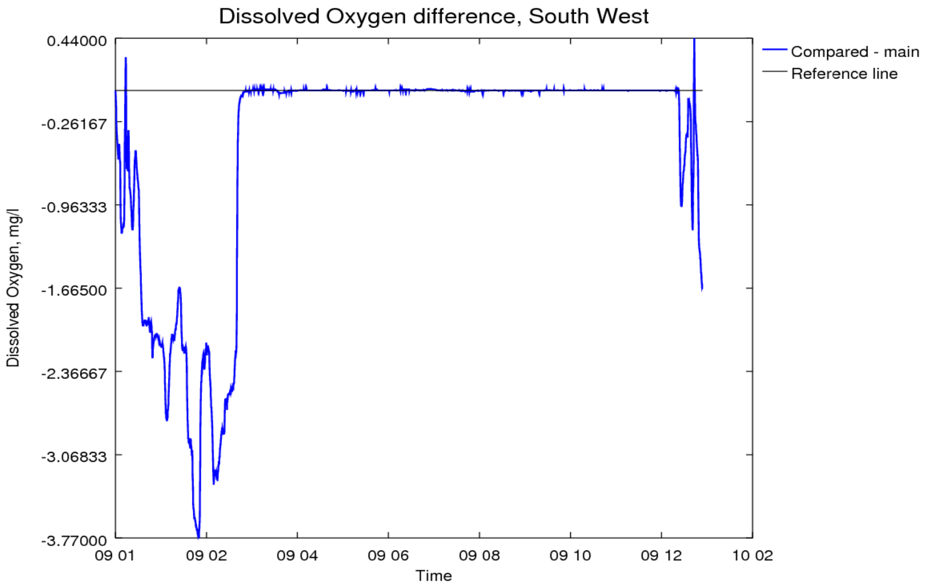
Dissolved Oxygen difference, South West
Compared - main
Reference line
0.44000
-0.26167
-0.96333
-1.66500
-2.36667
-3.06833
-3.77000
Dissolved Oxygen, mg/l
09 01
09 02
09 04
09 06
09 08
09 10
09 12
10 02
Time

Dissolved oxygen (reference with only light suppressed)

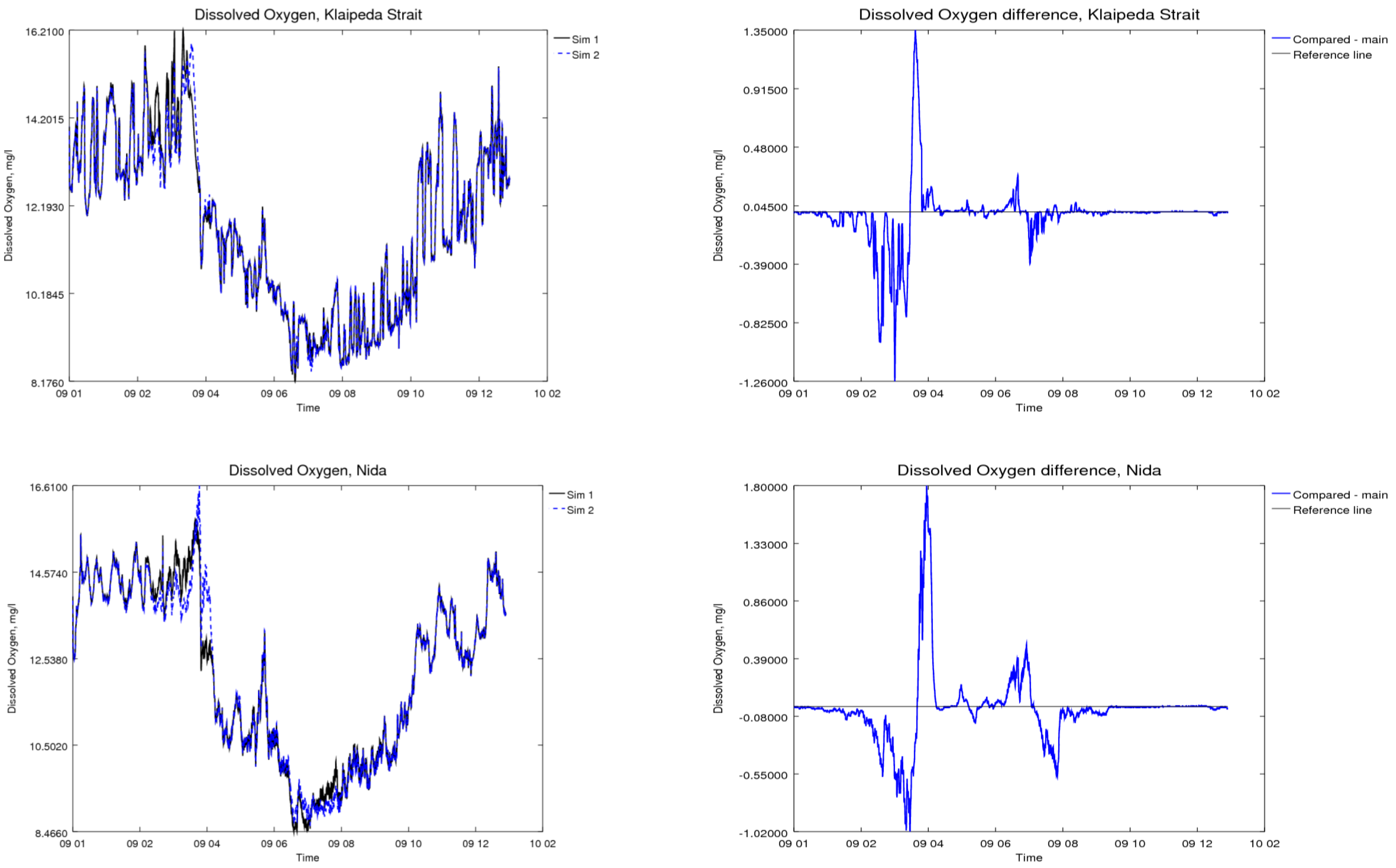

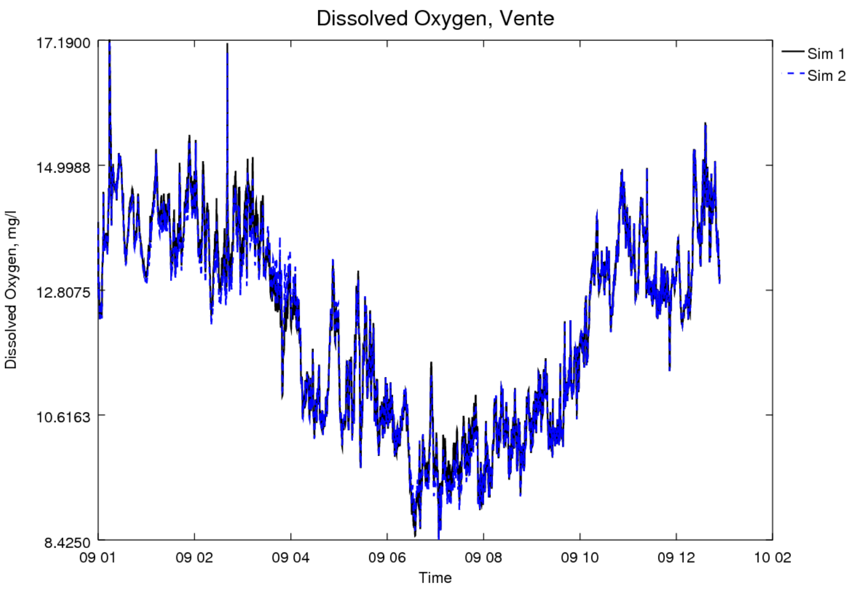
Dissolved Oxygen, Vente
Sim 1
Sim 2
Dissolved Oxygen, mg/l
17.1900
14.9988
12.8075
10.6163
8.4250
09 01
09 02
09 04
09 06
09 08
09 10
09 12
10 02
Time

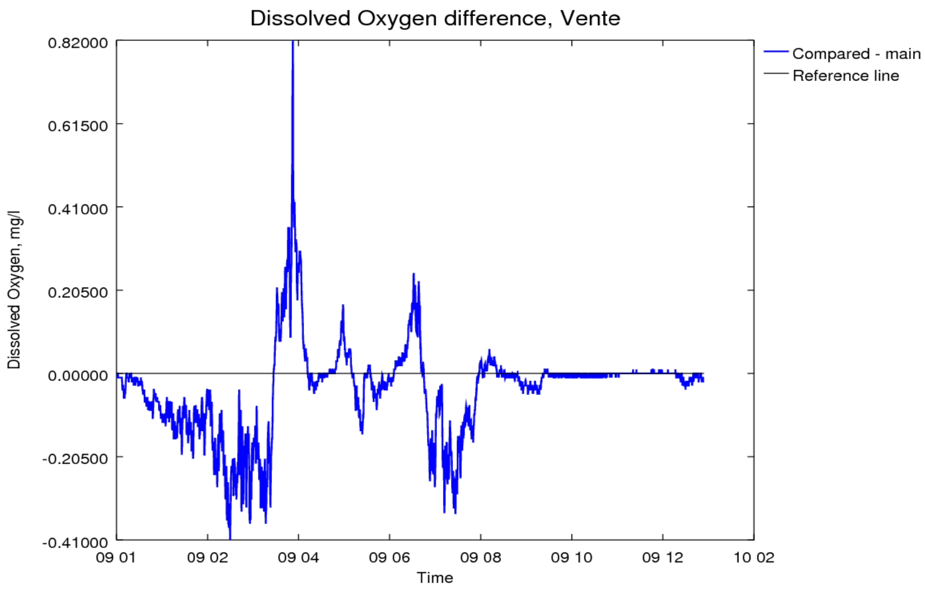
Dissolved Oxygen difference, Vente
Compared - main
Reference line
Dissolved Oxygen, mg/l
0.82000
0.61500
0.41000
0.20500
0.00000
-0.20500
-0.41000
09 01
09 02
09 04
09 06
09 08
09 10
09 12
10 02
Time

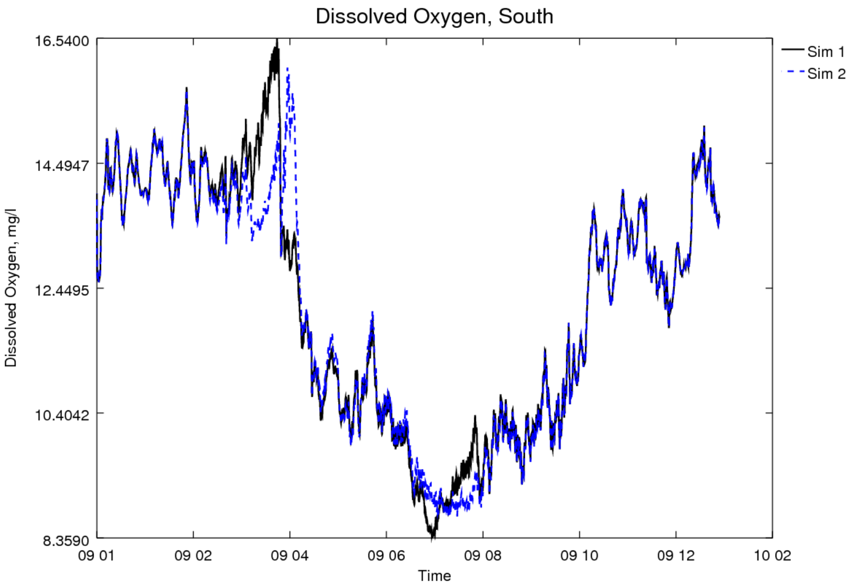
Dissolved Oxygen, South
Sim 1
Sim 2
Dissolved Oxygen, mg/l
16.5400
14.4947
12.4495
10.4042
8.3590
09 01
09 02
09 04
09 06
09 08
09 10
09 12
10 02
Time

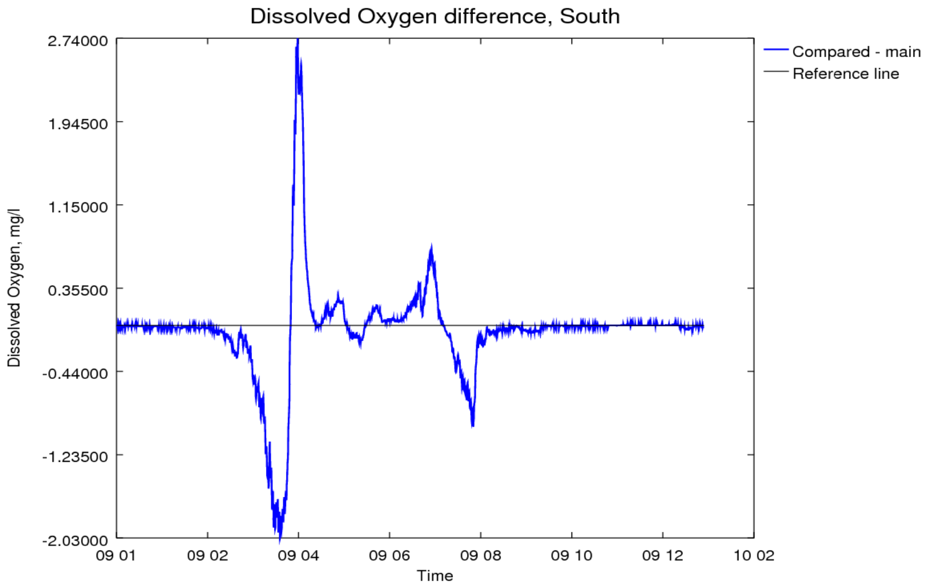
Dissolved Oxygen difference, South
Compared - main
Reference line
Dissolved Oxygen, mg/l
2.74000
1.94500
1.15000
0.35500
-0.44000
-1.23500
-2.03000
09 01
09 02
09 04
09 06
09 08
09 10
09 12
10 02
Time

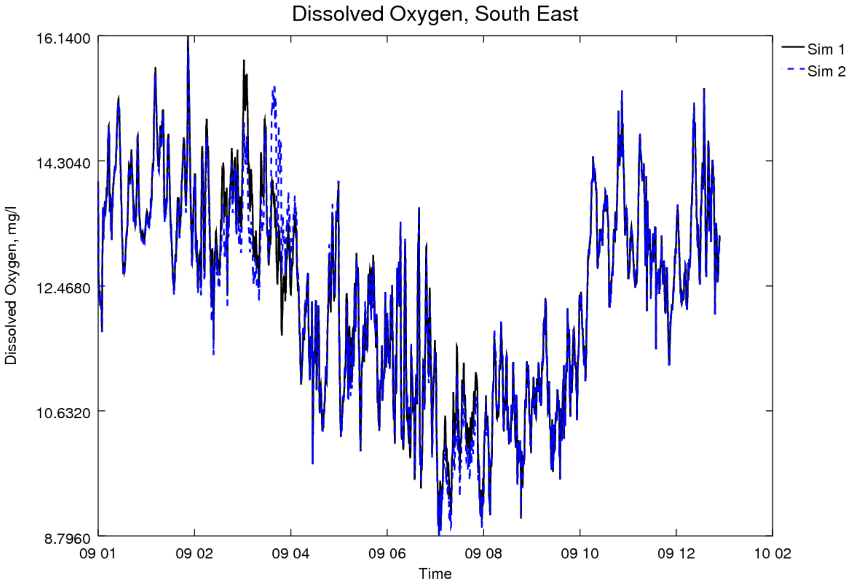
Dissolved Oxygen, South East
16.1400
14.3040
12.4680
10.6320
8.7960
09 01
09 02
09 04
09 06
09 08
09 10
09 12
10 02
Time
Dissolved Oxygen, mg/l
Sim 1
Sim 2

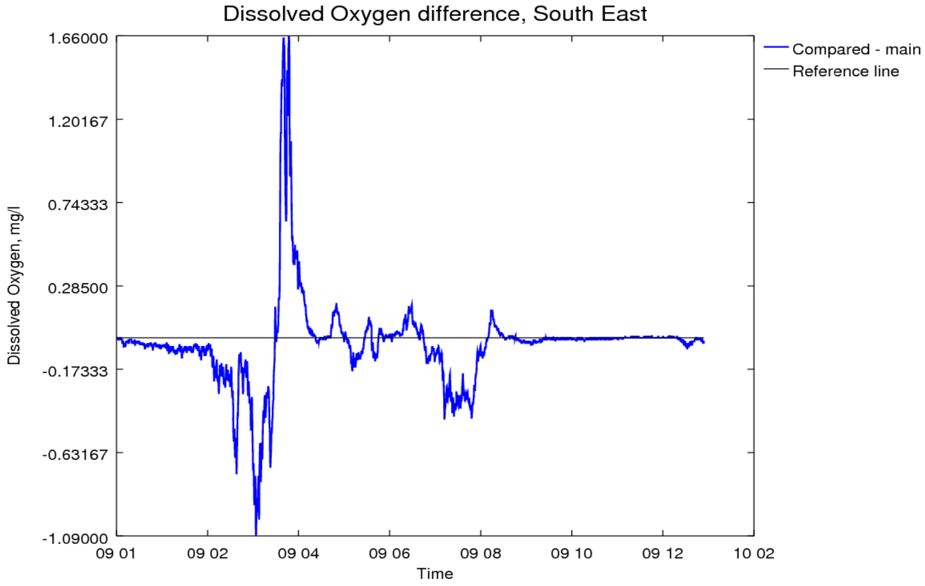
Dissolved Oxygen difference, South East
1.66000
1.20167
0.74333
0.28500
-0.17333
-0.63167
-1.09000
09 01
09 02
09 04
09 06
09 08
09 10
09 12
10 02
Time
Dissolved Oxygen, mg/l
Compared - main
Reference line

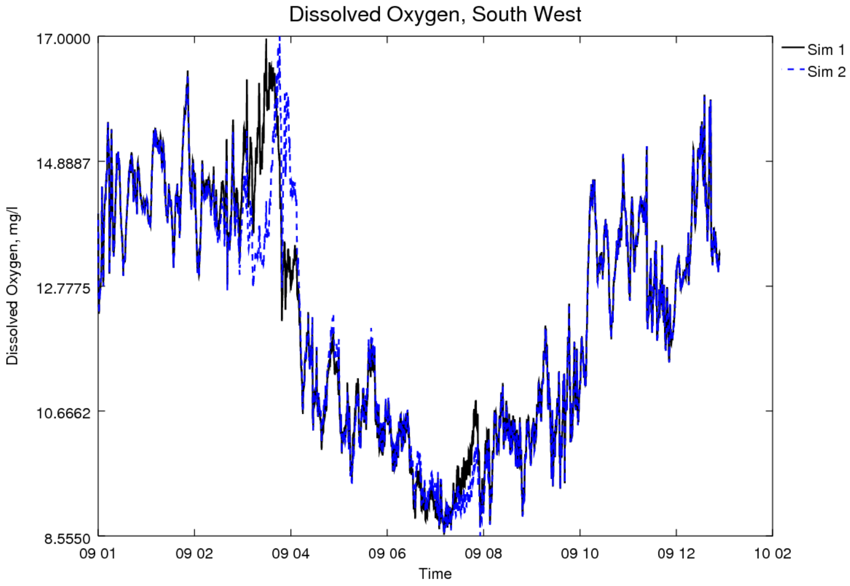
Dissolved Oxygen, South West
17.0000
14.8887
12.7775
10.6662
8.5550
09 01
09 02
09 04
09 06
09 08
09 10
09 12
10 02
Time
Dissolved Oxygen, mg/l
Sim 1
Sim 2

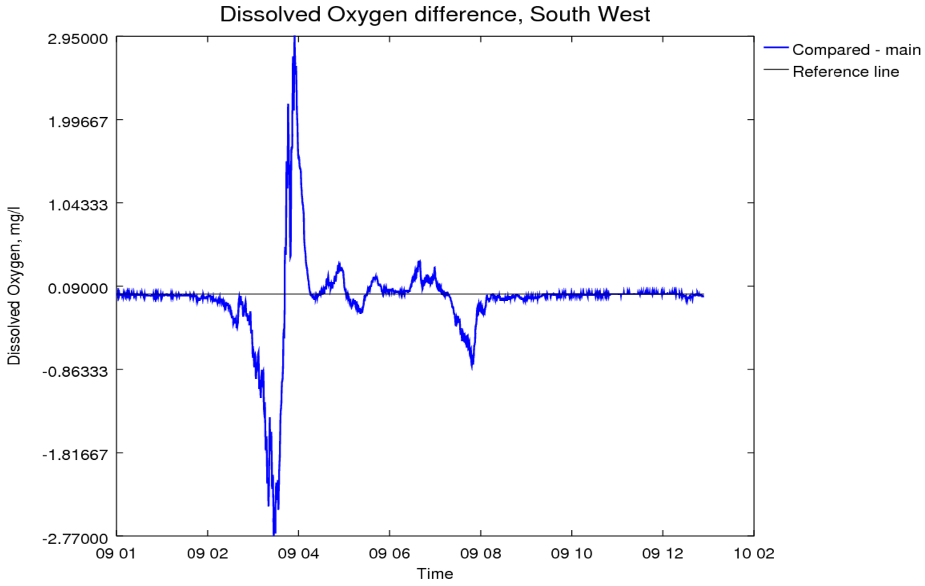
Dissolved Oxygen difference, South West
2.95000
1.99667
1.04333
0.09000
-0.86333
-1.81667
-2.77000
09 01
09 02
09 04
09 06
09 08
09 10
09 12
10 02
Time
Dissolved Oxygen, mg/l
Compared - main
Reference line

Dissolved oxygen (reference with only momentum suppressed)

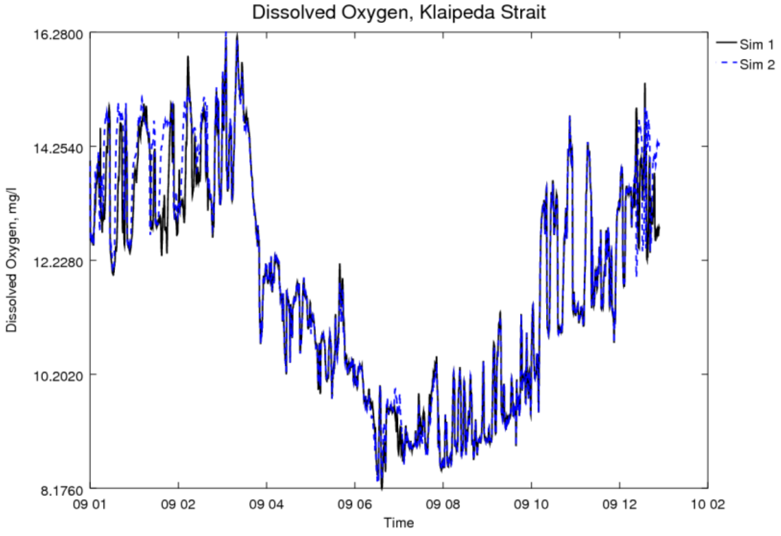

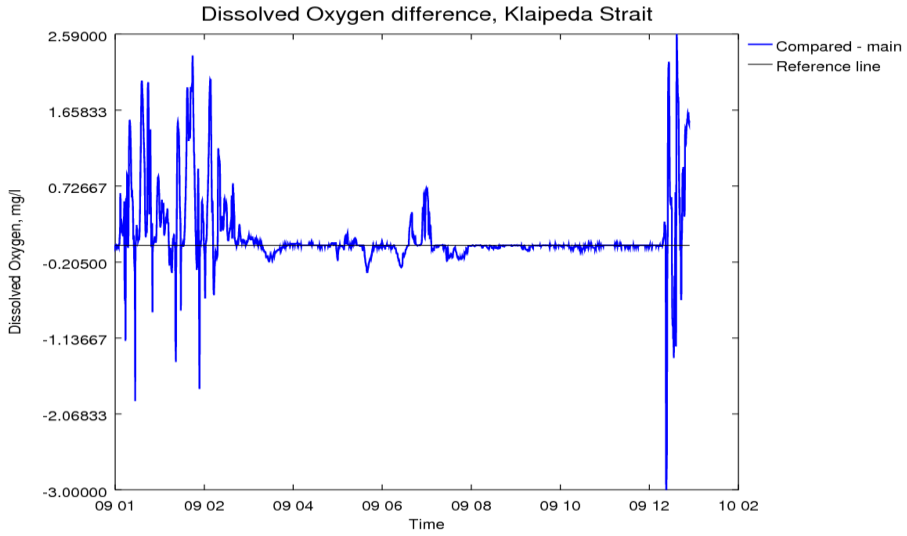

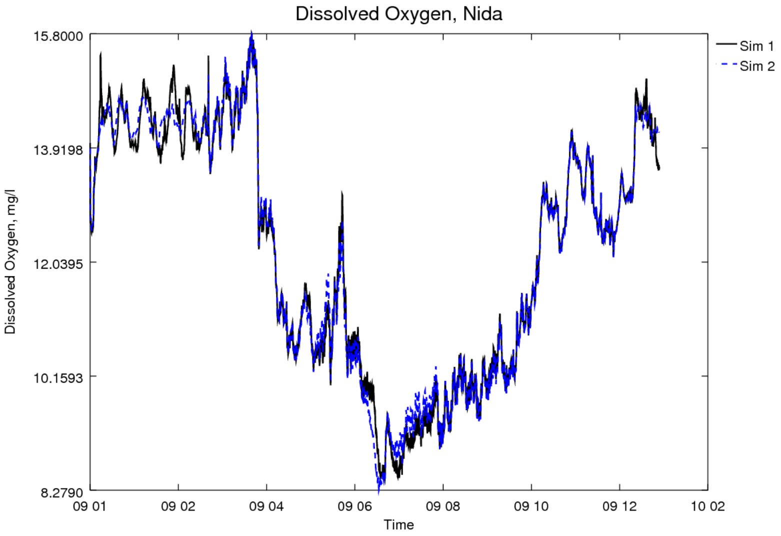

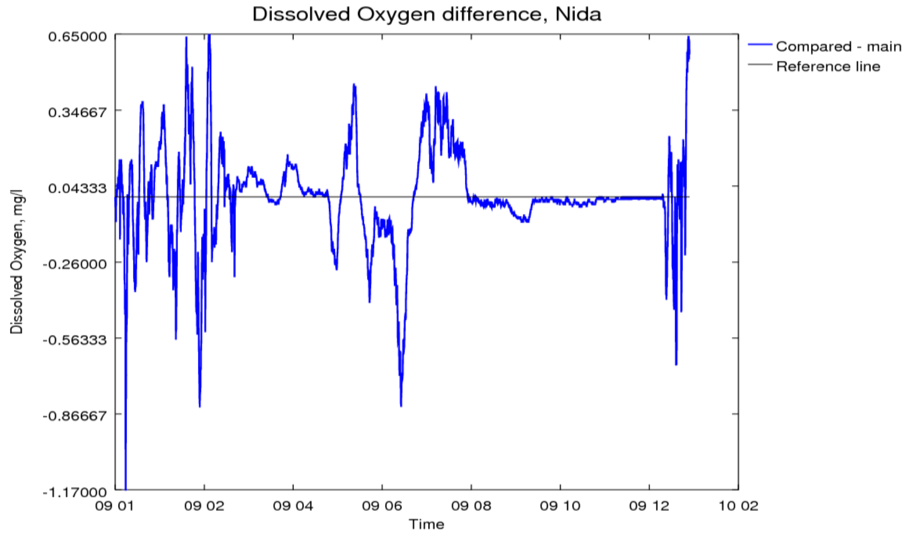

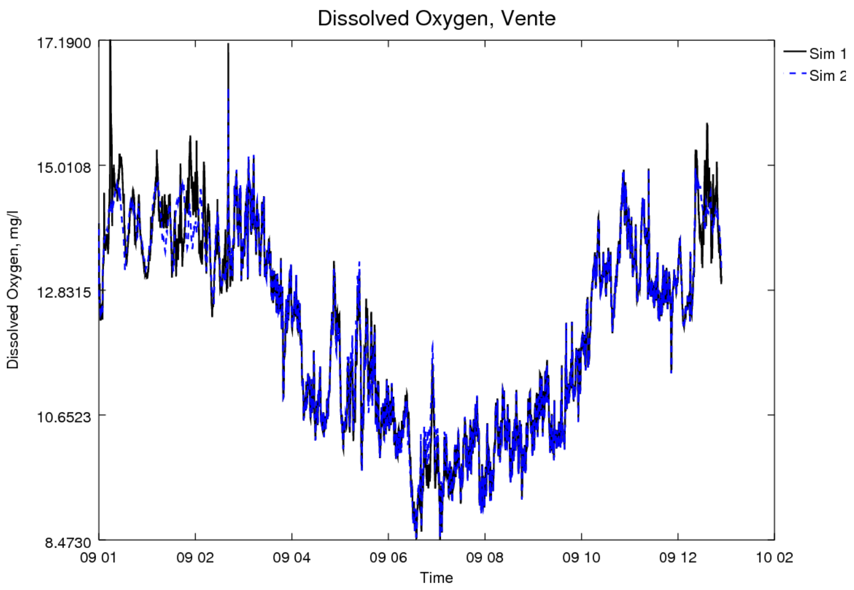
Dissolved Oxygen, Vente
Dissolved Oxygen, mg/l
17.1900
15.0108
12.8315
10.6523
8.4730
09 01
09 02
09 04
09 06
09 08
09 10
09 12
10 02
Time
Sim 1
Sim 2

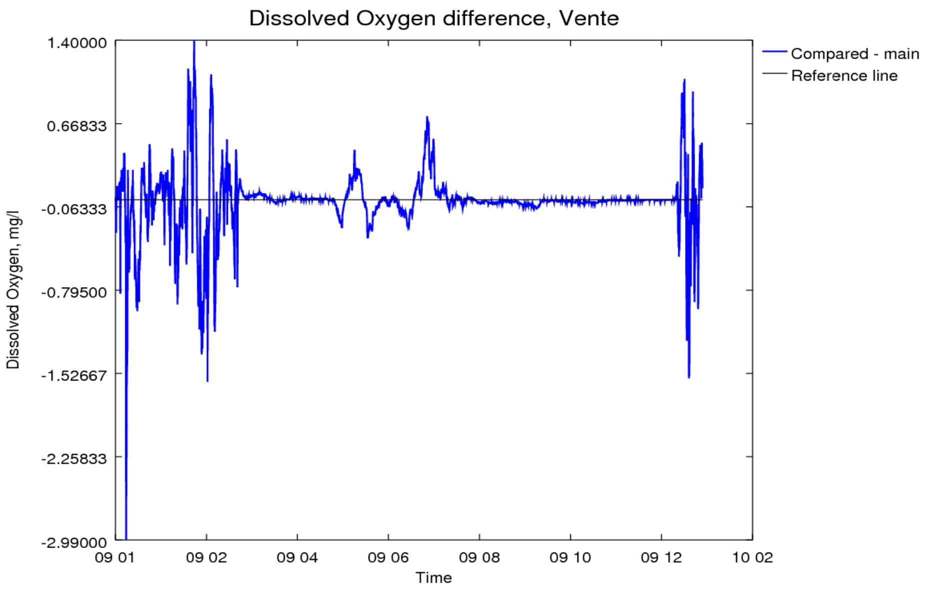
Dissolved Oxygen difference, Vente
Dissolved Oxygen, mg/l
1.40000
0.66833
-0.06333
-0.79500
-1.52667
-2.25833
-2.99000
09 01
09 02
09 04
09 06
09 08
09 10
09 12
10 02
Time
Compared - main
Reference line

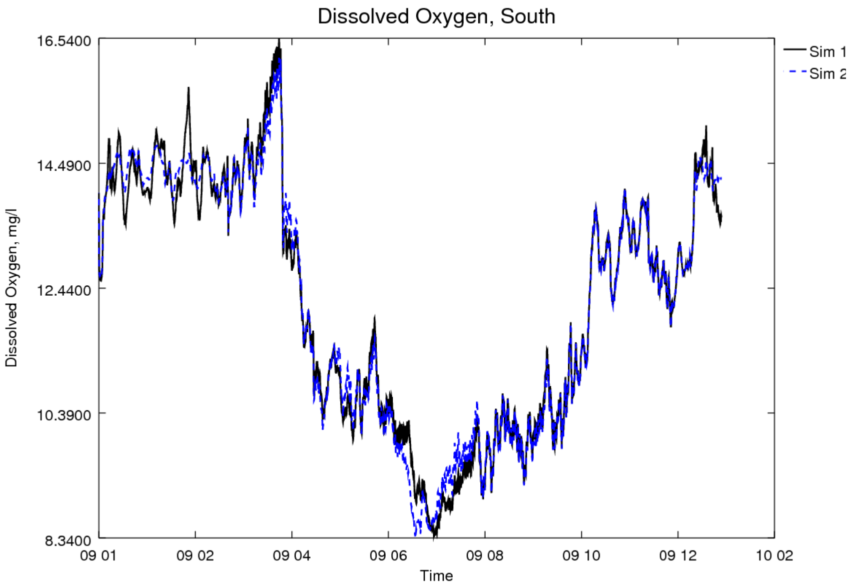
Dissolved Oxygen, South
Dissolved Oxygen, mg/l
16.5400
14.4900
12.4400
10.3900
8.3400
09 01
09 02
09 04
09 06
09 08
09 10
09 12
10 02
Time
Sim 1
Sim 2

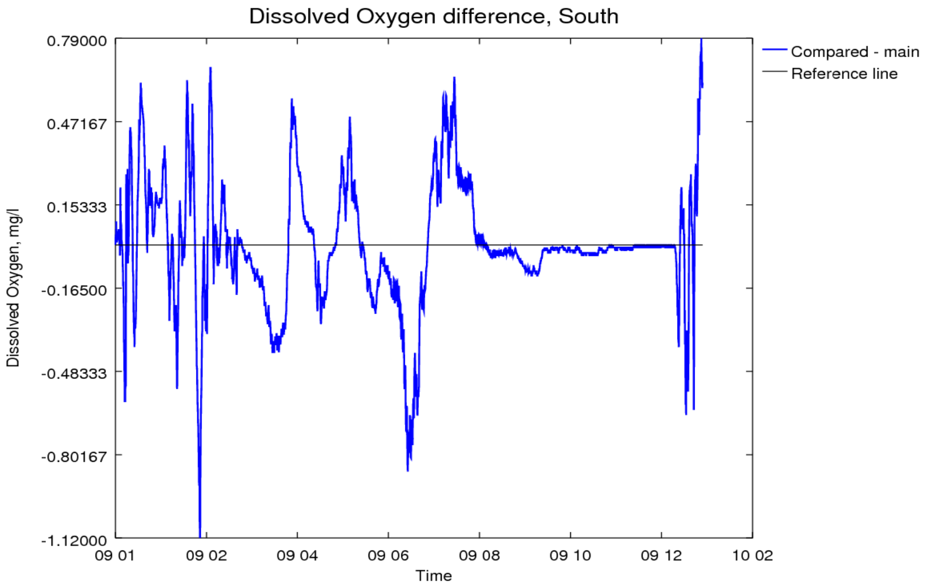
Dissolved Oxygen difference, South
Dissolved Oxygen, mg/l
0.79000
0.47167
0.15333
-0.16500
-0.48333
-0.80167
-1.12000
09 01
09 02
09 04
09 06
09 08
09 10
09 12
10 02
Time
Compared - main
Reference line

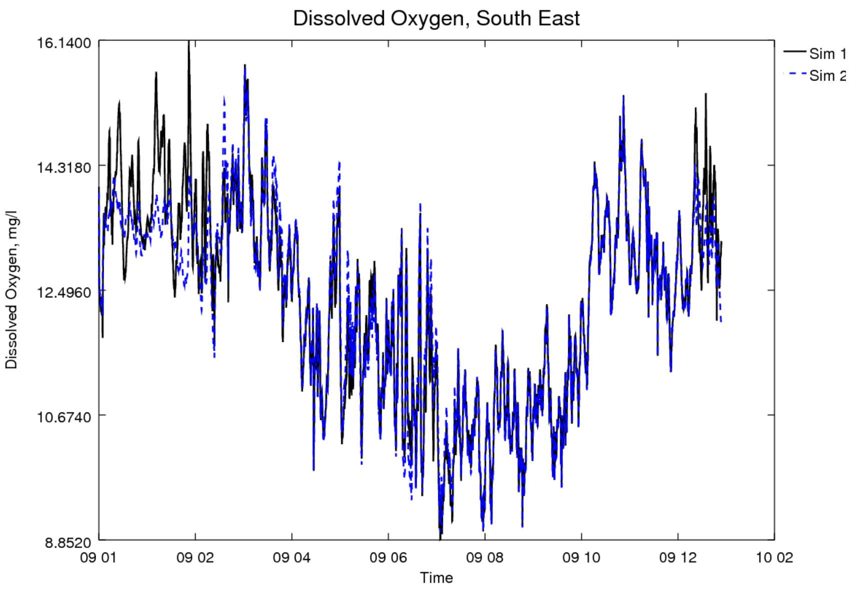
Dissolved Oxygen, South East
16.1400
14.3180
12.4960
10.6740
8.8520
Dissolved Oxygen, mg/l
09 01
09 02
09 04
09 06
09 08
09 10
09 12
10 02
Time
Sim 1
Sim 2

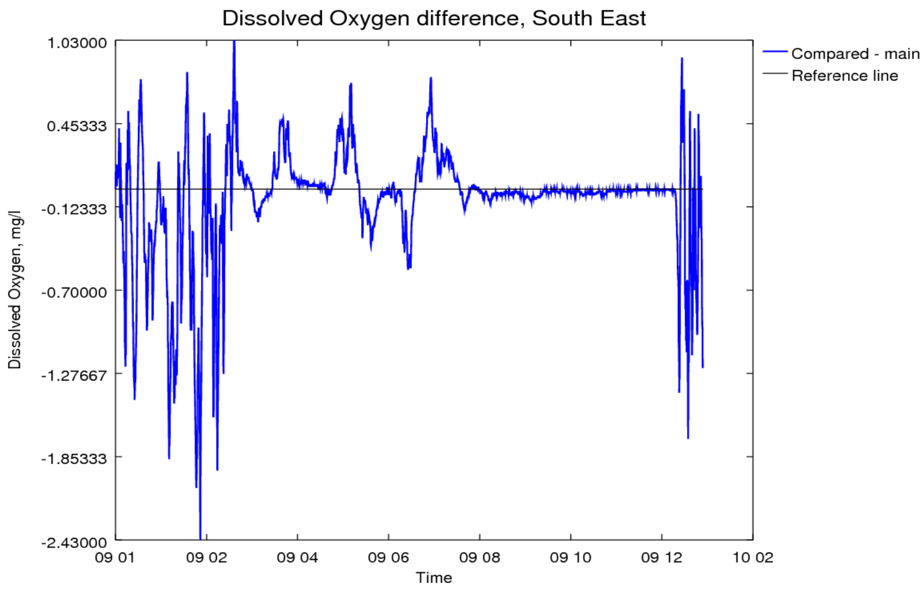
Dissolved Oxygen difference, South East
1.03000
0.45333
-0.12333
-0.70000
-1.27667
-1.85333
-2.43000
Dissolved Oxygen, mg/l
09 01
09 02
09 04
09 06
09 08
09 10
09 12
10 02
Time
Compared - main
Reference line

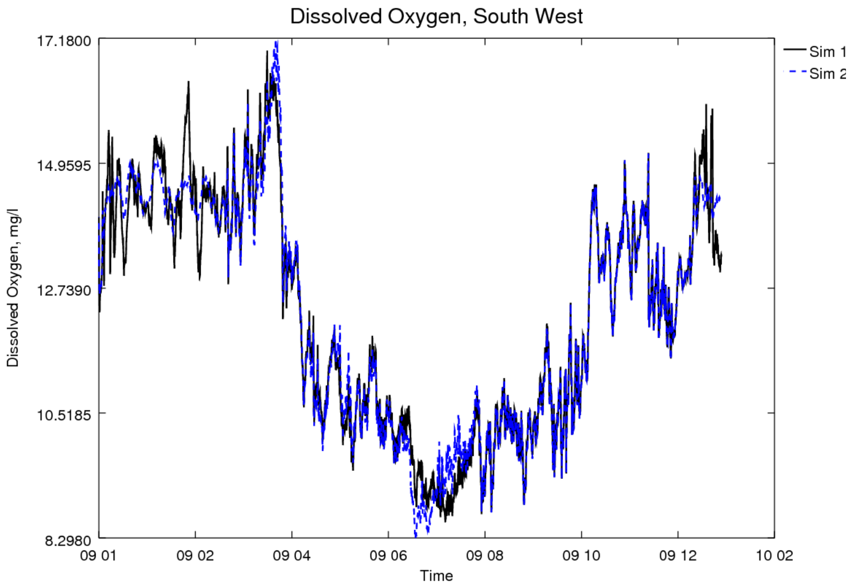
Dissolved Oxygen, South West
17.1800
14.9595
12.7390
10.5185
8.2980
Dissolved Oxygen, mg/l
09 01
09 02
09 04
09 06
09 08
09 10
09 12
10 02
Time
Sim 1
Sim 2

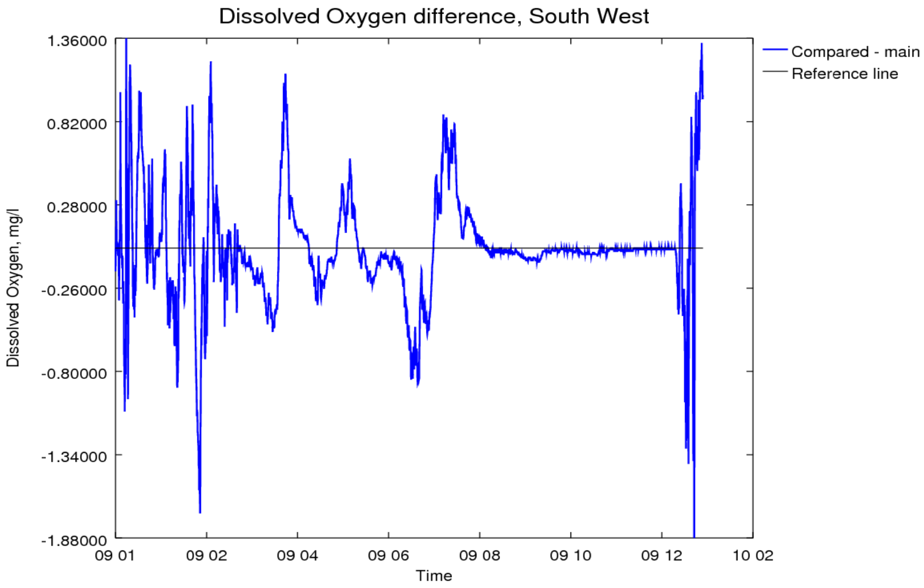
Dissolved Oxygen difference, South West
1.36000
0.82000
0.28000
-0.26000
-0.80000
-1.34000
-1.88000
Dissolved Oxygen, mg/l
09 01
09 02
09 04
09 06
09 08
09 10
09 12
10 02
Time
Compared - main
Reference line

Total phytoplankton (reference with only light suppressed)

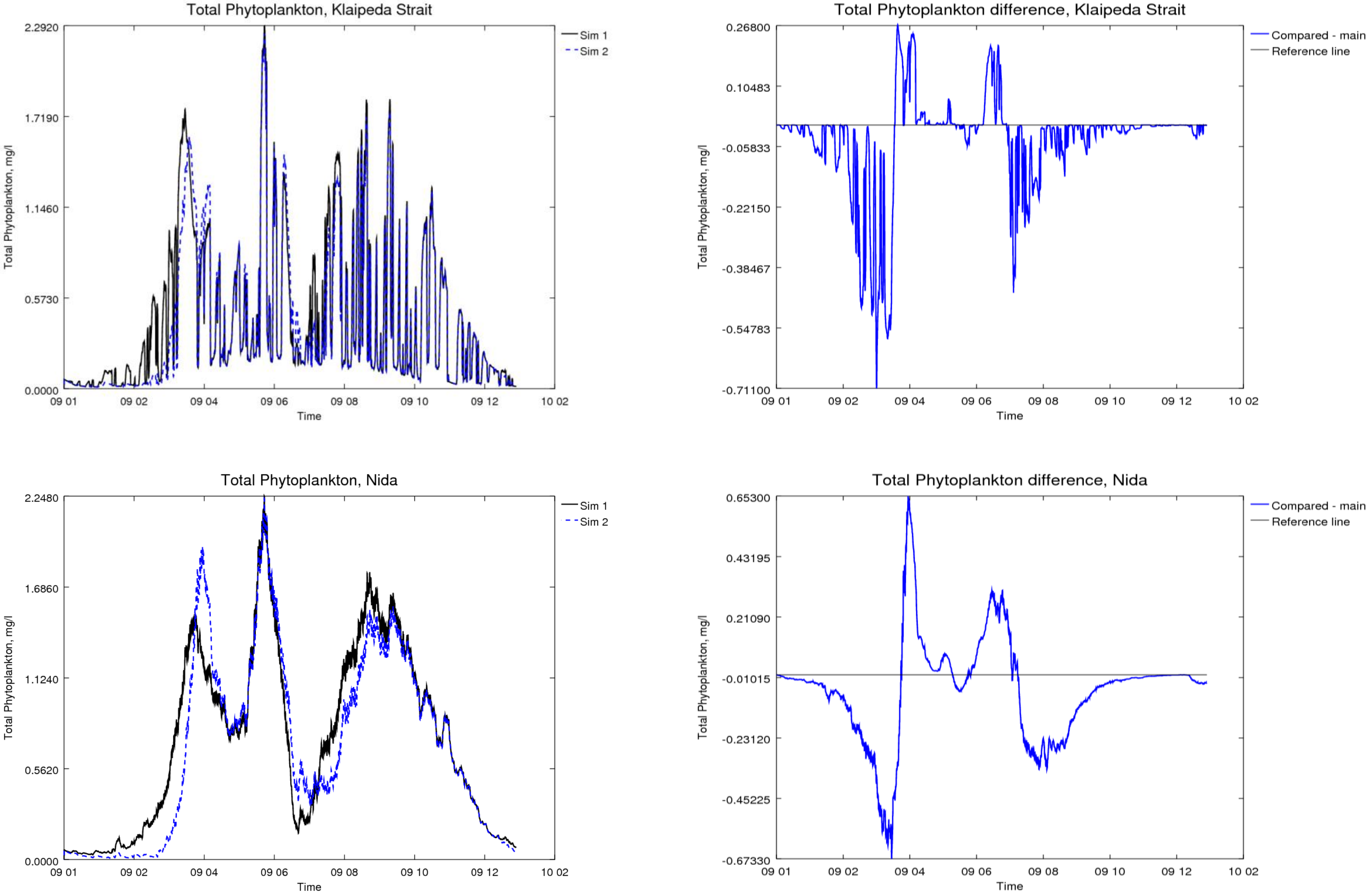

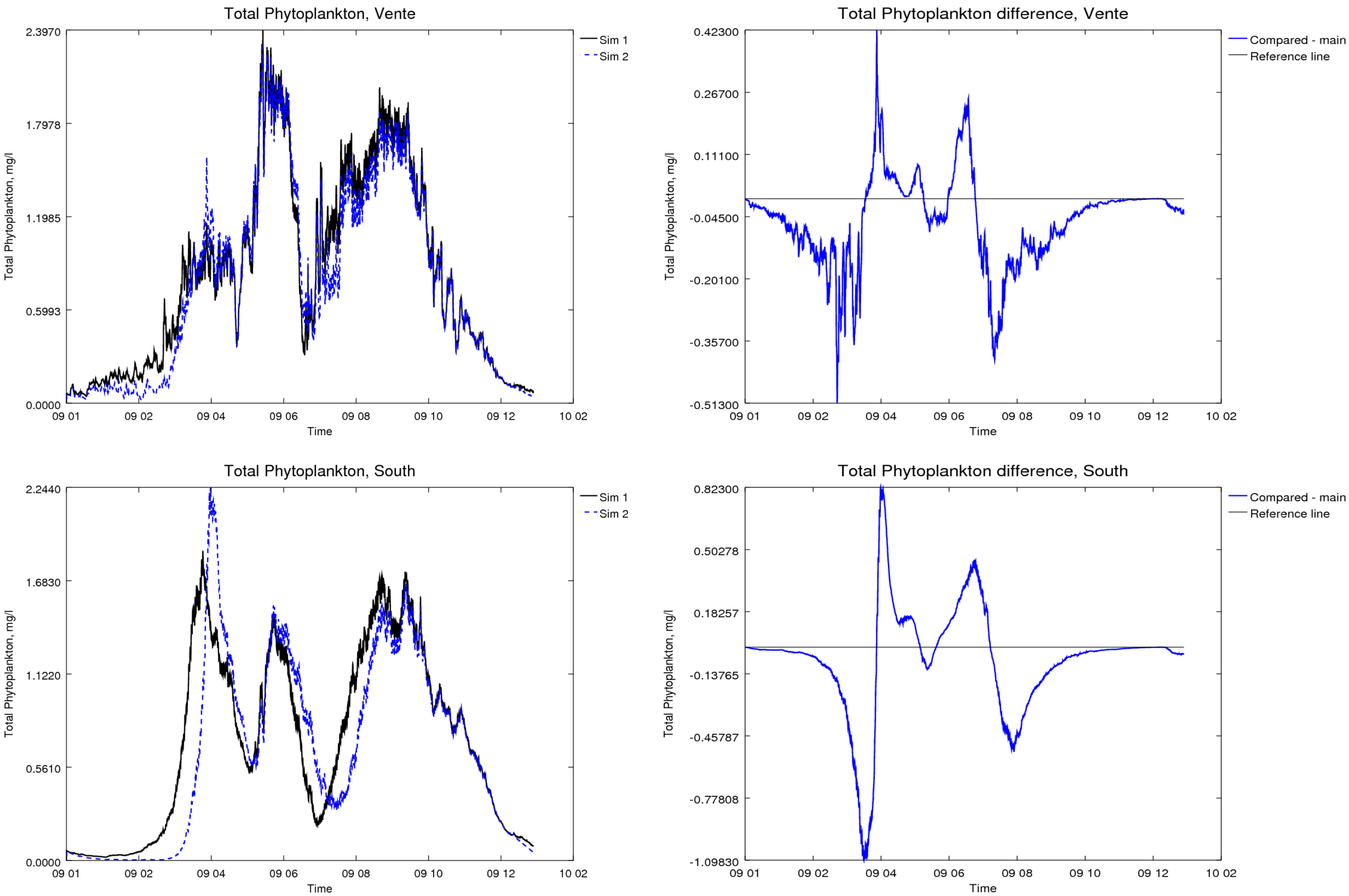

Total Phytoplankton, Vente
Sim 1
Sim 2
2.3970
1.7978
1.1985
0.5993
0.0000
Total Phytoplankton, mg/l
09 01
09 02
09 04
09 06
09 08
09 10
09 12
10 02
Time
Total Phytoplankton difference, Vente
Compared - main
Reference line
0.42300
0.26700
0.11100
-0.04500
-0.20100
-0.35700
-0.51300
Total Phytoplankton, mg/l
Time
Total Phytoplankton, South
2.2440
1.6830
1.1220
0.5610
0.0000
Total Phytoplankton difference, South
0.82300
0.50278
0.18257
-0.13765
-0.45787
-0.77808
-1.09830

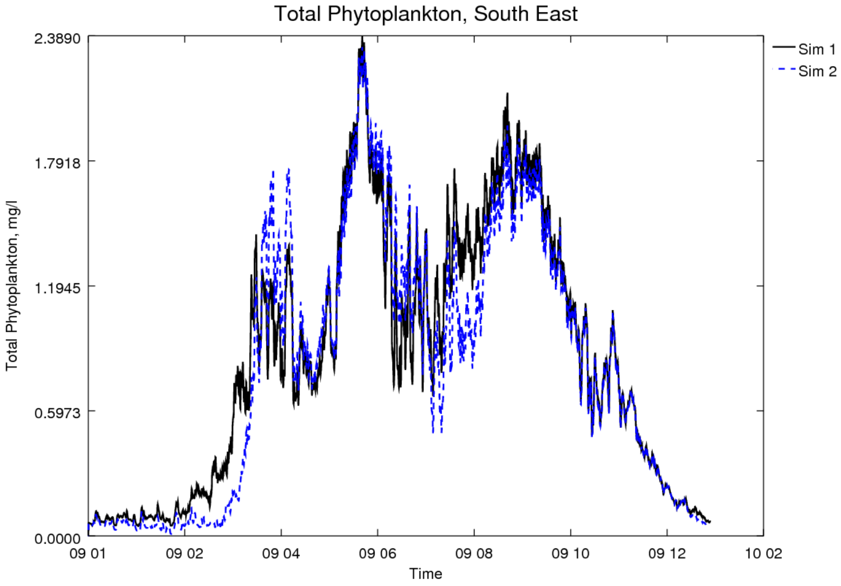
Total Phytoplankton, South East
Sim 1
Sim 2
Total Phytoplankton, mg/l
2.3890
1.7918
1.1945
0.5973
0.0000
09 01
09 02
09 04
09 06
09 08
09 10
09 12
10 02
Time

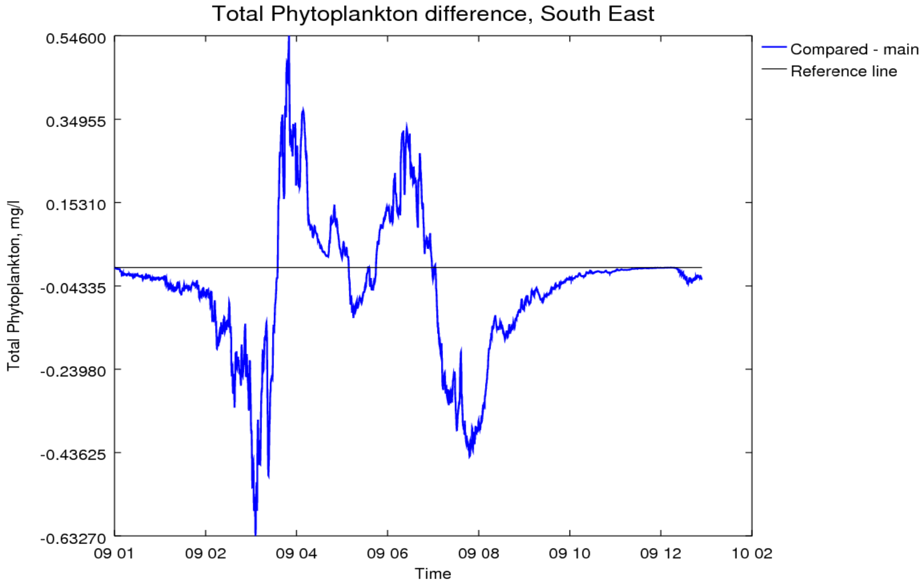
Total Phytoplankton difference, South East
Compared - main
Reference line
Total Phytoplankton, mg/l
0.54600
0.34955
0.15310
-0.04335
-0.23980
-0.43625
-0.63270
09 01
09 02
09 04
09 06
09 08
09 10
09 12
10 02
Time

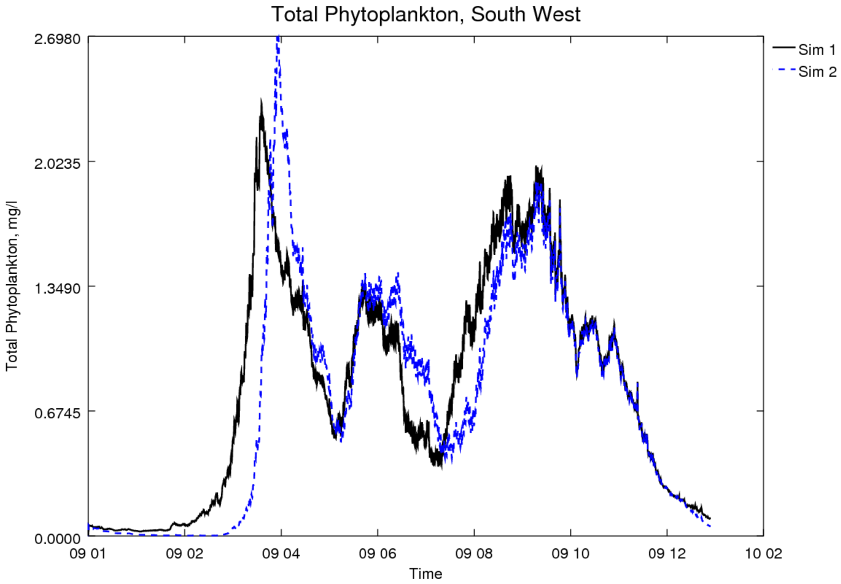
Total Phytoplankton, South West
Sim 1
Sim 2
Total Phytoplankton, mg/l
2.6980
2.0235
1.3490
0.6745
0.0000
09 01
09 02
09 04
09 06
09 08
09 10
09 12
10 02
Time

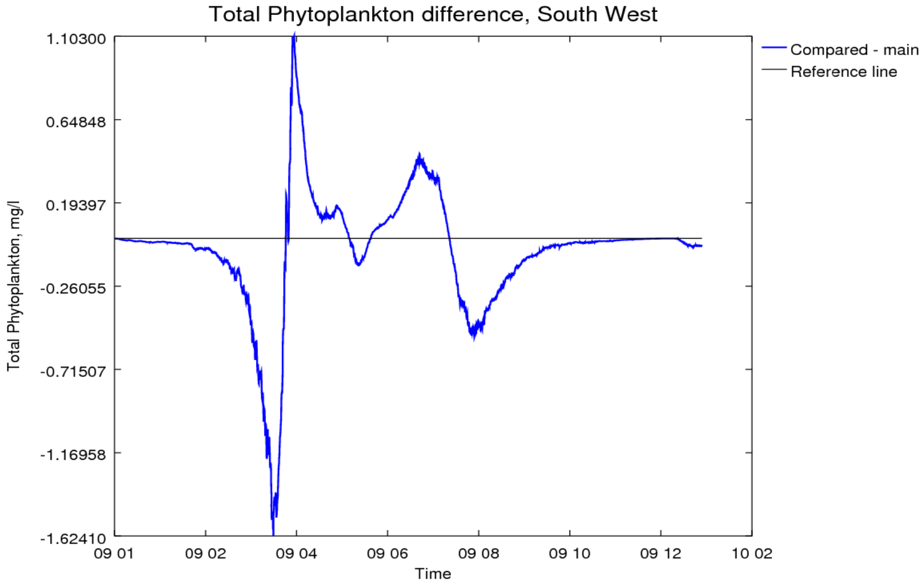
Total Phytoplankton difference, South West
Compared - main
Reference line
Total Phytoplankton, mg/l
1.10300
0.64848
0.19397
-0.26055
-0.71507
-1.16958
-1.62410
09 01
09 02
09 04
09 06
09 08
09 10
09 12
10 02
Time

Total phytoplankton (reference with only momentum suppressed)

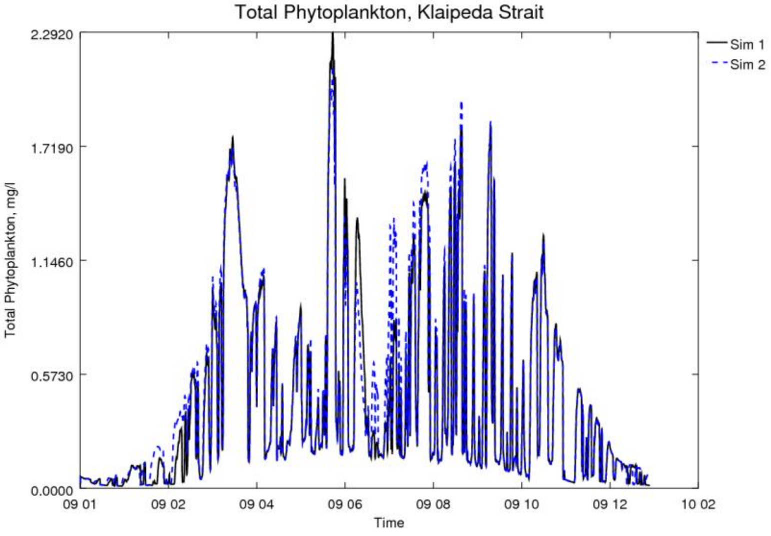

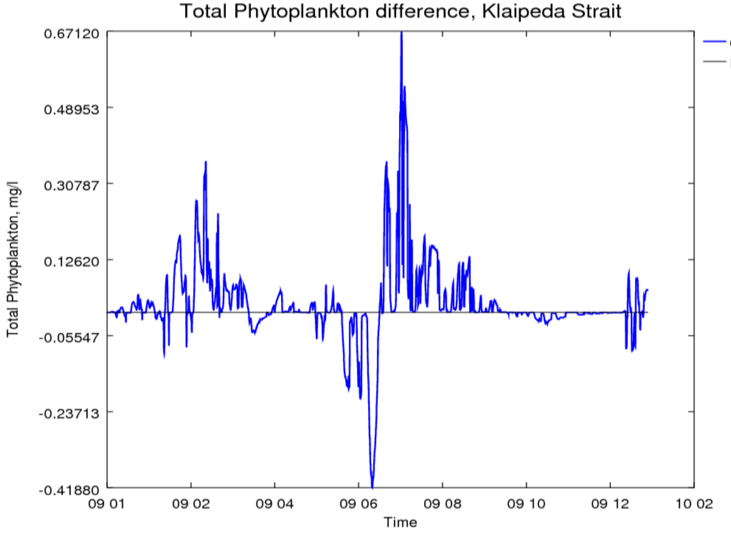

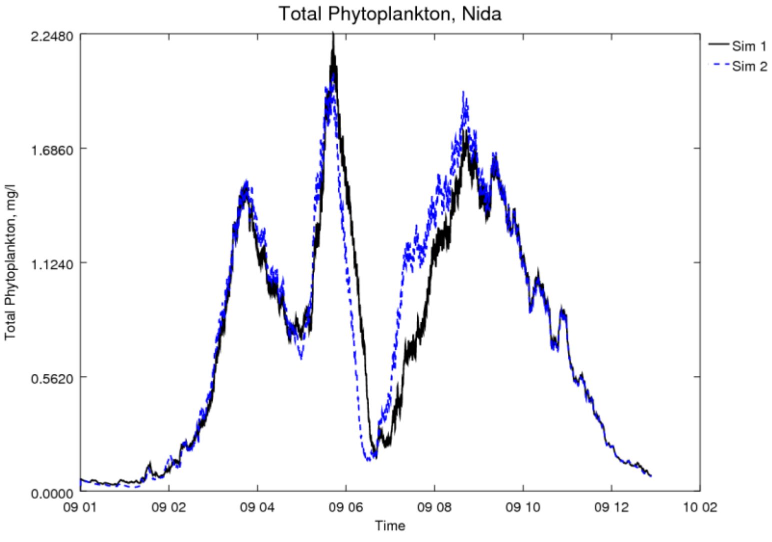

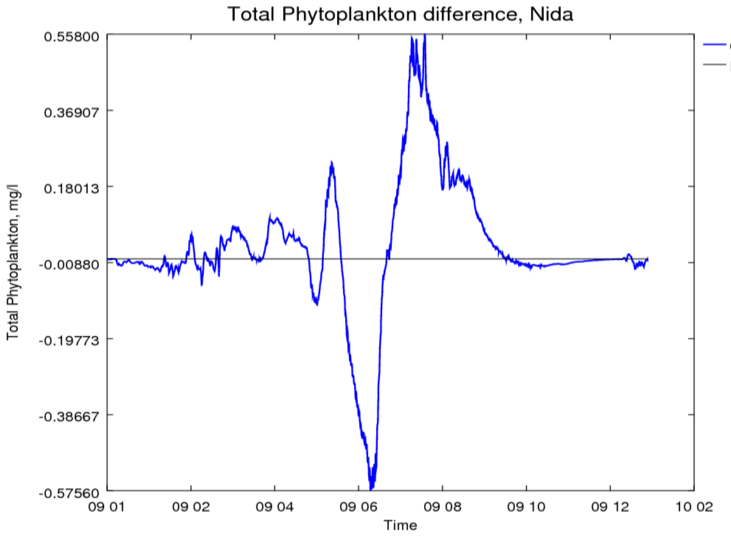

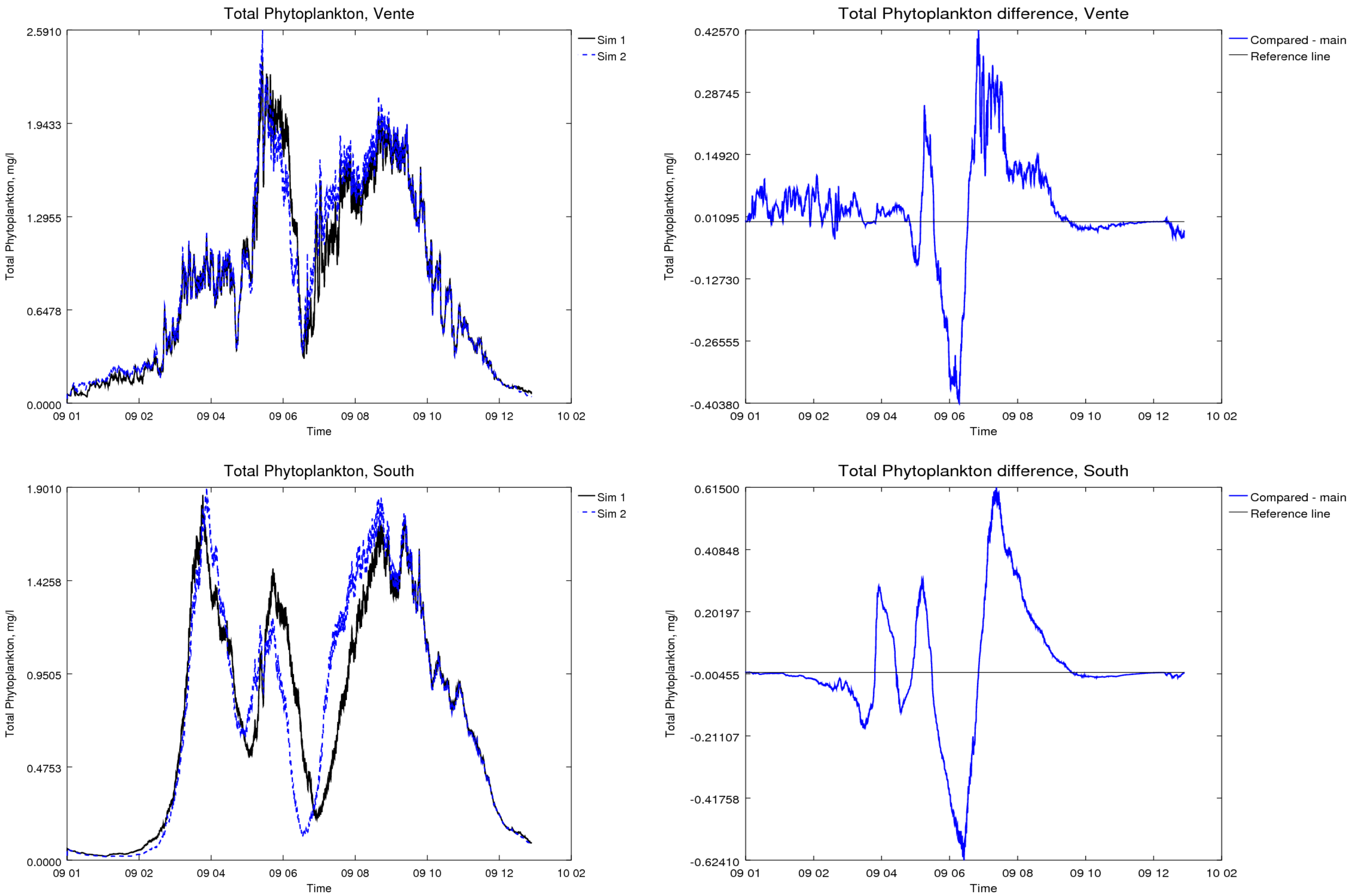

Total Phytoplankton, Vente
Sim 1
Sim 2
Total Phytoplankton, mg/l
2.5910
1.9433
1.2955
0.6478
0.0000
09 01
09 02
09 04
09 06
09 08
09 10
09 12
10 02
Time
Total Phytoplankton difference, Vente
Compared - main
Reference line
0.42570
0.28745
0.14920
0.01095
-0.12730
-0.26555
-0.40380
Total Phytoplankton, South
1.9010
1.4258
0.9505
0.4753
Total Phytoplankton difference, South
0.61500
0.40848
0.20197
-0.00455
-0.21107
-0.41758
-0.62410

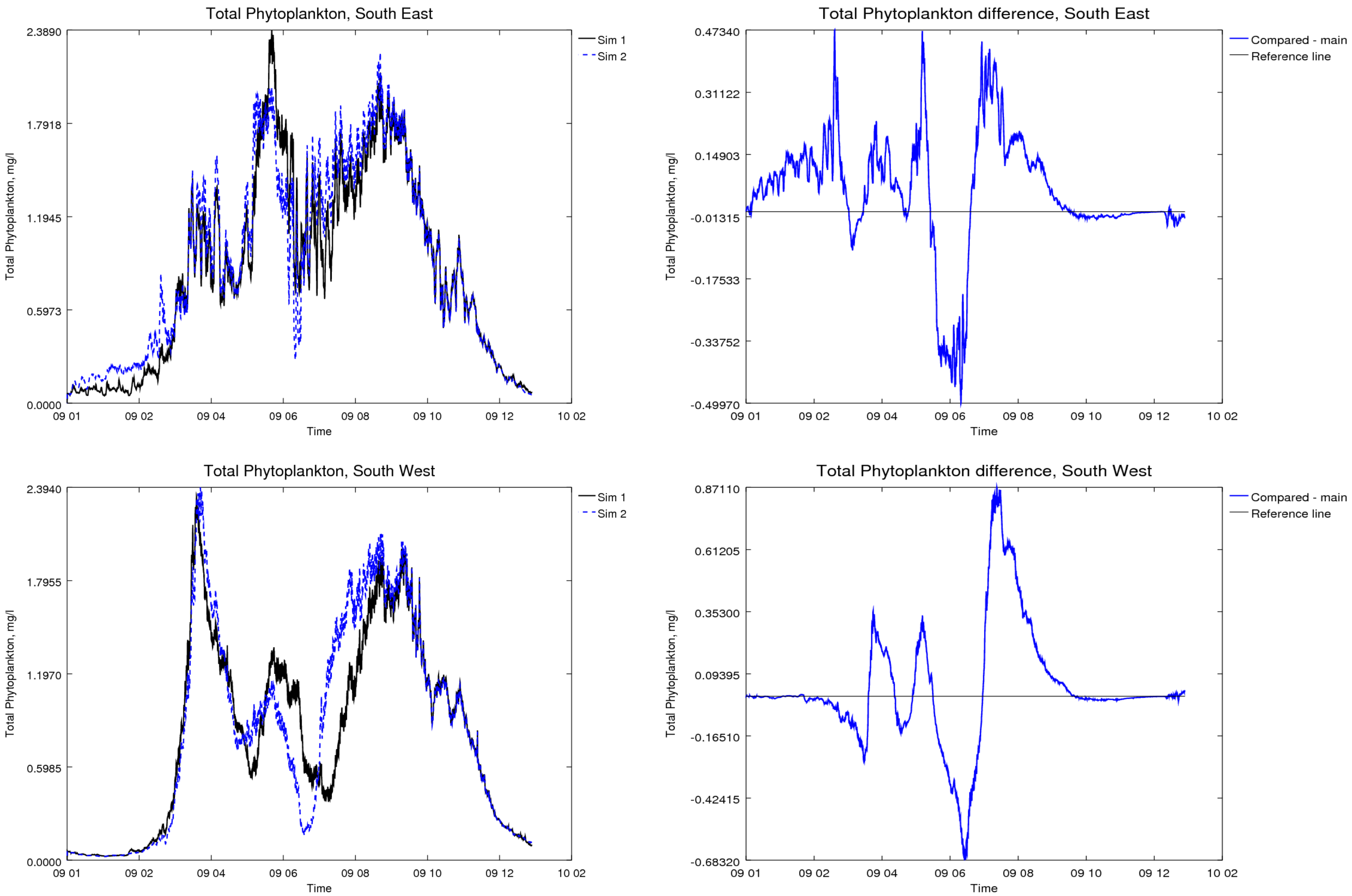

Total Phytoplankton, South East
2.3890
1.7918
1.1945
0.5973
0.0000
Total Phytoplankton, mg/l
09 01
09 02
09 04
09 06
09 08
09 10
09 12
10 02
Time
Sim 1
Sim 2
Total Phytoplankton difference, South East
0.47340
0.31122
0.14903
-0.01315
-0.17533
-0.33752
-0.49970
Total Phytoplankton, mg/l
Compared - main
Reference line
Total Phytoplankton, South West
2.3940
1.7955
1.1970
0.5985
0.0000
Total Phytoplankton difference, South West
0.87110
0.61205
0.35300
0.09395
-0.16510
-0.42415
-0.68320

Oxygen saturation (with and without natural ice cover conditions)

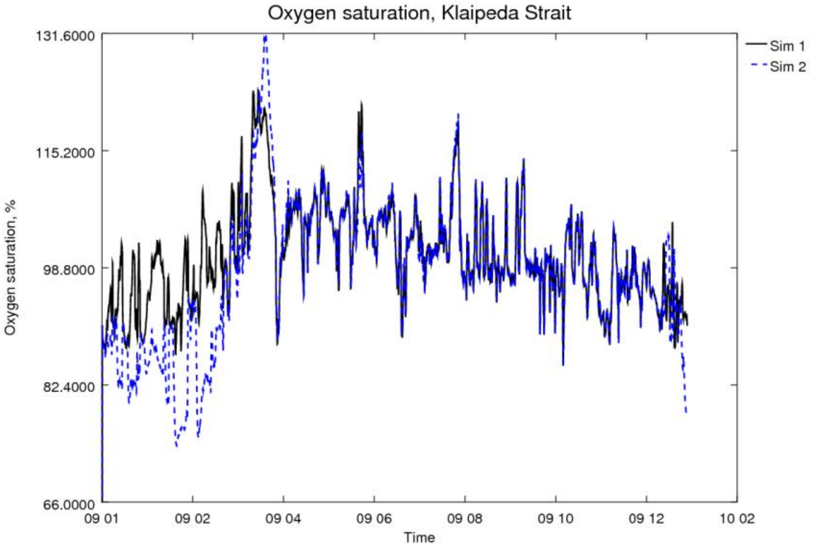

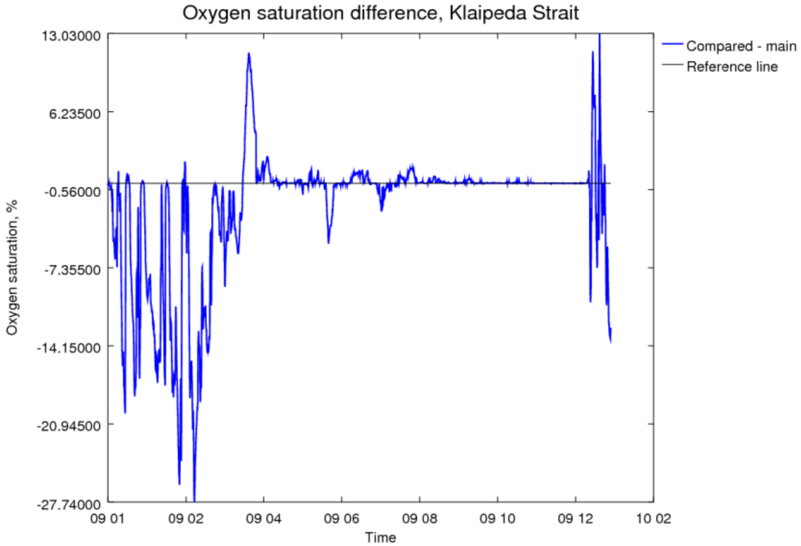

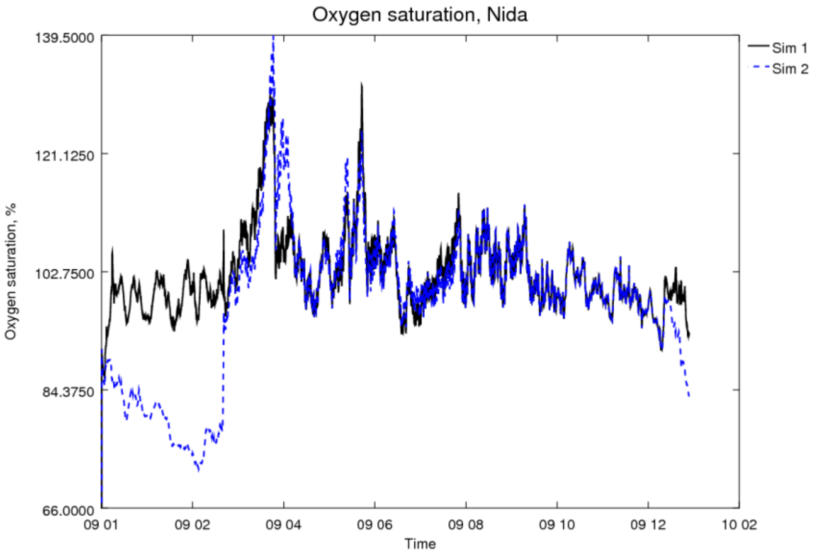

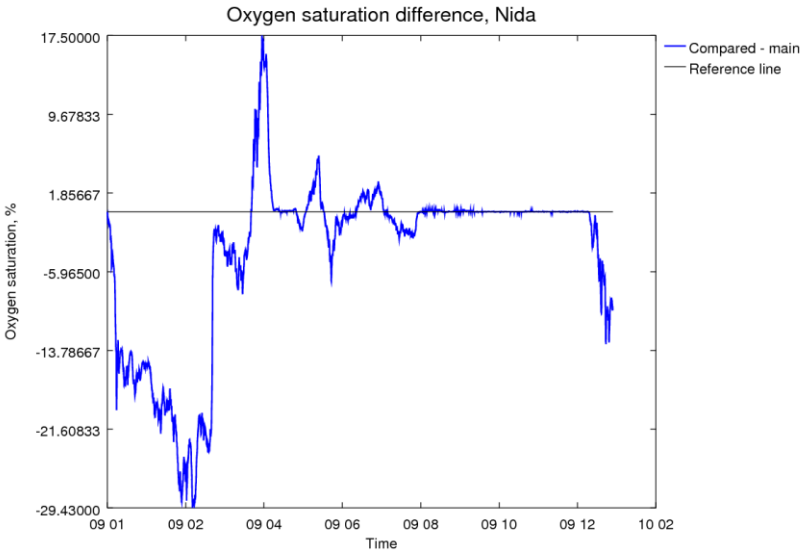

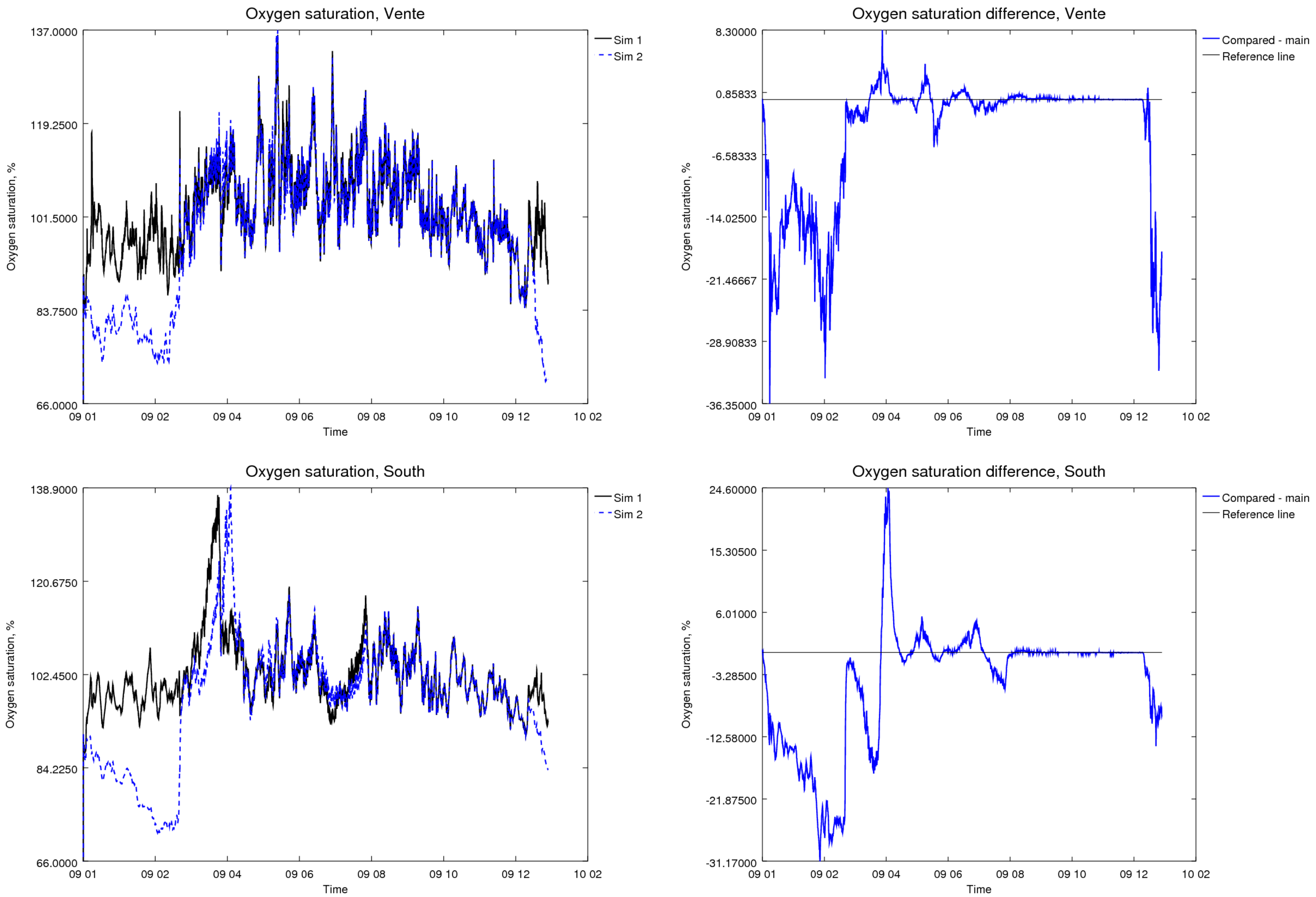

Oxygen saturation, Vente
137.0000
119.2500
101.5000
83.7500
66.0000
09 01
09 02
09 04
09 06
09 08
09 10
09 12
10 02
Time
Oxygen saturation, %
Sim 1
Sim 2
Oxygen saturation difference, Vente
8.30000
0.85833
-6.58333
-14.02500
-21.46667
-28.90833
-36.35000
Compared - main
Reference line
Oxygen saturation, South
138.9000
120.6750
102.4500
84.2250
66.0000
Oxygen saturation difference, South
24.60000
15.30500
6.01000
-3.28500
-12.58000
-21.87500
-31.17000

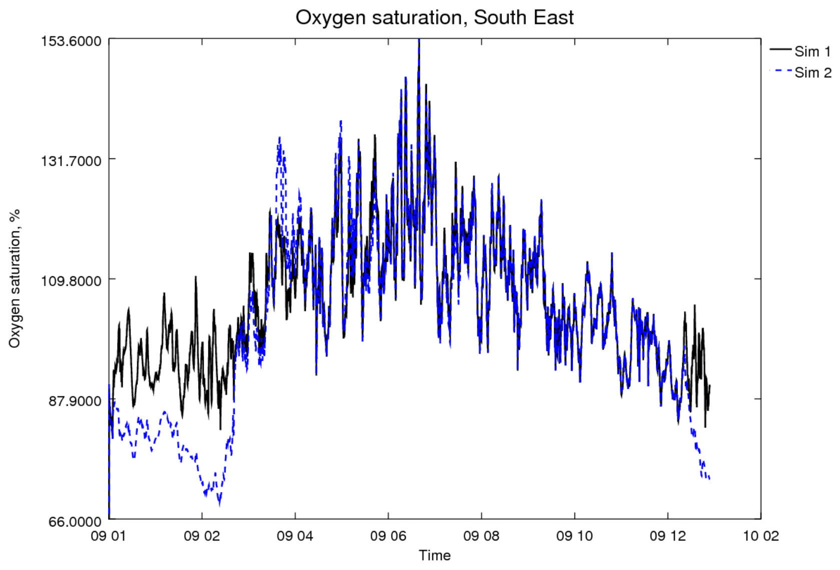
Oxygen saturation, South East
Sim 1
Sim 2
Oxygen saturation, %
Time

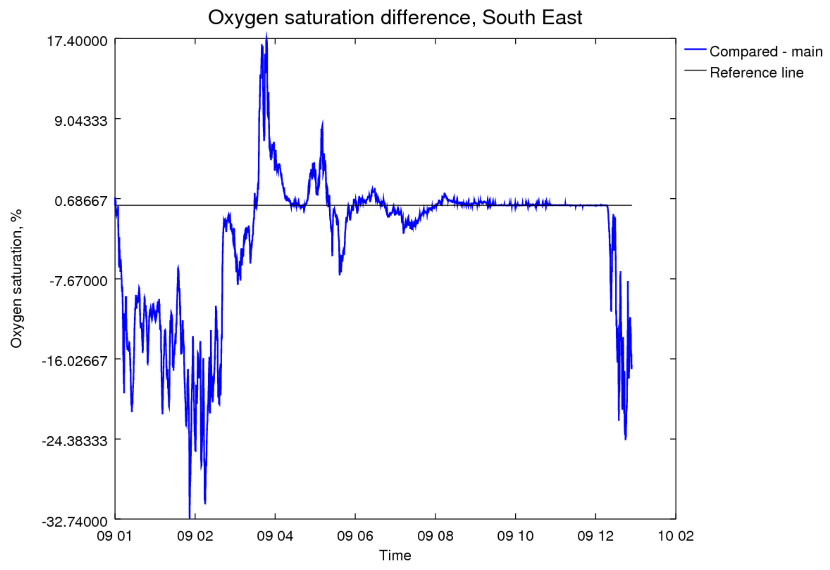
Oxygen saturation difference, South East
Compared - main
Reference line
Oxygen saturation, %
Time

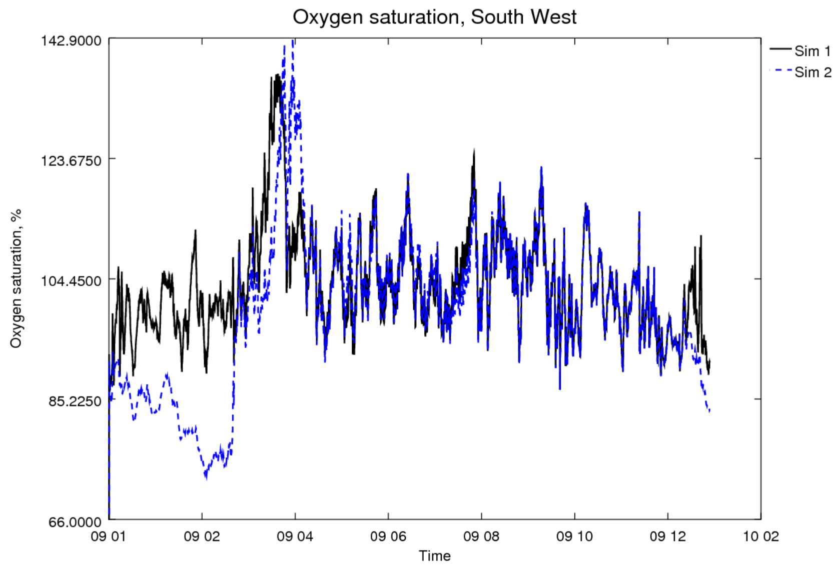
Oxygen saturation, South West
Sim 1
Sim 2
Oxygen saturation, %
Time

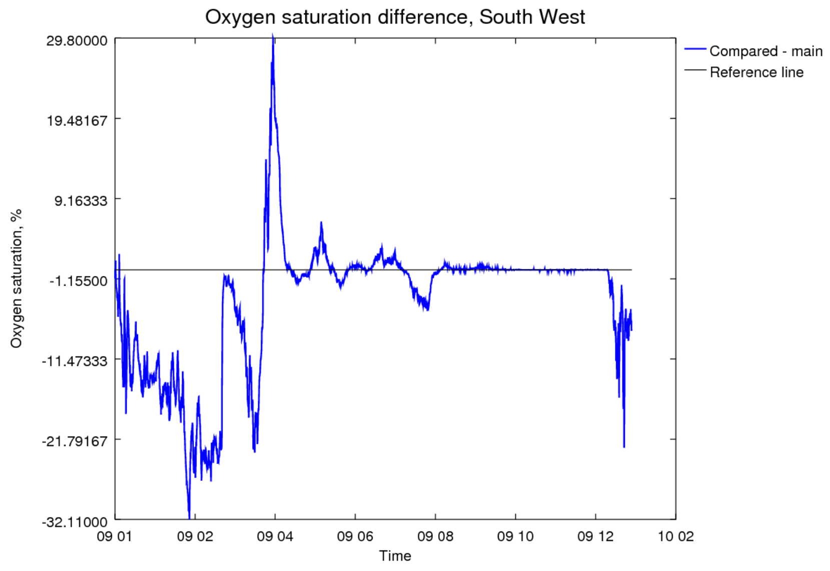
Oxygen saturation difference, South West
Compared - main
Reference line
Oxygen saturation, %
Time